Manganese Homeostasis in the Cyanobacterium *Synechocystis* sp. PCC 6803

Inaugural-Dissertation

zur Erlangung des Doktorgrades

der Mathematisch-Naturwissenschaftlichen Fakultät

der Heinrich-Heine-Universität Düsseldorf

vorgelegt von

Fabian Brandenburg

aus Düsseldorf

Düsseldorf, November 2017

aus dem Institut für Biochemie der Pflanzen

Heinrich-Heine-Universität Düsseldorf

Gedruckt mit Genehmigung der Mathematisch-

Naturwissenschaftlichen Fakultät der Heinrich-Heine-

Universität Düsseldorf

Referent: Prof. Dr. Andreas P. M. Weber

Korreferent: Prof. Dr. Peter Westhoff

Tag der mündlichen Prüfung: 18.12.2017

EIDESSTATTLICHE ERKLÄRUNG

Ich versichere an Eides Statt, dass diese Dissertation von mir selbständig und ohne unzulässige fremde Hilfe unter Beachtung der „Grundsätze zur Sicherung guter wissenschaftlicher Praxis an der Heinrich-Heine-Universität Düsseldorf“ erstellt worden ist.

Die Dissertation habe ich in der vorgelegten oder in ähnlicher Form noch bei keiner anderen Institution eingereicht.

Ich habe bisher keine erfolglosen Promotionsversuche unternommen.

Fabian Brandenburg

Düsseldorf, 03.11.2017

‘Don’t panic!’

Douglas Adams, The Hitchiker’s Guide to the Galaxy

Table of Contents

Preface

Following on a summary in English and German language, this PhD thesis introduces in the significance, mechanisms, and origin of photosynthesis, with a focus on the role of cyanobacteria and the importance of manganese homeostasis for photosynthetic organisms. The introduction concludes with a definition of the aim of this work. The main part of this thesis consists of three manuscripts.

The first manuscript, entitled 'The *Synechocystis* Manganese Exporter Mnx Is Essential for Manganese Homeostasis in Cyanobacteria', identifies the so far uncharacterized cyanobacterial protein Sll0615 as manganese export protein in the cyanobacterium *Synechocystis* sp. PCC 6803. The manuscript illustrates the importance of Sll0615 for manganese homeostasis and photosynthesis and has been published in in Plant Physiology (Brandenburg et al., 2017b).

Derived from the first manuscript, a novel protocol for the determination the cellular manganese content in *Synechocystis* sp. PCC 6803 has been published as a method paper entitled 'Determination of Mn Concentrations in *Synechocystis* sp. PCC 6803 Using ICP-MS' in Bio-protocol (Brandenburg et al., 2017a).

The third manuscript with the running title 'The *Synechocystis* hemi manganese Exchanger Hmx1 and Hmx2 Elucidate the Importance of Manganese Export in Manganese Homeostasis in Cyanobacteria' summarizes the results obtained so far for the two proteins Slr1170 and Ssr1558, and discusses their hypothetical function in manganese transport.

Finally, a concluding remark gives a résumé of the three manuscripts and places the scientific advances of this thesis in the wider context of scientific progression in manganese homeostasis over the past years.

The following manuscripts derived from the results obtained during the work on this thesis:

Brandenburg F, Schoffman H, Kurz S, Krämer U, Keren N, Weber APM, Eisenhut M (2017b) The *Synechocystis* Manganese Exporter Mnx is Essential for Manganese Homeostasis in Cyanobacteria. **Plant Physiology**, Vol. 173, 1798-1810.

Brandenburg F, Schoffman H, Keren N, Eisenhut M (2017a) Determination of Mn concentrations in *Synechocystis* sp. PCC6803 using ICP-MS. **Bio-protocol**, accepted.

Brandenburg F, Plett A, Weber APM, Eisenhut M (2017) The *Synechocystis* Hemi Manganese Exchangers Hmx1 and Hmx2 Elucidate the Importance of Manganese Export in Manganese Homeostasis in Cyanobacteria. In preparation.

Summary

Photosynthesis is considered the most important biological process on earth and the integral understanding of photosynthesis is one of the key goals for humankind. While the general mechanism of photosynthesis is well understood, many transport processes related to photosynthesis remain yet to be discovered.

Over 3 billion years ago, cyanobacteria-like prokaryotes were the first organisms performing oxygenic photosynthesis and are the origin of all chloroplasts of higher plants in a process called endosymbiosis. Nowadays, free-living cyanobacteria significantly account for the earth's net primary production and offer interesting biotechnological opportunities. Their ecological and economical relevance, together with their close relationship to the chloroplasts of all higher plants makes cyanobacteria excellent study objects for photosynthetic research.

The transition metal manganese is an essential micronutrient for organisms performing oxygenic photosynthesis, but has also detrimental effects when present in excess. Therefore, photosynthetic organisms like cyanobacteria need to maintain their internal manganese concentrations within a narrow range. The network of manganese homeostasis in the cyanobacterium *Synechocystis* sp. PCC 6803 has been investigated to some extend in the past and several key players are known. However, the current knowledge is limited to manganese import mechanisms. This thesis identifies the first export mechanisms for manganese in the cyanobacterium *Synechocystis* sp. PCC 6803. The results obtained illustrate the relevance of manganese export and elucidate the importance of strictly regulated manganese homeostasis for the cell.

Zusammenfassung

Photosynthese wird als der wichtigste biologische Prozess der Erde angesehen und das ganzheitliche Verständnis der Photosynthese ist eines der wichtigsten Ziele der Menschheit. Während der grundlegende Mechanismus der Photosynthese gut verstanden ist, verbleiben viele der Photosynthese zugehörigen Transportprozesse noch unbekannt.

Vor über 3 Milliarden Jahren, waren den heutigen Cyanobakterien ähnliche Prokaryoten die ersten Organismen die oxygene Photosynthese verrichteten und sind, durch einen Endosymbiose genannten Vorgang, der Ursprung aller Chloroplasten höherer Pflanzen. Heutzutage, tragen freilebende Cyanobakterien immer noch signifikant zur Nettoprimärproduktion der Erde bei und bieten interessante Möglichkeiten zur biotechnologischen Anwendung. Ihre ökologische und ökonomische Relevanz, zusammen mit ihrer engen Verwandtschaft zu den Chloroplasten aller höheren Pflanzen macht Cyanobakterien zu exzellenten Studienobjekten für die Erforschung der Photosynthese.

Das Übergangsmetall Mangan ist ein essentieller Mikronährstoff für Organismen die oxygene Photosynthese betreiben, hat aber auch schädliche Effekte, wenn es im Überfluss vorhanden ist. Dem entsprechend, müssen photosynthetische Organismen ihre internen Mangankonzentrationen in einem engen Rahmen konstant halten. Das Netzwerk der Manganhomöostase im Cyanobakterium *Synechocystis* sp. PCC 6803 wurde teilweise untersucht und mehrere Schlüsselspieler sind bekannt. Der gegenwärtige Wissensstand bleibt dennoch auf Importmechanismen für Mangan beschränkt. In dieser Dissertation werden die ersten Exportmechanismen im Cyanobakterium *Synechocystis* sp. PCC 6803 identifiziert. Die erlangten Erkenntnisse illustrieren die Relevanz des Exports von Mangan und verdeutlichen die Bedeutung strikt regulierter Manganhomöostase für die Zelle.

Introduction

Photosynthesis is the engine of life. The process not only provides the oxygen we breathe, but is also responsible for the initial formation of the ozone layer, which protects all life from solar ultraviolet (UV) radiation (Barber, 2003). Above all, most heterotrophic life – including humans – is strongly dependent on energy-rich carbon molecules fixed by photosynthetic organisms for nourishment and fuel. Thus, the integral understanding of photosynthesis is crucial for advances in agriculture, fuel production and other biotechnological approaches. The history of photosynthetic research dates back to the late 18th century, when the scholars Joseph Priestly and Jan Ingenhousz published the first qualitative description of photosynthesis (Raven *et al.* 1999). While especially many transport processes directly or indirectly involved in photosynthesis remain yet to be discovered, the general reaction mechanism of photosynthesis has become textbook knowledge.

General Mechanism of Oxygenic Photosynthesis

Photosynthesis is a process in which cells use light energy to oxidize water (H_2O) in order to form complex and energy rich carbon molecules by the reduction of carbon dioxide (CO_2). In general, photosynthesis takes place in specialized cell compartments named chloroplasts and consists of the so-called light reaction and the Calvin-Benson-Bassham cycle.

The light reaction of photosynthesis, takes place in a membrane system inside the chloroplasts named the thylakoid membrane. The thylakoid membrane forms an enclosed compartment, which harbors all proteins complexes conducting the light reaction. Two photosystems (PSI and PSII) use light energy to excite electrons, which are transported along the thylakoid membrane, in order to generate the energy-rich

molecule adenosine triphosphate (ATP) and the reduction equivalent nicotinamide adenine dinucleotide phosphate ($NADP^+$, or NADPH in its reduced form).

The excited electrons are generated in the PSII reaction center P680. Light energy absorbed in the light-harvesting complexes (LHCs) of the photosystems powers the reaction. Upon absorption of light energy, P680 undergoes charge separation and passes excited electrons along the electron transport chain in the thylakoid membrane (Zouni et al., 2001). The oxidized P680 ($P680^+$) – one of the strongest biological oxidizing agents known – withdraws electrons from a manganese-oxygen-calcium (Mn_4O_5Ca) cluster (Mn cluster) which is part of the so called oxygen-evolving complex (OEC) in PSII (Rappaport et al., 2002). Eventually, the Mn cluster conducts the splitting of water and thereby regenerates the electrons passed across the electron transport chain. The splitting of water, a unique process in nature, results in the formation of molecular oxygen (O_2) and protons (H^+). Most organisms on earth depend on the O_2 released in this reaction, whereas the H^+ contribute to the formation of the H^+ gradient across the thylakoid membrane required for ATP formation.

The protein complex plastoquinol-plastocyanin reductase (cytochrome b_6f complex) transports the electrons, excited by PSII, to PSI via the isoprenoid quinone plastoquinone and the small protein plastocyanine. In this process, cytochrome b_6f complex also transports protons across the thylakoid membrane into the thylakoid lumen, creating a proton gradient across the thylakoid membrane. The transported electrons are excited further by PSI and are transferred to ferredoxin-$NADP^+$ reductase (FNR) via the iron-sulfur protein ferredoxin. FNR reduces $NADP^+$ to NADPH. Finally, the enzyme ATP synthase uses the proton gradient, generated by cytochrome b_6f complex and the water-splitting reaction, to conduct the condensation of adenosine diphosphate (ADP) and inorganic phosphate to ATP. Both, ATP and NADPH fuel the Calvin-Benson-Bassham-Cycle to fix CO_2 from the atmosphere in order to synthesize energy-rich carbohydrates.

Cyanobacteria, the origin of Photosynthesis and the rise of Atmospheric Oxygen

Before the rise of photosynthesis, the earths' atmosphere was composed of methane (CH_4), CO_2, and nitrogen (N_2) and the first organisms performed a strictly anaerobic metabolism (Hohmann-Marriott and Blankenship, 2011). It is believed that early life used hydrogen (H_2), ferrous iron (Fe^{2+}), or hydrogen sulfide (H_2S) as electron donor for redox reactions in order to synthesize energy-rich molecules and fuel their metabolism (Hohmann-Marriott and Blankenship, 2011). Hence, it is hypothesized that the first living cells developed in the oceans near hydrothermal vents, which leak H_2, CO_2 and other important components for anaerobic life out of the ocean ground (Martin et al., 2016). Moreover, these hydrothermal vents provide tolerable temperatures of 60-70°C in comparison to the 400°C of a so called black smoker or the 2°C of the surrounding water at the given depth (Martin et al., 2016).

The exact timing of the evolution of the first photoautotrophic organisms is still under debate, but analysis of stromatolites and morphological resemblance of microfossils with modern cyanobacteria lead to the hypothesis that cyanobacteria-like prokaryotes were among the first organisms on earth performing oxygenic photosynthesis (Awramik, 1992; Hohmann-Marriott and Blankenship, 2011). With the ability to oxidize H_2O, the early cyanobacteria had access to an unlimited source of electrons and H^+ for the first time, which allowed the expansion to new habitats (Dismukes et al., 2001).

The release of O_2 as a byproduct of photosynthesis also changed the composition of the atmosphere and oceans dramatically (Figure 1). About 2.4 billion years ago, oxygen levels in the atmosphere rose for the first time above levels that can be explained exclusively by the photolysis of H_2O caused by UV radiation (Figure 1). This is referred to as the 'Great Oxidation Event' (GOE) and is hypothesized to be a direct result from the evolution of oxygenic photosynthesis (Buick, 2008). Intriguingly, the earliest microfossils of cyanobacteria date as early as 3.3-3.5 billion years ago, about 1 billion years before

the GOE (Sternberger et al., 1987). However, the O_2 from the first local oxygenated aquatic environments may not have ended up in the atmosphere for example due to the oxidation of Fe^{2+} of hydrothermal origin to iron oxides or reactions of O_2 with atmospheric CH_4 (Awramik, 1992; Canfield et al., 2006). The latter may have even caused the Huronian glaciation, the second of five glaciation periods of the earth (Kopp et al., 2005). Taken together, these events may explain the time delay between the first evolution of oxygenic photosynthesis and the GOE. Additionally, a most recent genomic comparison of cyanobacteria and closely related phyla dates the origin of cyanobacterial oxygenic photosynthesis relatively late in their evolution to about 2.5-2.6 billion years ago and supports a direct causation of oxygenic photosynthesis and the rise of O_2 in the atmosphere (Soo et al., 2017).

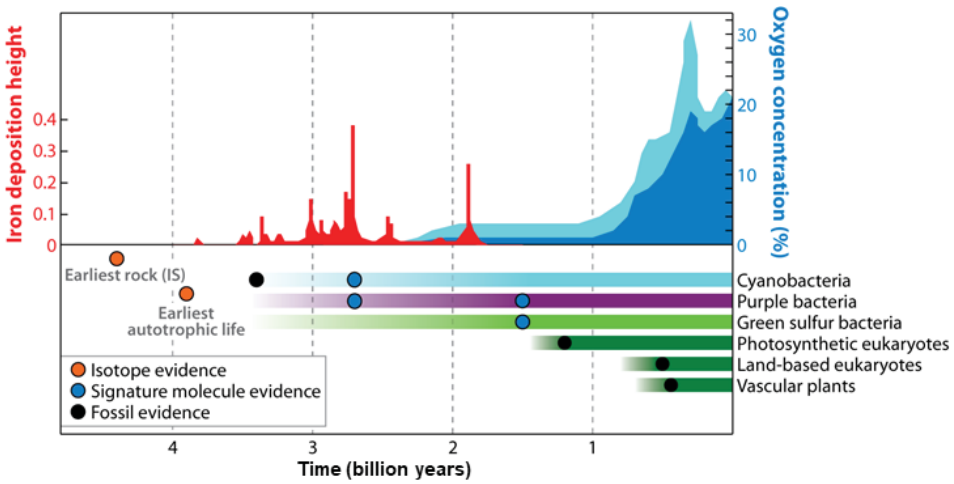

Figure 1: Evolution of photosynthesis in geological context. Precipitated iron oxides appear in sediments with the first evidence of autotrophic life before significant amounts of oxygen accumulate in the atmosphere (4-2 billion years before present). The evolution of photosynthetic eukaryotes and land-based plants is linked to the increase of atmospheric oxygen to today's concentration of 20%. Modified after Hohmann-Mariott and Blankenship (2011).

What is certain is that the changed composition of the atmosphere and oceans drastically changed the path of evolution. The evolution of oxygenic photosynthesis enabled the evolution of advanced life by promoting the formation of an ozone shield in the stratosphere protecting life from solar UV radiation (Blankenship, 1992) and by

changing the redox balance on earth (Hohmann-Marriott and Blankenship, 2011). The so far strictly anaerobic organisms were forced to either adapt to the increasing concentrations of O_2, become specialists to local anaerobic niches, or become extinct (Hohmann-Marriott and Blankenship, 2011). On the other hand, organisms which successfully adapted to the increased O_2 levels in their environment, benefited from an 18-times higher production of ATP per metabolic input (as hexose sugar) of aerobic compared to anaerobic metabolism (Dismukes et al., 2001) and eventually evolved the metabolic networks we know today.

In a second step, the oxygen concentration of the atmosphere raised to the current 20% (Figure 1), caused by the evolution of photosynthetic eukaryotes dating back about 1 billion years ago (Hohmann-Marriott and Blankenship, 2011). Phylogenetic analysis led to the conclusion that most likely all plastids from eukaryotic algae and plants originate from a single endosymbiotic event occurring about 1 to 1.5 billion years ago (Cavalier-Smith 2000; Weber *et al.* 2006), in which a eukaryotic, heterotrophic cell engulfed a free-living cyanobacterium but did not digest it (Chan & Bhattacharya 2010). The incorporation was followed by the establishment of an exchange system for fixed carbon starting a symbiotic relationship (Weber et al., 2006). Gene transfer from the cyanobacterium to the host cell nucleus finally resulted in cell organelle that today we call the chloroplast (Weber et al., 2006).

The Cyanobacterial Model Organism *Synechocystis sp.* PCC 6803

Nowadays, free-living cyanobacteria still account for 20-30% of the earth's primary photosynthetic production and are candidates for a variety of biotechnological applications. While the usefulness of cyanobacteria for biomass production is under debate, the use for the production of high value chemical compounds offers interesting economic opportunities (Cotton et al., 2015). These opportunities and cyanobacteria's

close relationship to the plastids of all eukaryotic phototrophs makes it an interesting research subject for photosynthetic research.

Cyanobacteria belong to the domain of prokaryotes but form a separate phylum as they possess chlorophyll a and perform oxygenic photosynthesis (Bryant, 1994; Ruggiero et al., 2015). For this instance, they were thought to be eukaryotic algae until electron microscopy and biochemical analysis could reveal this prospect (Bryant, 1994). The unicellular, freshwater cyanobacterium *Synechocystis* sp. PCC 6803 (*Synechocystis*) is the most popular model organism among the cyanobacteria. In contrast to plants, the thylakoid systems of *Synechocystis* form ring shaped structures inside and in close proximity to the plasma membrane (Figure 2 A). Several regions where the thylakoids converge towards the plasma membrane are visible on electron microscopic images (Figure 2 B). These regions are the so-called biogenesis or repair centers and are believed to be important during the assembly and repair of PSII (Stengel et al., 2012; Nickelsen and Rengstl, 2013; Heinz et al., 2016)

Synechocystis is a gram-negative bacterium and surrounded by an outer and a cytoplasmic membrane which border an intermembrane space called periplasm (Figure 2 C) (Al-Amoudi *et al.* 2004). Certain nutrients, for example Mn are known to be stored predominantly in the periplasm (Keren et al., 2002).

The complete genome of *Synechocystis* became available in 1996 (Kaneko et al., 1996; Kaneko and Tabata, 1997). The genome consists of a single chromosomal plasmid of approximately 3.5 mega base pairs (Mbp), containing roughly 3,000 protein coding genes (Kaneko et al., 1996). *Synechocystis* is highly polyploid and contains more than 200 genome copies in exponential phase and more than 50 in stationary phase (Griese et al., 2011). In comparison, the likewise unicellular salt-water species *Synechococcus* PCC 7942 contains about 3-4 genome copies, regardless of the growth phase. Besides the chromosomal plasmid, *Synechocystis* contains several smaller (2.3-5.2 kilo base

pairs, kbp) and larger (44-120 kbp) plasmids of different sizes (Kaneko et al., 2003). As the genes encoded on most plasmids are uncharacterized, their exact function remains unknown. However, 75% of the sequence of the 100 kbp plasmid pSYSA encode three different clustered regularly interspaced short palindromic repeats (CRISPR) systems, mediating antiviral defense (Kopfmann and Hess, 2013). The presence of seven simultaneously active toxin-antitoxin systems to ensure the maintenance of the plasmid through post-segregational killing mechanisms elucidates the importance of the plasmid (Kopfmann and Hess, 2013).

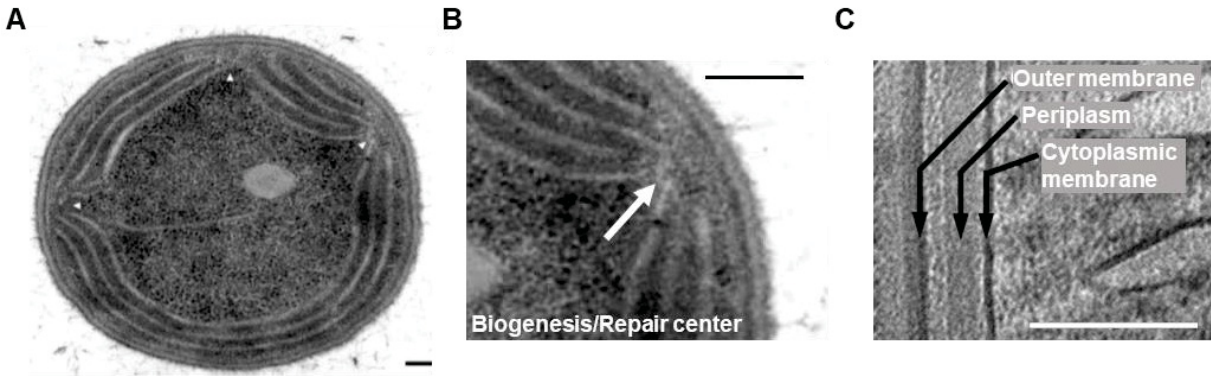

Figure 2: Electron microscopic images of *Synechocystis*. (A) The thylakoid membranes form ring shaped structures inside the plasma membrane. Triangles indicate the biogenesis or repair centers (taken from Heinz et al., 2016). (B) Close up of the biogenesis or repair center (arrow). These regions, where the thylakoid membranes are close to the plasma membrane are thought to be important for PSII biogenesis and repair (modified after Heinz et al., 2016). (C) Outer membrane and cytoplasmic membrane enclose and intermembrane space called the periplasm (modified after Al-Amoudi et al., 2004). Black scale bars are 200 nm, white scale bar is 100 nm.

Standard cultivation conditions for *Synechocystis* include moderate temperatures of around 30°C, light intensities of 60-100 µmol photons m^{-2} s^{-1}, and a pH of 7.5 in a defined medium called BG-11 (Rippka et al., 1979). The use of a defined medium allows the precise manipulation of the chemical environment the culture is facing. Protocols to delete (Hagemann and Zuther, 1992; Hagemann et al., 1997; Eisenhut et al., 2006) or overexpress (Lagarde et al., 2000) target genes are available and well established.

The Role of Manganese in Photosynthesis and Cell Function

For photoautotrophic organisms, performing oxygenic photosynthesis Mn is an essential nutrient. Mn serves as catalytically active metal, or fulfills an activating role for several proteins (Hänsch and Mendel, 2009). As described earlier, a cluster of four Mn ions is part of the OEC and catalyzes the water-splitting reaction to provide electrons for the photosynthetic electron reaction chain (Goussias et al., 2002). The four Mn ions provide four positive charges, which bind two H_2O molecules at the same time. The binding of two instead of one H_2O molecule allows the formation of O_2 instead of reactive oxygen species (ROS) (Millaleo et al., 2010). ROS are well known to cause oxidative damage to proteins, deoxyribonucleic acid (DNA) and lipids (Apel and Hirt, 2004).

In addition, Mn is part of the active site of enzymes such as Mn superoxide dismutase, Mn catalase, pyruvate carboxylase, phosphoenolpyruvate carboxykinase (Ducic and Polle, 2005), and acts as direct cofactor of a variety of enzymes (~35 in plants) (Burnell, 1988). Mn is also involved in ATP synthesis (Pfeffer et al., 1986), the reactions of Ribulose-1,5-bisphosphate carboxylase/oxygenase (RuBisCO) (Houtz et al., 1988), and the biosynthesis of fatty acids and proteins (Ness and Woolhouse, 1980). Given the manifoldness of cellular processes in which Mn plays a role, there are surprisingly few studies on the symptoms of Mn deficiency. This might be because Mn is needed in trace concentrations and it has been reported that for *Synechocystis* Mn concentrations as low as 100 nanomolar (nM) are sufficient for growth without any physiological effect (Salomon and Keren, 2011).

While low concentrations of Mn are beneficial and even essential for photosynthetic cells, high concentrations of Mn have negative impact on multiple cellular functions. Mn is known to compete with Fe for functional sites in the magnesium branch of tetrapyrrole biosynthesis and inhibits this pathway at the step of protoprophyrin IX

synthesis (Csatorday et al., 1984). Furthermore, the PSI reaction center proteins, PsaA and PsaB are less abundant when Mn is present in excess and PSI activity is impaired accordingly (Millaleo et al., 2013). Consequently, excess Mn is associated with reduced growth, reduced pigment content (chlorophyll a, b and carotenoids), as well as chlorotic and necrotic leaf areas in plants (Macfie and Taylor, 1992). Several authors also report a connection between excess Mn and photo-oxidative stress. Discussed mechanisms are the direct generation of ROS in a Fenton reaction (Lynch and St.Clair, 2004) or the disabling of antioxidant systems for example by ascorbate depletion of the chloroplast (Gonzalez et al., 1998).

It has become clear that photosynthetic organisms need to maintain their cellular Mn homeostasis carefully, in order to ensure sufficient Mn supply without accumulating toxic concentrations of Mn. While the Mn concentrations cyanobacteria face in their natural habitats are typically in the nM range (Chester and Stoner, 1974; Sunda and Huntsman, 1988; Sterner et al., 2004; Morel, 2008), plants growing in soils characterized as acidic – which are about 25% of the soils worldwide being used for agriculture – frequently face toxic concentrations of Mn (Lynch and St.Clair, 2004). In consequence, plants have evolved multiple tolerance strategies to address this challenge, whereas for cyanobacteria Mn tolerance mechanisms have not been described, yet.

Manganese Transport and Tolerance Strategies in Cyanobacteria and Plants

In cyanobacteria, Mn uptake through the outer membrane is mediated likely, similar to other gram negative bacteria, through specific porins (Public, 1985) and about 80% of the total cellular Mn content are stored in the periplasm (Keren et al., 2002). It is hypothesized that the membrane potential is involved in building up and maintaining this Mn-pool in a light-dependent manner (Keren et al., 2002) together with soluble Mn-binding proteins like MncA (Tottey et al., 2008). The tetratricopeptide repeat protein

PratA has been shown to mediate the capture of Mn^{2+} by a precursor of D1 in the periplasm (Stengel et al., 2012). This makes the biogenesis of PSII independent of intracellular Mn concentrations and transport activities. Active import into the cytoplasm is mediated by the high affinity ATP-binding cassette (ABC-) type transporter MntCAB (Bartsevich and Pakrasi, 1995; Bartsevich and Pakrasi, 1996). This transporter is expressed under starvation conditions to import Mn stored in the periplasmic storage in order to maintain normal cell activity (Bartsevich and Pakrasi, 1996; Keren et al., 2002). However, Mn uptake into the cytosol can be measured in *mntCAB* knockout lines demonstrating the presence of a second Mn import system, which is hypothesized to be highly specific and induced by µM amounts of Mn (Bartsevich and Pakrasi, 1996). Intracellular Mn transporter or Mn exporter are not known in cyanobacteria.

Since plants are multicellular organisms, the Mn transport network is more complex. The uptake of Mn from the soil to the chloroplast sink involves approximately 15 individual transport processes (Hell and Stephan, 2003). Similar to cyanobacteria, free Mn cations are absorbed from the rhizosphere by negatively charged cell wall constituents of the root cells (Clarkson, 1988; Humphires et al., 2007). The root protein LeGlp1 is thought to play an important role in this process because its N-terminal metal binding domain has been shown to bind Mn in transgenic tobacco (Takahashi and Sugiura, 2001). After active uptake into the root via the transport protein NRAMP1 (Cailliatte et al., 2010), Mn is transported through the xylem to the photosynthetic active tissues (Millaleo et al., 2010). Only a few Mn transporters are known inside the plant cell. The protein AtIRT1 is located in the plasma membrane and facilitates the import of Mn into the cell (Ducic & Polle 2005; Pittman 2005). AtECA1 and AtECA3 are transporting Mn into the endoplasmatic reticulum and into the Golgi apparatus, respectively (Mills et al., 2008). NRAMP3 as well as NRAMP4 are Mn transporters located in the vacuole membrane (Oomen et al., 2009). Interestingly, no homologs of MntCAB or other Mn transporters were found in chloroplasts (Shcolnick and Keren, 2006).

As a first barrier in their set of Mn tolerance mechanisms, plants limit Mn uptake by lowering metal uptake in general (Hall, 2002). On the cellular level, Mn is excreted via secretory pathway vesicles after import into the Golgi apparatus (Ducic and Polle, 2005). However, accumulation of Mn in the vacuole and the formation of insoluble complexes of Mn with phosphate (Dučić and Polle, 2007) or the formation and exudation of malate-Mn-complexes appears to be of greater relevance (Chen et al., 2015). Even though transport across different membranes is required for all of the described mechanisms, only a few manganese transport proteins are known in plants and none in the chloroplast. Identifying novel metal transport pathways relevant for photosynthesis are therefore of great significance from both an ecological and agricultural point of view and pose an intriguing scientific question (Shcolnick and Keren, 2006).

The GreenCut Protein Family UPF0016

In 2007, the complete genome of the unicellular green algae *Chlamydomonas rheinhardtii* (*Chlamydomonas)* became available (Merchant et al., 2007). Comparison of the 6968 protein families, which contain *Chlamydomonas* proteins, with the genomes of the also unicellular green algae *Ostreococcus*, the land plant *Arabidopsis thaliana* and the moss *Physcomitrella patens* revealed a set of 349 protein families which have a single *Chlamydomonas* protein but no proteins of non-photosynthetic organisms (Merchant et al., 2007). This set of proteins was named the GreenCut and is hypothesized to be enriched for proteins with important functions in or related to photosynthesis. In 2011, several newly sequenced genomes were included in the analysis. The extended set of GreenCut proteins now consists of 597 proteins and has been named GreenCut2 (Karpowicz et al., 2011). 83 proteins of the GreenCut2 are assigned to the functional category 'transport', from which 38 had no known function

assigned (Karpowicz et al., 2011). Members of the unknown protein family 0016 (UPF0016) are part of this list of 38 proteins.

Proteins belonging to UPF0016 are well conserved and can be found in all eukaryotes and many bacteria (Demaegd et al., 2014). In yeast, a member of UPF0016, the Gcr1-dependent translation factor1 (GDT1), has been characterized as Golgi-localized Ca^{2+} transporter and it has been proposed that members of UPF0016 function as secondary active cation/H^+ antiporter (Demaegd et al., 2013). Interestingly, Ca transporters also accept Mn as transport substrate frequently (Socha and Guerinot, 2014).

Members of UP0016 consist of two repeated domains with a highly conserved ExGD motif in the first of three predicted trans-membrane spans (Demaegd et al., 2013). The repeats are oriented in an antiparallel manner (Figure 3) (Demaegd et al., 2013), a feature commonly associated with secondary transporters (Vinothkumar and Henderson, 2010). The proteins are either encoded by one gene resulting in a homodimer, two genes resulting in a heterodimer, or one gene that has undergone an internal duplication encoding for a two-domain protein (Demaegd et al., 2014).

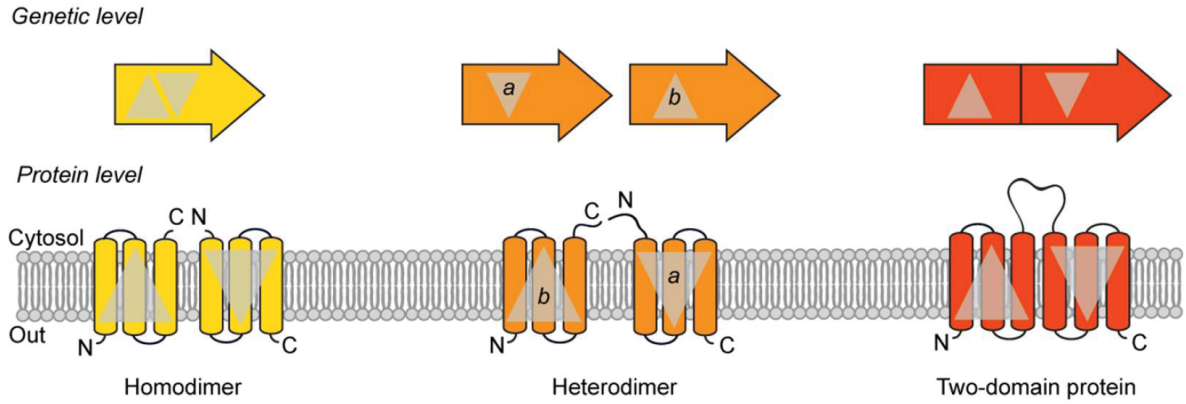

Figure 3: Illustration of the possible structures of members of UPF0016 on genetic and protein level. Evolutionary states of UPF0016 members on the genetic (top) and the protein (bottom) level. Top panel: Arrows indicate genes. Grey triangles and inverted triangles indicate the orientation of the encoded proteins in the membrane as up, down or dual. Bottom panel: Triangles indicate the UPF0016 proteins/domains with three trans-membrane spans each either in the up or down topology. Taken from Demaegd *et al.* (2014).

Aim of This Thesis

Oxygenic photosynthesis originated in cyanobacteria more than 3 billion years ago and has influenced evolution drastically. Nowadays, photosynthesis is widely accepted as the most important biological process on earth, providing the vast majority of the primary production on this planet. Thus, the integral understanding of photosynthesis is one of the key goals of humankind.

While the general mechanisms of photosynthesis are well understood, many aspects such as transport processes directly or indirectly involved in photosynthesis remain unidentified. The transition metal Mn is an important micronutrient for photosynthetic organisms but causes severe toxic effects when present in excess. In consequence, only a small window exists in which photosynthetic organisms need to maintain the cellular concentrations of Mn carefully. Nonetheless, a limited number of manganese transport proteins have been discovered in plants and none of these proteins localizes to the chloroplast. Due to their endosymbiotic relationship to the chloroplasts of all photosynthetic eukaryotes, cyanobacteria are an interesting tool for photosynthetic research. The unicellular, freshwater cyanobacterium *Synechocystis* sp. PCC 6803 is one of the most popular model organisms among the cyanobacteria due to its well-established cultivation protocols and the ability to knockout and overexpress specific genes of interest.

This thesis aims to identify novel manganese-transport proteins in *Synechocystis* to give insight into the intricate network of manganese homeostasis in cyanobacteria.

Analysis of transport proteins exclusively related to photosynthetic organisms (GreenCut2 ressource) revealed a promising candidate for metal transport in the cyanobacterium *Synechocystis* sp. PCC 6803. The protein Sll0615 is a member of the highly conserved unknown proteins family 0016, which shows features of secondary

transporters involved in metal transport. Hence, the characterization of Sll0615 was the inception of this thesis.

In the course of the work with Sll0615, two additional members of the unknown protein family 0016, the proteins Slr1170 and Ssr1558, have been identified as candidates for an additional transport protein involved in manganese homeostasis and were included in the analysis.

REFERENCES

Al-Amoudi A, Norlen LPO, Dubochet J (2004) Cryo-electron microscopy of vitreous sections of native biological cells and tissues". J Struct Biol **148**: 131–135

Apel K, Hirt H (2004) Reactive oxygen species: metabolism, oxidative stress, and signal transduction. Annu Rev Plant Biol **55**: 373–399

Awramik SM (1992) The oldest records of photosynthesis. Photosynth Res **33**: 75–89

Barber J (2003) Photosystem II: the engine of life. Q Rev Biophys **36**: 71–89

Bartsevich V V, Pakrasi HB (1995) Molecular identification of an ABC transporter complex for manganese : analysis of a cyanobacterial mutant strain impaired in the photosynthetic oxygen evolution process. EMBO J **14**: 1845–1853

Bartsevich V V, Pakrasi HB (1996) Manganese Transport in the Cyanobacterium *Synechocystis* sp . PCC 6803. J Biol Chem **271**: 26057–26061

Blankenship RE (1992) Origin and early evolution of photosynthesis. Photosynth Res **33**: 91–111

Bryant DA (1994) Advances in Photosynthesis - The Molecular Biology of Cyanobacteria.

Buick R (2008) When did oxygenic photosynthesis evolve? Philos Trans R Soc B Biol Sci **363**: 2731–2743

Burnell J (1988) The Biochemistry of Manganese in Plants. Manganese in Soils and Plants. pp 125–137

Cailliatte R, Schikora A, Briat J-F, Mari S, Curie C (2010) High-affinity manganese uptake by the metal transporter NRAMP1 is essential for Arabidopsis growth in low manganese conditions. Plant Cell **22**: 904–917

Canfield DE, Rosing MT, Bjerrum C (2006) Early anaerobic metabolisms. Philos Trans R Soc Lond B Biol Sci **361**: 1819-1834-1836

Cavalier-smith T (2000) Membrane heredity and early chloroplast evolution. Trends Plant Sci **5**: 174–182

Chan, C. X. & Bhattacharya D (2010) The origin of plastids. Nat Educ **3**: 84

Chen Z, Sun L, Liu P, Liu G, Tian J, Liao H (2015) Malate Synthesis and Secretion Mediated by a Manganese-Enhanced Malate Dehydrogenase Confers Superior Manganese Tolerance in Stylosanthes guianensis. Plant Physiol **167**: 176–88

Chester R, Stoner JH (1974) The distribution of zin, nickel, manganese, cadmium, copper, and iron in some surface waters from the world ocean. Mar Chem **2**: 17–32

Clarkson DT (1988) The Uptake and Translocation of Manganese by Plant Roots. Developments Plant Soil Sci **33**: 101–111

Cotton CAR, Douglass JS, De Causmaecker S, Brinkert K, Cardona T, Fantuzzi A, Rutherford AW, Murray JW (2015) Photosynthetic constraints on fuel from microbes. Front Bioeng Biotechnol **3**: 1–5

Csatorday K, Gombos Z, Szalontai B (1984) Mn^{2+} and Co^{2+} toxicity in chlorophyll biosynthesis. Proc Natl Acad Sci **81**: 476–478

Demaegd D, Colinet A-S, Deschamps A, Morsomme P (2014) Molecular Evolution of a Novel Family of Putative Calcium Transporters. PLoS One **9**: e100851

Demaegd D, Foulquier F, Colinet A-S, Gremillon L, Legrand D, Mariot P, Peiter E, Van Schaftingen E, Matthijs G, Morsomme P (2013) Newly characterized Golgi-localized family of proteins is involved in calcium and pH homeostasis in yeast and human cells. Proc Natl Acad Sci U S A **110**: 6859–64

Dismukes GC, Klimov V V, Baranov S V, Kozlov YN, Dasgupta J, Tyryshkin A (2001) The origin of atmospheric oxygen on Earth: The innovation of oxygenic photosynthesis. PNAS **98**: 2170–2175

Ducic T, Polle A (2005) Transport and detoxiification of manganese and copper in plants. Brazilian J Plant Physiol **17**: 103–112

Dučić T, Polle A (2007) Manganese toxicity in two varieties of Douglas fir (Pseudotsuga menziesii var. viridis and glauca) seedlings as affected by phosphorus supply. Funct Plant Biol **34**: 31–40

Eisenhut M, Kahlon S, Hasse D, Ewald R, Lieman-Hurwitz J, Ogawa T, Ruth W, Bauwe H, Kaplan A, Hagemann M (2006) The Plant-Like C2 Glycolate Cycle and the Bacterial-Like

Glycerate Pathway Cooperate in Phosphoglycolate Metabolism in Cyanobacteria. Plant Physiol **142**: 333–342

Gonzalez A, Steffen KL, Lynch JP (1998) Light and Excess Manganese - Implications for Oxidative Stress in Common Bean. Plant Physiol **118**: 493–504

Goussias C, Boussac A, Rutherford W (2002) Photosystem II and photosynthetic oxidation of water: an overview. Philos Trans R Soc Lond B Biol Sci **357**: 1369–1381

Griese M, Lange C, Soppa J (2011) Ploidy in cyanobacteria. FEMS Microbiol Lett **323**: 124–131

Hagemann M, Schoor A, Jeanjean R, Zuther E, Joset F (1997) The stpA gene from *Synechocystis* sp. strain PCC 6803 encodes the glucosylglycerol-phosphate phosphatase involved in cyanobacterial osmotic response to salt shock. J Bacteriol **179**: 1727–1733

Hagemann M, Zuther E (1992) Selection and characterization of mutants of the cyanobacterium *Synechocystis* sp. PCC 6803 unable to tolerate high salt concentrations. Arch Microbiol **158**: 429–434

Hall JL (2002) Cellular mechanisms for heavy metal detoxification and tolerance. J Exp Bot **53**: 1–11

Hänsch R, Mendel RR (2009) Physiological functions of mineral micronutrients (Cu, Zn, Mn, Fe, Ni, Mo, B, Cl). Curr Opin Plant Biol **12**: 259–66

Heinz S, Liauw P, Nickelsen J, Nowaczyk M (2016) Analysis of photosystem II biogenesis in cyanobacteria. Biochim Biophys Acta - Bioenerg **1857**: 274–287

Hell R, Stephan UW (2003) Iron uptake, trafficking and homeostasis in plants. Planta **216**: 541–551

Hohmann-Marriott MF, Blankenship RE (2011) Evolution of Photosynthesis. Annu Rev Plant Biol **62**: 515–548

Houtz RL, Nable RO, Cheniae GM (1988) Evidence for Effects on the in Vivo Activity of Ribulose-Bisphosphate Carboxylase/Oxygenase during Development of Mn Toxicity in Tobacco. Plant Physiol **86**: 1143–1149

Humphires J, Stangoulis J, Graham R (2007) Manganese. Handb. Plant Nutr. pp 351–366

Kaneko T, Nakamura Y, Sasamoto S, Watanabe A, Kohara M (2003) Structural Analysis of Four Large Plasmids Harboring in a Unicellular Cyanobacterium, *Synechocystis* sp . PCC 6803. DNA Res **228**: 221–228

Kaneko T, Sato S, Kotani H, Tanaka A, Asamizu E, Nakamura Y, Miyajima N, Hirosawa M, Sugiura M, Sasamoto S, et al (1996) Sequence analysis of the genome of the unicellular

cyanobacterium *Synechocystis* sp. strain PCC6803. II. Sequence determination of the entire genome and assignment of potential protein-coding regions. DNA Res **3**: 109–136

Kaneko T, Tabata S (1997) Complete Genome Structure of the Unicellular Cyanobacterium *Synechocystis* sp. PCC6803. Plant Cell Physiol **38**: 1171–1176

Karpowicz SJ, Prochnik SE, Grossman AR, Merchant SS (2011) The greenCut2 resource, a phylogenomically derived inventory of proteins specific to the plant lineage. J Biol Chem **286**: 21427–21439

Keren N, Kidd MJ, Penner-hahn JE, Pakrasi HB (2002) A Light-Dependent Mechanism for Massive Accumulation of Manganese in the Photosynthetic Bacterium Dynechocystis sp. PCC 6803. Biochemistry **41**: 15085–15092

Kopfmann S, Hess WR (2013) Toxin-antitoxin systems on the large defense plasmid pSYSA of synechocystis sp. pCC 6803. J Biol Chem **288**: 7399–7409

Kopp RE, Kirschvink JL, Hilburn I a, Nash CZ (2005) The Paleoproterozoic snowball Earth: A climate disaster triggered by the evolution of oxygenic photosynthesis. Proc Natl Acad Sci U S A **102**: 11131–6

Lagarde D, Beuf L, Vermaas W (2000) Increased Production of Zeaxanthin and Other Pigments by Application of Genetic Engineering Techniques to *Synechocystis* sp. Strain PCC 6803. Appl Environ Microbiol **66**: 63–72

Lynch JP, St.Clair SB (2004) Mineral stress: the missing link in understanding how global climate change will affect plants in real world soils. F Crop Res **90**: 101–115

Macfie S, Taylor G (1992) The effects of excess manganese on photosynthetic rate and concentration of chlorophyll in Triticum aestivum grown in solution culture. Plant Physiol **85**: 467–475

Martin W, Weiss M, Neukirchen S, Nelson-Sathi S, Sousa F (2016) Physiology, phylogeny, and LUCA. Microb Cell **3**: 451–456

Merchant SS, Prochnik SE, Vallon O, Harris EH, Karpowicz SJ, Witman GB, Terry A, Salamov A, Fritz-Laylin LK, Maréchal-Drouard L, et al (2007) The *Chlamydomonas* genome reveals the evolution of key animal and plant functions. Science (80-) **318**: 245–250

Millaleo R, Ivanov AG, Mora ML, Alberdi M (2010) Manganese as Essential and Toxic Element for Plant: Transport, Accumulation and Resistance Mechanisms. Journale Soil Sci Plant Nutr.ition **10**: 476–494

Millaleo R, Reyes-Díaz M, Alberdi M, Ivanov AG, Krol M, A HNP (2013) Excess manganese differentially inhibits photosystem I versus II in *Arabidopsis thaliana*. J Exp Bot **64**: 343–354

Mills RF, Doherty ML, López-Marqués RL, Weimar T, Dupree P, Palmgren MG, Pittman JK, Williams LE (2008) ECA3, a Golgi-localized P2A-type ATPase, plays a crucial role in manganese nutrition in *Arabidopsis*. Plant Physiol **146**: 116–28

Morel FMM (2008) The co-evolution of phytoplankton and trace element cycles in the oceans. Geobiology **6**: 318–324

Ness PJ, Woolhouse HW (1980) RNA Synthesis in Phaseolus Chloroplasts. **31**: 235–245

Nickelsen J, Rengstl B (2013) Photosystem II assembly: from cyanobacteria to plants. Annu Rev Plant Biol **64**: 609–635

Oomen RJFJ, Wu J, Lelièvre F, Blanchet S, Richaud P, Barbier-Brygoo H, Aarts MGM, Thomine S (2009) Functional characterization of NRAMP3 and NRAMP4 from the metal hyperaccumulator *Thlaspi caerulescens*. New Phytol **181**: 637–650

Pfeffer PE, Tu SI, Gerasimowicz W V, Cavanaugh JR (1986) In vivo ^{31}P NMR studies of corn root tissue and its uptake of toxic metals. Plant Physiol **80**: 77–84

Pittman JK (2005) Managing the manganese: molecular mechanisms of manganese transport and homeostasis. New Phytol **167**: 733–742

Public N (1985) Molecular Basis of Bacterial Outer Membrane Permeability. **49**: 1–32

Rappaport F, Guergova-kuras M, Nixon PJ, Diner BA, Lavergne J, Rappaport F, Guergova-kuras M, Nixon PJ, Diner BA (2002) Kinetics and Pathways of Charge Recombination in Photosystem II Kinetics and Pathways of Charge Recombination in Photosystem II. Biochemistry **41**: 8518–8527

Rippka R, Deruelles J, Waterbury JB, Herdman M, Stanier RY (1979) Generic Assignments, Strain Histories and Properties of Pure Cultures of Cyanobacteria. J Gen Microbiol **111**: 1–61

Ruggiero MA, Gordon DP, Orrell TM, Bailly N, Bourgoin T, Brusca RC, Cavalier-Smith T, Guiry MD, Kirk PM (2015) A higher level classification of all living organisms. PLoS One **10**: 1–60

Salomon E, Keren N (2011) Manganese limitation induces changes in the activity and in the organization of photosynthetic complexes in the cyanobacterium *Synechocystis* sp. strain PCC 6803. Plant Physiol **155**: 571–9

Shcolnick S, Keren N (2006) Metal Homeostasis in Cyanobacteria and Chloroplasts . Balancing Benefits and Risks to the Photosynthetic Apparatus. Plant Physiol **141**: 805–810

Socha AL, Guerinot M Lou (2014) Mn-euvering manganese: the role of transporter gene family members in manganese uptake and mobilization in plants. Front Plant Sci **5**: 106

Soo RM, Hemp J, Parks DH, Fischer WW, Hugenholtz P (2017) On the origins of oxygenic photosynthesis and aerobic respiration in Cyanobacteria. Science (80-) **355**: 1436–1440

Stengel A, Gügel IL, Hilger D, Rengstl B, Jung H, Nickelsen J (2012) Initial steps of photosystem II de novo assembly and preloading with manganese take place in biogenesis centers in *Synechocystis*. Plant Cell **24**: 660–675

Sternberger A, Harwell W, Hockfield S, Johansen J, Frederiksen K, Mckav R, Zipursky SL, Benzer S, Ferrus A, Lee MC, et al (1987) Early Archean (3.3-Billion to 3.5-Billion-Year-Old) Microfossils from Warrawoona Group, Australia. Science (80-) **237**: 70–73

Sterner RW, Smutka TM, McKay RML, Xiaoming Q, Brown ET, Sherrell RM (2004) Phosphorus and trace metal limitation of algae and bacteria in Lake Superior. Limnol Oceanogr **49**: 495–507

Sunda WG, Huntsman SA (1988) Effect of sunlight on redox cycles of manganese in the southwestern Sargasso Sea. Deep Sea Res Part A, Oceanogr Res Pap **35**: 1297–1317

Takahashi M, Sugiura M (2001) Strategies for uptake of a soil micronutrient, manganese, by plant roots. RIKEN Rev 76–77

Tottey S, Waldron KJ, Firbank SJ, Reale B, Bessant C, Sato K, Cheek TR, Gray J, Banfield MJ, Dennison C, et al (2008) Protein-folding location can regulate manganese-binding versus copper- or zinc-binding. Nature **455**: 1138–42

Vinothkumar KR, Henderson R (2010) Structures of membrane proteins. Q Rev Biophys. doi: 10.1017/S0033583510000041

Weber APM, Linka M, Bhattacharya D (2006) Single, Ancient Origin of a Plastid Metabolite Translocator Family in Plantae from an Endomembrane-Derived Ancestor. Eukaryot Cell **5**: 609–612

Zouni A, Witt H-T, Kern J, Fromme P, Krauss N, Saenger W, Orth P (2001) Crystal structure of photosystem II from *Synechococcus elongatus* at 3.8 A resolution. Nature **409**: 739–743

Manuscript I

The *Synechocystis* Manganese Exporter Mnx Is Essential for Manganese Homeostasis in Cyanobacteria

The *Synechocystis* Manganese Exporter Mnx Is Essential for Manganese Homeostasis in Cyanobacteria[1]

Fabian Brandenburg, Hanan Schoffman, Samantha Kurz, Ute Krämer, Nir Keren, Andreas P. M. Weber, and Marion Eisenhut

Institute of Plant Biochemistry, Cluster of Excellence on Plant Science, Heinrich Heine University, 40225 Duesseldorf, Germany (F.B., S.K., A.P.M.W., M.E.); Department of Plant and Environmental Sciences, Institute of Life Sciences, Hebrew University of Jerusalem, 91904 Jerusalem, Israel (H.S., N.K.); and Department of Plant Physiology, Ruhr University, 44801 Bochum, Germany (U.K.)

ORCID IDs: 0000-0002-5910-765X (F.B.); 0000-0002-6853-1399 (S.K.); 0000-0001-7870-4508 (U.K.); 0000-0003-0970-4672 (A.P.M.W.); 0000-0002-2743-8630 (M.E.).

The essential micronutrient manganese (Mn) functions as redox-active cofactor in active sites of enzymes and, thus, is involved in various physiological reactions. Moreover, in oxygenic photosynthetic organisms, Mn is of special importance, since it is central to the oxygen-evolving complex in photosystem II. Although Mn is an essential micronutrient, increased amounts are detrimental to the organism; thus, only a small window exists for beneficial concentrations. Accordingly, Mn homeostasis must be carefully maintained. In contrast to the well-studied uptake mechanisms in cyanobacteria, it is largely unknown how Mn is distributed to the different compartments inside the cell. We identified a protein with so far unknown function as a hypothetical Mn transporter in the cyanobacterial model strain *Synechocystis* sp. PCC 6803 and named this protein Mnx for Mn exporter. The knockout mutant Δ*mnx* showed increased sensitivity toward externally supplied Mn and Mn toxicity symptoms, which could be linked to intracellular Mn accumulation. ^{54}Mn chase experiments demonstrated that the mutant was not able to release Mn from the internal pool. Microscopic analysis of a Mnx::yellow fluorescent protein fusion showed that the protein resides in the thylakoid membrane. Heterologous expression of *mnx* suppressed the Mn-sensitive phenotype of the *Saccharomyces cerevisiae* mutant Δ*pmr1*. Our results indicate that Mnx functions as a thylakoid Mn transporter and is a key player in maintaining Mn homeostasis in *Synechocystis* sp. PCC 6803. We propose that Mn export from the cytoplasm into the thylakoid lumen is crucial to prevent toxic cytoplasmic Mn accumulation and to ensure Mn provision to photosystem II.

The transition metal manganese (Mn) plays a vital role in multiple cellular processes (Hänsch and Mendel, 2009). Mn is either part of the active site or serves as an activator for approximately 35 different enzymes (Hebbern et al., 2009). Important Mn-dependent enzymes include Mn-superoxide dismutase and Mn-catalase (Hänsch and Mendel, 2009), which serve in the detoxification of reactive oxygen species (ROS). Mn also is of central importance in carbohydrate, lipid, and lignin biosynthesis (Tobergte and Curtis, 2012). In oxygenic photosynthetic organisms, the most prominent role of Mn is in the oxygen-evolving complex (OEC) of PSII, where Mn is incorporated into a Mn_4O_5Ca cluster that mediates the splitting of water into oxygen, protons, and electrons (Nelson and Junge, 2015). While the oxygen is released, the extracted electrons are fed into the photosynthetic electron transfer chain. Thus, limited intracellular Mn content leads to a reduction of photosynthesis and growth (Salomon and Keren, 2011). However, despite its vital importance in cellular metabolism, Mn in excess amounts also can cause detrimental effects. Several Mn toxicity mechanisms are discussed, including the direct generation of ROS in a Fenton-like reaction mediated by free Mn^{2+} ions or the competition of Mn with other metal ions for incorporation into the active site of enzymes, thus changing their activity (Lynch and St. Clair, 2004). To ensure sufficient Mn supply for cellular needs while avoiding toxic overaccumulation at the same time, cellular Mn homeostasis needs to be carefully maintained, especially in oxygenic photosynthetic organisms.

In the cyanobacterium *Synechocystis* sp. PCC 6803 (hereafter *Synechocystis*), the biological role and regulation of Mn homeostasis has been partially investigated. Keren et al. (2002) demonstrated that cyanobacterial

[1] This work was supported by the German Science Foundation (grant no. EI 945/3-1 to M.E., grant no. KR 1967/3-3 to U.K., and grant no. EXC 1028 to A.P.M.W) and the Israeli Science Foundation (grant no. 2733/16 to N.K.).

*Address correspondence to m.eisenhut@uni-duesseldorf.de.

The author responsible for distribution of materials integral to the findings presented in this article in accordance with the policy described in the Instructions for Authors (www.plantphysiol.org) is: Marion Eisenhut (m.eisenhut@uni-duesseldorf.de).

F.B., M.E., N.K., and A.P.M.W. designed the study; F.B., M.E., S.K., and H.S. carried out laboratory experiments; F.B., M.E., N.K., U.K., and A.P.M.W. interpreted the data; F.B. and M.E. wrote the article; N.K., U.K., S.K., H.S., and A.P.M.W. edited and approved the article.

www.plantphysiol.org/cgi/doi/10.1104/pp.16.01895

Downloaded from www.plantphysiol.org on March 23, 2017 - Published by www.plantphysiol.org
Copyright © 2017 American Society of Plant Biologists. All rights reserved.

cells contain two separate Mn pools. Up to 80% of the cellular content accumulates in the periplasmic space, probably attached to the outer membrane or bound to soluble Mn-binding proteins, such as MncA (Tottey et al., 2008). The cytoplasm was found to contain only small amounts of Mn (Keren et al., 2002). That is, the periplasm serves as an Mn storage site from where the metal is mobilized upon demand. Either Mn is imported into the cytoplasm by active transport or preloaded into PSII directly from the periplasm. The active import into the cytoplasm is mediated by the high-affinity ATP-binding cassette (ABC)-type transporter MntCAB (Bartsevich and Pakrasi, 1995, 1996), which is active only under Mn limitation conditions to provide sufficient Mn supply for cell function. The presence of a second, constitutively active but lower-affinity Mn importer in the plasma membrane also was suggested (Bartsevich and Pakrasi, 1996). Possibly, iron (Fe) transporters, such as FutABC, catalyze the transport of Mn by a piggybacking mechanism and, thus, are responsible for the constitutive Mn uptake (Sharon et al., 2014). Along with its functionality, expression of the *mntCAB* operon is under the control of a two-component regulatory system and only transcribed under Mn-limiting conditions (Ogawa et al., 2002; Yamaguchi et al., 2002). The environmental Mn availability is monitored by the Mn sensor ManS. It functions as a sensory His kinase that binds Mn^{2+} ions under Mn-sufficient conditions, autophosphorylates, and then activates the response regulator ManR by phosphorylation. In its phosphorylated state, ManR represses transcription of the *mntCAB* operon (Ogawa et al., 2002; Yamaguchi et al., 2002). Preloading of PSII with Mn^{2+} ions was demonstrated recently to be mediated by PratA, a tetratricopeptide repeat protein (Stengel et al., 2012). Since this step takes place in biogenesis centers at the cell periphery, it is assumed that Mn is loaded directly from periplasmic storage into PSII (Stengel et al., 2012) independently of internal Mn concentrations and transport activities.

In contrast to the knowledge about Mn import and its regulation, the mechanisms for managing intracellular Mn homeostasis and distribution are largely unknown in cyanobacteria. For example, intracellular Mn-binding proteins or Mn exporters have not been revealed so far. In this study, we identified and characterized a thylakoid membrane protein that is important for the export of Mn and named the protein Mnx. By the generation and characterization of a knockout mutant and overexpression line, we demonstrate that the maintenance of intracellular Mn homeostasis is highly important in *Synechocystis* and that Mnx plays a central role in Mn management. According to our results, we present a model in which Mnx is critical for mitigating cytoplasmic Mn accumulation and the provision of Mn to the OEC, thus maintaining efficient photosynthesis.

RESULTS

Identification of a Candidate Mn Transporter

Since Mn is of central importance especially in all organisms performing oxygenic photosynthesis, we assumed that the transport protein should be conserved throughout cyanobacteria, algae, and land plants. Thus, to search for a candidate Mn exporter, we explored the inventory of the so-called GreenCut2, which comprises a set of all proteins that are encoded in the genomes of Viridiplantae (green algae and land plants) but not in or highly diverged in the genomes of nonphotosynthetic organisms (Karpowicz et al., 2011). Among the 597 GreenCut proteins in the green alga *Chlamydomonas reinhardtii*, which is used as a reference organism for the GreenCut, 83 proteins are assigned to the functional category transport, 45 with known and 38 with unknown functions (Karpowicz et al., 2011). We concentrated only on those proteins that were predicted to localize to the chloroplast in Viridiplantae, were of unknown function, and were strictly conserved, meaning encoded in at least 95% (at least 35 of 37 analyzed genomes; Karpowicz et al., 2011) of the analyzed cyanobacterial genomes. The final set of five transport proteins (Supplemental Table S1) contained the protein CPLD63, which belongs to the unknown protein family 0016 (UPF0016). This GreenCut protein seemed to be a promising candidate, since another member of UPF0016, the Gcr1-dependent translation factor1 (GDT1), was proposed to function as a Golgi-localized Ca^{2+}/H^{+} antiporter in yeast (*Saccharomyces cerevisiae*; Demaegd et al., 2013), and Ca^{2+}-transporting systems are known to frequently also accept Mn^{2+} as a substrate (Socha and Guerinot, 2014). The *Synechocystis* genome contains the gene *sll0615*, encoding an orthologous protein to CPLD63. Thus, we selected Sll0615 as a candidate protein to test for Mn export function in the cyanobacterium and designated Sll0615 as Mnx.

Deletion of Mnx Results in Sensitivity toward Externally Supplied Mn

To test the function of Mnx, we generated a *Synechocystis* mutant line, Δ*mnx*, by insertional inactivation (Fig. 1A). Full segregation of the Δ*mnx* mutant line and the complete loss of *mnx* transcripts (Fig. 1, B and C) demonstrated that Mnx was not essential under the standard conditions used. Additionally, we generated a complementation line, Δ*mnx/OEX*, in which the expression of *mnx* is under the control of the strong *psbAII* promoter (Lagarde et al., 2000) in the Δ*mnx* mutant background (Fig. 1, A and B). According to real-time quantitative PCR (RT-qPCR) analysis, the abundance of *mnx* transcript was 7-fold elevated in the Δ*mnx/OEX* line compared with the wild type (Fig. 1C). Therefore, this line was considered as both a complementation line and an overexpression line.

We hypothesized that Mnx functions as an Mn exporter. Thus, we tested the mutant for sensitivity toward externally supplied Mn. When we treated the cells with increasing Mn concentrations, we observed that the Δ*mnx* mutant was not able to grow on BG11 medium with elevated Mn concentration (Fig. 2A). The commonly used BG11 medium (Rippka et al., 1979) contains 9 μM $MnCl_2$. At this concentration and on medium without $MnCl_2$ (0 μM), wild-type and Δ*mnx* cells grew comparably

Downloaded from www.plantphysiol.org on March 23, 2017 - Published by www.plantphysiol.org
Copyright © 2017 American Society of Plant Biologists. All rights reserved.

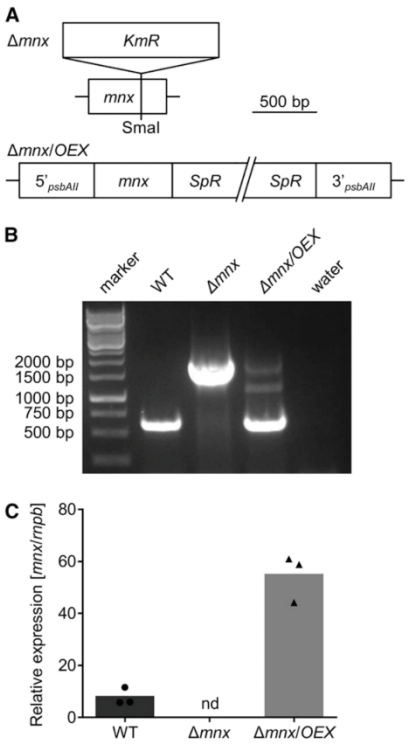

Figure 1. Generation of *mnx* knockout and overexpression lines. A, The knockout mutant Δ*mnx* was generated by insertion of a kanamycin resistance cassette (*KmR*) into the coding sequence of the *mnx* gene at the unique *Sma*I restriction site. The overexpression line Δ*mnx*/*OEX* was generated by reintroducing *mnx* under the control of the strong *psbAII* promoter into the genetic background of Δ*mnx*. Using homologous recombination, *mnx* was integrated into the *psbAII* locus. For selection, a gene encoding a spectinomycin resistance cassette (*SpR*) was included. B, The genotypes of the mutants were verified by PCR using gene-specific primers for amplification of *mnx*. Water was used as a negative control. WT, Wild type. C, The transcript abundance of *mnx* was analyzed by RT-qPCR. nd, Not detectable.

well. However, in response to a slightly increased concentration of 12.5 μM $MnCl_2$, growth of the mutant was retarded, while higher concentrations of $MnCl_2$ resulted in a lethal phenotype of the Δ*mnx* mutant. The rescued growth of the Δ*mnx/OEX* line proved that the Mn sensitivity was indeed caused by the loss of Mnx and not by any secondary mutation (Fig. 2A). We also tested the sensitivity toward additional divalent transition metals, since Mn transporters are known at least in plants as being promiscuous for their substrates (Socha and Guerinot, 2014). Growth of the Δ*mnx* mutant was not distinguishable from that of the wild type in response to 12.5-fold elevated concentrations of Ca^{2+} ions or 3-fold Fe^{2+}, Cu^{2+}, Zn^{2+}, and Co^{2+} ions in the BG11 medium (Fig. 2B). Also, the addition of Cd^{2+} or Ni^{2+} ions, which are not contained in standard BG11 medium, did not affect the growth of the Δ*mnx* mutant. The dose-dependent and metal-specific phenotype observed here provided, to our knowledge, the first indications that Mnx conveys resistance to elevated Mn amounts, likely by a specific export of Mn.

The Δ*mnx* Mutant Shows Symptoms of Mn Toxicity

The Mn-dependent phenotype of the mutant was studied in more detail. To implement Mn limitation conditions, we precultivated all lines in BG11 medium without Mn. Mn depletion for 5 d did not restrict growth or chlorophyll content in any strain (Fig. 3, A–C). After preincubation, the cultures were supplemented with either 9 or 150 μM $MnCl_2$ to apply standard or high Mn concentrations (Fig. 3, B and C). As a control, the Mn limitation conditions were continued (Fig. 3A). Application of both 0 and 9 μM $MnCl_2$ did not affect the growth and chlorophyll amounts in either culture (Fig. 3, A and B; Supplemental Fig. S1, A and B). However, after the addition of 150 μM $MnCl_2$, growth of the Δ*mnx* mutant was impaired and also chlorophyll amounts decreased significantly (Fig. 3C; Supplemental Fig. S1, A and B). The negative effect of the high-Mn treatment on Δ*mnx* cells was additionally reflected by strongly reduced photosynthetic activity, as indicated by reduced oxygen evolution (Fig. 3D). Under Mn-depleted conditions, oxygen evolution was not significantly different between the lines. However, 4 h after the addition of 9 μM $MnCl_2$, oxygen evolution was reduced significantly by 30%, and 4 h after the addition of 150 μM $MnCl_2$, it was reduced significantly by 70% (Fig. 3D). In contrast, the overexpression line Δ*mnx/OEX* showed a significant increase in photosynthesis 4 h after the addition of 9 μM $MnCl_2$ or 150 μM $MnCl_2$ compared with the wild type (Fig. 3C). Importantly, the significant difference between the wild type and the overexpression line results from a decrease in the activity of the wild type with increasing concentration of Mn but not from an increase in photosynthesis of the overexpression line (Fig. 3D). The detrimental effect of 150 μM $MnCl_2$ on the growth of Δ*mnx* cells is shown in Figure 3E.

The Δ*mnx* Mutant Mounts a High-Light-Sensitive Phenotype

The observation that photosynthetic activity was affected after the addition of $MnCl_2$ in the Δ*mnx* mutant prompted us to investigate the inhibition mechanism in more detail. We did not observe significantly reduced photosynthetic activity under Mn depletion (Fig. 3D) and, thus, expected that the negative effect of Mn in the Δ*mnx* mutant was not due to reduced incorporation of Mn into de novo assembled PSII but rather was caused by Mn-dependent effects on the photosynthesis apparatus. To test this hypothesis, we analyzed the lines at standard Mn concentrations (9 μM) but two different light intensities. Our standard growth light conditions were 100 μmol photons m^{-2} s^{-1}. For high-light conditions,

Downloaded from www.plantphysiol.org on March 23, 2017 - Published by www.plantphysiol.org
Copyright © 2017 American Society of Plant Biologists. All rights reserved.

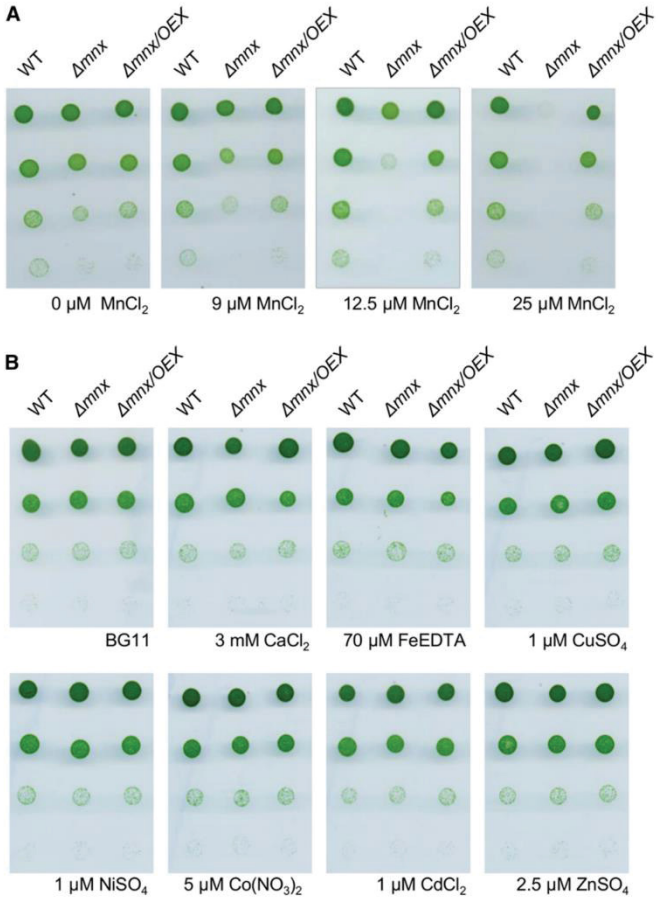

Figure 2. Sensitivity of *Synechocystis* wild type (WT), Δ*mnx* mutant, and Δ*mnx/OEX* line toward divalent transition metals. Cells of the mid log phase were diluted to an optical density at 750 nm (OD_{750}) of 0.25. Two microliters of these cultures and subsequent 1:10, 1:100, and 1:1,000 dilutions were spotted onto BG11 plates supplemented with different transition metals as indicated. Photographs were taken after incubation for 4 d. A, Growth of cells on BG11 medium containing 0, 9, 12.5, or 25 μM $MnCl_2$. Nine micromolar is the standard concentration of $MnCl_2$ in BG11 medium. B, Growth of cells on BG11 medium containing elevated levels of divalent transition metals. The concentrations were 12.5-fold elevated for Ca^{2+} and 3-fold elevated for Fe^{2+}, Cu^{2+}, Zn^{2+}, and Co^{2+} ions compared with standard BG11 medium. Additionally, Cd^{2+} and Ni^{2+} ions were tested, which are not contained in standard BG11 medium.

the cultures were exposed to a light intensity of 1,000 μmol photons m^{-2} s^{-1}. Similar to the results of the Mn treatment (Fig. 3), Δ*mnx* was impaired significantly in growth and chlorophyll content under high-light conditions (Fig. 4, A and B; Supplemental Fig. S1, C and D). Also, the photosynthetic activity in the Δ*mnx* mutant was reduced significantly after 4 h of high-light treatment (Fig. 4C). To distinguish whether photoinhibition or recovery was changed due to the lack of Mnx, all three lines were first incubated in BG11 medium containing the standard 9 μM $MnCl_2$ under high-light conditions for 45 min and then shifted back to standard growth light conditions. Oxygen evolution was measured to determine photosynthetic activity. While the photoinactivation rate was comparable between the wild type, the Δ*mnx* mutant, and the Δ*mnx/OEX* line (Fig. 4D), the recovery time was increased significantly for Δ*mnx*. The mutant needed 2.7 times longer to recover to 50% of its initial photosynthetic rate (Fig. 4E). The detrimental effect of 1,000 μmol photons m^{-2} s^{-1} on the growth of Δ*mnx* cells is shown in Figure 4F.

Lack of Mnx Leads to an Increased Intracellular Mn Pool

Both reduced chlorophyll accumulation (Csatorday et al., 1984; Clairmont et al., 1986) and photosynthetic activity (Millaleo et al., 2013) were described earlier as typical symptoms of critical Mn accumulation in oxygenic photosynthetic organisms. To investigate whether the observed phenotype of the Δ*mnx* mutant was caused by Mn accumulation, we quantified the cellular Mn amounts. The intracellular Mn pools were reduced strongly after 5 d of Mn depletion treatment and not significantly different between the three lines (Fig. 5). Significant overaccumulation (3-fold) in the intracellular Mn pool was observed specifically for the Δ*mnx* mutant after Mn addition, while the intracellular Mn levels of the Δ*mnx/OEX*

Downloaded from www.plantphysiol.org on March 23, 2017 - Published by www.plantphysiol.org
Copyright © 2017 American Society of Plant Biologists. All rights reserved.

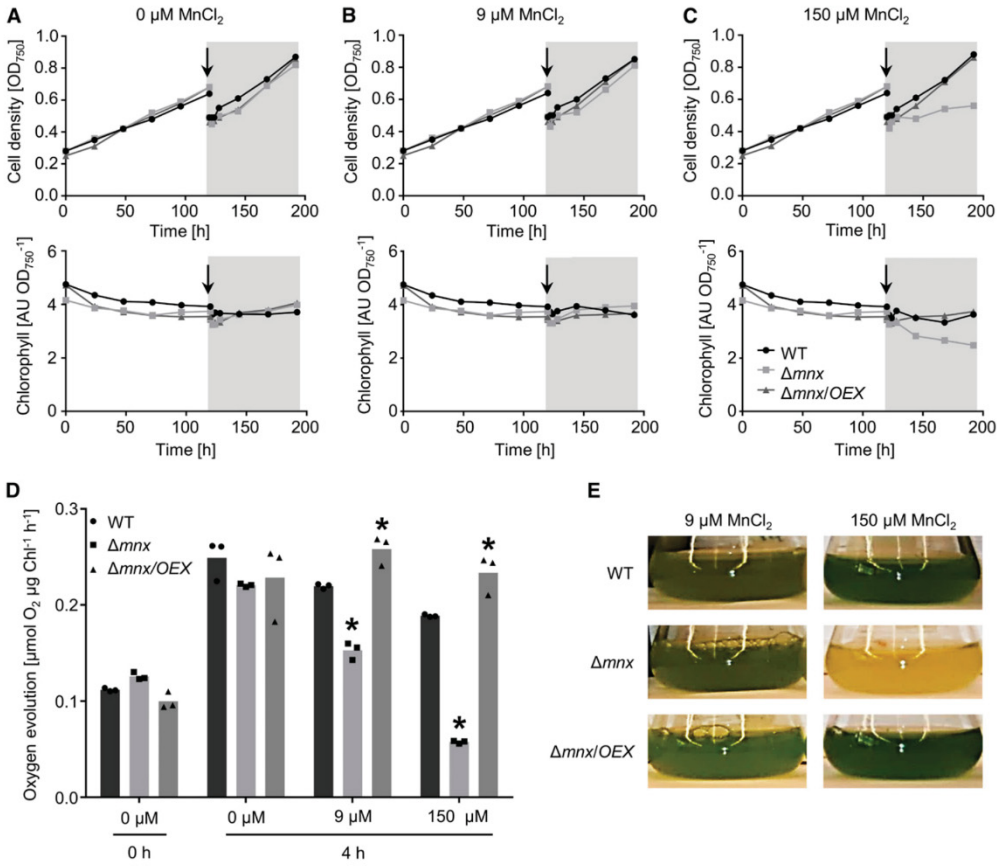

Figure 3. Effects of Mn treatment on physiological parameters of the wild type (WT), Δ*mnx* mutant, and Δ*mnx/OEX* line. A to C, During the first 5 d, the cultures were grown in Mn-free medium (white areas). For the remaining 3 d, the cultures were diluted and treated with 0 μM (A), 9 μM (B), or 150 μM (C) $MnCl_2$. Growth (top row) and chlorophyll content (bottom row) were monitored over a time course of 8 d. The addition of $MnCl_2$ is indicated with the arrows and the gray areas. One representative result of four independent experiments is shown. D, Before (0 h) and 4 h after treatment, additional samples were taken for oxygen evolution measurements. Values shown are means of three independent experiments. Asterisks indicate significant changes to the respective wild-type value according to a two-way ANOVA ($P \leq 0.05$). E, Mn-dependent lethal phenotype of the Δ*mnx* mutant. Shown are photographs of the cultures after 3 d of growth in BG11 medium containing 9 or 150 μM $MnCl_2$. AU, Arbitrary units.

line and the wild type were equal (Fig. 5). Thus, the intracellular Mn levels provided further evidence that Mnx is involved in Mn export out of the cell.

Loss of Intracellular ^{54}Mn Is Impaired in the Δ*mnx* Mutant

To examine whether, in fact, the export was affected by the loss of *mnx*, we performed in vivo ^{54}Mn chase experiments (Fig. 6). After the cells had been incubated for 3 d in BG11 medium supplemented with ^{54}Mn, which allowed the incorporation of ^{54}Mn into internal pools and into proteins, cells were washed and further cultivated in BG11 medium without the radioactive isotope. During the whole experiment, the final concentration of $MnCl_2$ was kept constantly at the standard 9 μM. In all three lines, the intracellular signal of the radioactive ^{54}Mn isotope declined most strongly within the first 30 min. However, the ^{54}Mn contents in the Δ*mnx* mutant stably remained at 80% of the starting amount. In contrast, wild-type and Δ*mnx/OEX* cells displayed a monotonous decrease of the radioactive signal. The decrease of ^{54}Mn in wild-type and Δ*mnx/OEX* cells was significantly higher throughout the whole experiment in comparison with the Δ*mnx* mutant, with a total loss of ~80% of the

Downloaded from www.plantphysiol.org on March 23, 2017 - Published by www.plantphysiol.org
Copyright © 2017 American Society of Plant Biologists. All rights reserved.

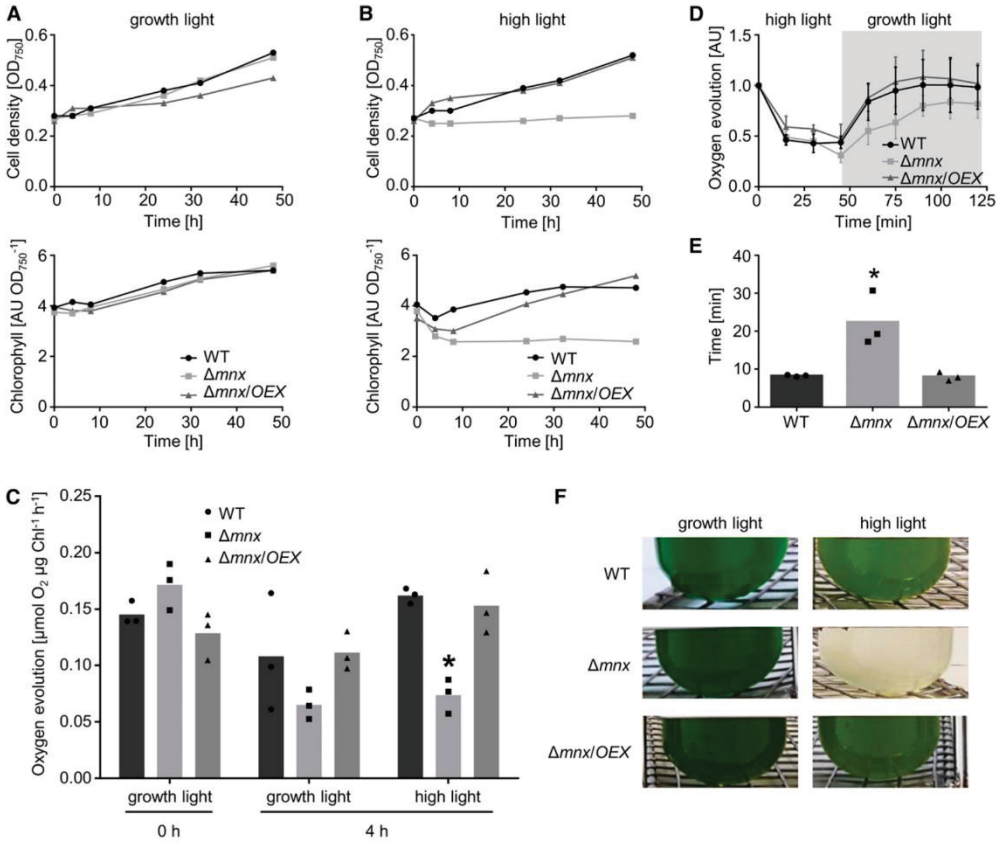

Figure 4. Effects of high-light treatment on physiological parameters of the wild type (WT), Δ*mnx* mutant, and Δ*mnx/OEX* line. A and B, The cultures were grown either under standard growth light (100 μmol photons m^{-2} s^{-1}; A) or high-light (1,000 μmol photons m^{-2} s^{-1}; B) conditions. Growth (top row) and chlorophyll content (bottom row) were monitored over a time course of 48 h. C, Additional samples were taken before (0 h) and 4 h after exposure to growth light and high-light conditions, respectively, for oxygen evolution measurements. Values shown are means of three independent experiments. D, For photoinhibition and recovery studies, cultures were shifted to high-light (1,000 μmol photons m^{-2} s^{-1}; white area) conditions. After 45 min, the cultures were shifted back to 100 μmol photons m^{-2} s^{-1} (gray area) and the recovery of photosynthetic activity was monitored. Means and SD of three independent experiments are shown as the oxygen evolution relative to the corresponding time point 0 min for each line. E, The time that each culture needs for one-half-maximal recovery was calculated from D. F, The high-light-dependent lethal phenotype of the Δ*mnx* mutant. Shown are photographs of the cultures after 48 h of growth under growth light (100 μmol photons m^{-2} s^{-1}) or high-light (1,000 μmol photons m^{-2} s^{-1}) conditions. Asterisks indicate significant changes to wild-type values according to a two-way ANOVA ($P \leq 0.05$). AU, Arbitrary units.

radioactive signal for both the wild type and the overexpression line Δ*mnx/OEX* within the 4-h course (Fig. 6).

Mnx Resides in the Thylakoid Membrane

To investigate the subcellular localization of the Mnx protein, we generated a mutant line, *mnx*::*yfp*, expressing a Mnx protein with a C-terminal enhanced yellow fluorescent protein (eYFP) fusion. The biological functionality of the Mnx::YFP fusion proteins was confirmed by demonstrating unrestricted growth of the *mnx*::*yfp* line at Mn concentrations that are lethal for the Δ*mnx* mutant (Supplemental Fig. S2B). For confocal fluorescence microscopy, we mixed *mnx*::*yfp* and wild-type cells to have both cell lines on the same image. The YFP signal showed a complete overlap with the chlorophyll autofluorescence signal, indicating the localization of Mnx::YFP in the thylakoid membrane. In some cases,

Downloaded from www.plantphysiol.org on March 23, 2017 - Published by www.plantphysiol.org
Copyright © 2017 American Society of Plant Biologists. All rights reserved.

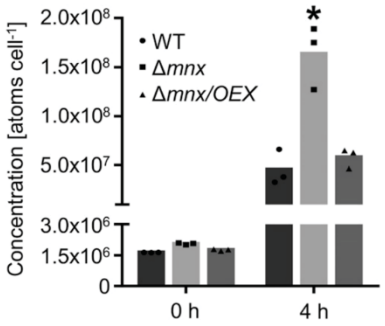

Figure 5. Intracellular Mn accumulation in the wild type (WT), Δ*mnx* mutant, and Δ*mnx/OEX* line. Cells were grown under Mn-limiting conditions for 5 d and then treated with 200 μM $MnCl_2$. Inductively coupled plasma mass spectrometry (ICP-MS) analysis was performed after starvation (0 h) and 4 h after treatment with $MnCl_2$. Each bar represents three biological replicates. The asterisk indicates a significant change to the respective wild-type value according to a two-way ANOVA ($P \leq 0.05$).

we observed locally increased YFP signals (Fig. 7). To analyze the spatial distribution in more detail, we furthermore quantified the signal intensities of a circumferential profile for the two *mnx*::*yfp* cells and found the YFP and chlorophyll autofluorescence signals positively correlated (Supplemental Fig. S3B). A slight patchiness with regard to the YFP signal also was observed for both cells. We detected regions where the autofluorescence was low while YFP fluorescence peaked (Supplemental Fig. S3B). For wild-type cells, we did not detect a signal in the YFP channel with the settings used (Fig. 7). The different intensities in the autofluorescence probably resulted from the unequal arrangement of *mnx*::*yfp* and wild-type cells, with the wild-type cells being ~0.2 μm increased in comparison with the wild type cells (Supplemental Fig. S3).

Expression of Mnx Suppresses the Phenotype of a Yeast Mn Transport Mutant

To further prove that Mnx facilitates the transport of Mn and does not act as a regulatory Mn receptor protein, we employed a heterologous yeast mutant suppression assay. In *Saccharomyces cerevisiae* cells, Mn^{2+} and Ca^{2+} ions are imported into the secretory pathway by a P-type Ca^{2+}/Mn^{2+} ATPase, PMR1, that resides in the Golgi apparatus membrane (Dürr et al., 1998). The corresponding mutant Δ*pmr1* accumulates Mn in the cytoplasm (Lapinskas et al., 1995) and cannot survive on medium containing 2 mM $MnCl_2$ (Maeda et al., 2004). Heterologous expression of the cyanobacterial Mnx protein suppressed the Mn-sensitive phenotype of the Δ*pmr1* mutant (Fig. 8), which strongly supports a role of Mnx in Mn export from the cytoplasm.

DISCUSSION

Mnx Facilitates the Export of Mn from the Cytoplasm in *Synechocystis*

Mn homoeostasis in oxygenic photosynthetic organisms needs to be carefully sustained to avoid limited provision of Mn^{2+} ions to the OEC of PSII, on the one hand, and inhibitory effects due to cytoplasmic Mn accumulation, on the other hand. In search of an Mn exporter in the cyanobacterium *Synechocystis*, we identified the protein Mnx encoded by the open reading frame *sll0615* as a promising candidate. In this study, we provide several independent lines of evidence that Mnx, in fact, functions in the export of Mn from the cytoplasm.

The knockout mutant Δ*mnx* showed high sensitivity toward externally supplied Mn. Already, a treatment with only 1.4-fold elevated $MnCl_2$ concentration (12.5 μM) had a strong negative impact on the mutant, while a 2.8-fold concentration (25 μM) was lethal for Δ*mnx* (Fig. 2A). Different physiological mechanisms for Mn toxicity were suggested. First, Mn can compete with other divalent metal ions, such as magnesium, Fe, or calcium (Ca), for incorporation into the active sites of enzymes and, thus, modifies enzymatic activities. For this reason, chlorophyll biosynthesis is inhibited in cyanobacteria (Csatorday et al., 1984) and plants (Clairmont et al., 1986) upon Mn intoxication. Furthermore, excess Mn inhibits Rubisco activity (Houtz et al., 1988; Nable et al., 1988) and photosynthetic activity (Millaleo et al., 2013) for the same reason. Second, free Mn possibly functions as a redox-active metal in a Fenton-like reaction with the generation of most reactive OH· radicals. However, it is assumed that, in vivo, the reduction potential of Mn is not low enough to catalyze this toxic reaction (Kehres and Maguire, 2003). Our physiological analyses revealed that the mutant line Δ*mnx* showed several of the described symptoms of Mn toxicity. Chlorophyll accumulation in Δ*mnx* cells was reduced after the application of Mn (Fig. 3, B and C; Supplemental Fig. S1B), likely as a consequence of Mn-inhibited chlorophyll biosynthesis. Also, photosynthetic activity was lower in the mutant as a function of external Mn concentration (Fig. 3D). The enhanced generation of OH· radicals was not investigated in this study and cannot be excluded as another reason for the lethality of Δ*mnx* cells upon exposure to high Mn concentrations.

ICP-MS analysis (Fig. 5) supported the hypothesis that the observed physiological symptoms were actually caused by intracellular Mn overaccumulation in the Δ*mnx* mutant. The intracellular Mn level was 3-fold higher in Δ*mnx* than in wild-type cells, and this elevation was obviously sufficient to negatively influence the performance of the mutant cells. Similar behavior was observed for a mutant in the plasma membrane Mn efflux system, MntE, in *Streptococcus pneumoniae*. Incubation with 300 μM $MnCl_2$ resulted in 5-fold increased intracellular Mn amounts compared with wild-type cells, and high Mn concentrations in the growth medium led to severe growth inhibition (Rosch et al., 2009). Our results are in the same range and demonstrate the strict need for the maintenance of Mn homeostasis.

Downloaded from www.plantphysiol.org on March 23, 2017 - Published by www.plantphysiol.org
Copyright © 2017 American Society of Plant Biologists. All rights reserved.

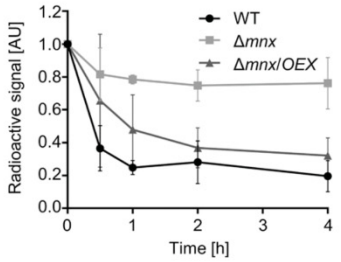

Figure 6. Radioactive trace experiments. Cells limited for Mn were incubated with radioactive ^{54}Mn for 3 d. After washing and transfer to label-free BG11 medium, the decay of the radioactivity signal was followed over a time course of 4 h. Radioactivity at time point 0 h was set to 100%, and subsequent values were normalized to this time point. Values shown are means and SD of three biological replicates. WT, Wild type; AU, arbitrary units.

Also, mutants in the Mn uptake regulatory system, ManSR, showed intracellular Mn accumulation and symptoms of intoxication upon high-Mn treatment (Zorina et al., 2016), which, in the *manS* and *manR* mutants, is essentially caused by uncontrolled Mn uptake via the Mn ABC-type transporter MntCAB (Bartsevich and Pakrasi, 1995). According to DNA microarray analysis of these mutants, *mnx* expression is not controlled by the two-component system ManSR (Yamaguchi et al., 2002). To prove that the membrane protein Mnx is not a Mn sensor but functions as a translocator, we employed a yeast mutant phenotype suppression assay. The strong growth phenotype of the Mn-sensitive yeast mutant Δ*pmr1* (Maeda et al., 2004) could be suppressed on Mn-containing medium by the expression of *Synechocystis mnx* (Fig. 8). Thus, we suggest that Mnx, indeed, functions as a transporter and not as a signaling or regulatory protein.

The measured intracellular Mn content comprises the Mn pools of cytoplasm, thylakoid membrane, and thylakoid lumen. Accordingly, three alternative hypotheses for Mnx function are conceivable: Mnx facilitates Mn export from the cytoplasm into (1) the periplasm, (2) the thylakoid lumen, or (3) export from the thylakoid lumen into the cytoplasm. To distinguish between these options, we determined the subcellular localization of Mnx.

According to the fluorescence microscopy images (Fig. 7), Mnx resides in the thylakoid membrane, which is in agreement with a recent global proteomics study in *Synechocystis* (Liberton et al., 2016), finding Mnx essentially in the thylakoid membrane fraction. However, we cannot rule out that minor amounts of Mnx also reside in the plasma membrane. In Arabidopsis (*Arabidopsis thaliana*), the homologous protein PHOTOSYNTHESIS AFFECTED MUTANT71 (PAM71) resides in the thylakoid membrane as well (Schneider et al., 2016). PAM71 is suggested to facilitate Mn uptake from the chloroplast stroma into the thylakoid lumen in antiport with protons, thus providing Mn for incorporation into the OEC of PSII (Schneider et al., 2016). For other members of the UPF0016, a proton-coupled antiport mode is proposed (Demaegd et al., 2013). In accordance, we anticipate that Mnx serves in Mn transport from the cytoplasm to the thylakoid lumen of illuminated *Synechocystis* cells.

We observed phenotypic changes only upon treatment with Mn. All other divalent metals tested, Ca^{2+}, Fe^{2+}, Cu^{2+}, Ni^{2+}, Co^{2+}, Cd^{2+}, or Zn^{2+}, did not negatively impact the Δ*mnx* mutant (Fig. 2B), indicating that Mnx facilitates the transport of Mn with rather high specificity. This high specificity of Mnx for Mn was surprising, since metal transporters are typically promiscuous regarding their substrate (Socha and Guerinot, 2014). For example, members of the NRAMP family transport a broad range of metals. For the Arabidopsis proteins AtNRAMP3 and AtNRAMP4, a function in both Fe and Mn transport was demonstrated (Lanquar et al., 2005, 2010). However, since it is conceivable that, for some metals, such as Ca or Fe, more efficient compensatory mechanisms exist than for Mn, and for that reason we do not see any effect, we cannot rule out that other metals also are transported by Mnx.

Toward the Biological Function of Mnx in Cyanobacteria

The current knowledge about proteins involved in cellular Mn homeostasis is described in the introduction and summarized in Figure 9. We have identified Mnx as a new player in the management of cyanobacterial Mn homoeostasis that facilitates Mn transport from the cytoplasm into the thylakoid lumen. However, what is the critical biological function of Mn export from the cytoplasm into the thylakoid lumen?

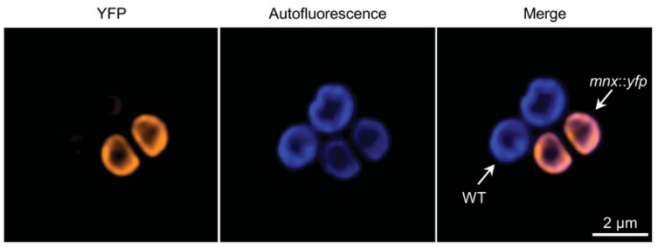

Figure 7. Subcellular localization of the Mnx::YFP protein. *mnx*::*yfp* cells, expressing the Mnx protein with a C-terminal fusion to YFP, were mixed with wild-type (WT) cells as a negative control and inspected by confocal fluorescence microscopy. YFP fluorescence is shown in orange and chlorophyll autofluorescence in blue. Shown is stack 5 of a total series of nine z-stacks. The complete series of z-stacks is shown in Supplemental Figure S3.

Downloaded from www.plantphysiol.org on March 23, 2017 - Published by www.plantphysiol.org
Copyright © 2017 American Society of Plant Biologists. All rights reserved.

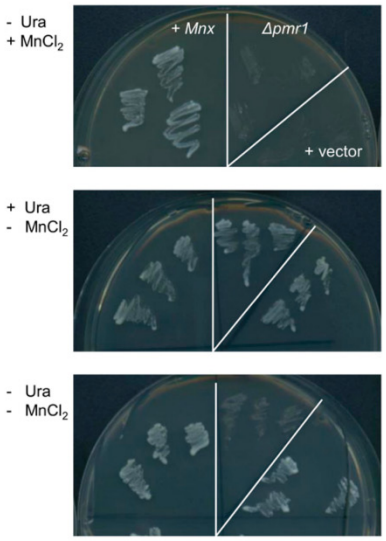

Figure 8. Expression of *Synechocystis mnx* in the *S. cerevisiae* mutant Δ*pmr1*. Mutant Δ*pmr1* cells, Δ*pmr1* cells containing the empty vector pDR196 (+ vector), and Δ*pmr1* cells carrying the vector with *mnx* as an insert (+ *Mnx*) were verified by PCR and streaked on synthetic medium with (+) or without (−) 2 mM $MnCl_2$. For selection, uracil (Ura) was added (+) or omitted (−). Photographs were taken after 4 d of incubation at 30°C.

Function 1

Mnx sequesters free Mn into the thylakoid lumen to mitigate harmful effects. Cytoplasmic Mn accumulation leads to detrimental effects, as discussed above, and needs to be avoided. Thus, Mn is sequestered by the Mnx protein into the thylakoid lumen, where Mn likely does no harm. High environmental Mn concentrations, as provided in our experimental setup, lead to cytoplasmic Mn accumulation. Since Mn concentrations in aquatic habitats are in the range of 0.1 to 10 nM (Salomon and Keren, 2015), this scenario is not very likely to occur in nature. Alternatively, cytoplasmic Mn accumulation could result from the release of this metal during protein turnover and degradation. According to our results, the major path to eliminate intracellular Mn basically involves Mnx and passage through the thylakoid lumen. In our ^{54}Mn chase experiments, the knockout mutant Δ*mnx* retained about 80% of the intracellular radioactive signal, while in the wild type and the overexpression line, the signal decreased rapidly to about 20% (Fig. 6). Thus, the data show that more than 70% of the internal Mn pool is rapidly turned over and exported to the periplasm within 1 h in wild-type and Mnx overexpression cultures (Fig. 6). The remaining approximately 20% of the intracellular Mn pool is probably bound to proteins that are stable over the observed period of time. Furthermore, the results indicate that Δ*mnx* is unable to export Mn resulting from intracellular protein turnover even under unstressed conditions (i.e. 9 μM $MnCl_2$ in the standard BG11 medium). Every cell division causes a dilution of cytoplasmic Mn, which likely contributes to mutant survival in the standard conditions. The intriguing result that Mnx contributes significantly to the release of Mn into the periplasm, although the transporter resides in the thylakoid membrane, remains to be explained. Interestingly, a similar behavior was demonstrated for a mutant in the thylakoid Na^+/H^+ transporter Nhas3 in *Synechocystis*. Although the transporter resides in the thylakoid membrane, the *nhaS3* knockdown mutant showed increased sensitivity toward elevated Na^+ concentrations in the medium (Tsunekawa et al., 2009).

Function 2

Mnx contributes to Mn supply to the OEC. In cyanobacteria, major intracellular Mn amounts presumably are contained in the Mn_4O_5Ca cluster of the OEC, since, in chloroplasts, roughly 80% of Mn is associated with PSII (Anderson et al., 1964). The cluster is bound by the D1 protein and stabilized by the extrinsic, lumenal PSII subunits PsbO, PsbP, PsbQ, PsbU, and PsbV in cyanobacteria (Nickelsen and Rengstl, 2013). It is suggested that the loading of pre-D1 protein with Mn takes place in biogenesis centers and is mediated by the PratA protein (Stengel et al., 2012). The D1 protein is damaged continuously by light and needs to be repaired (i.e. replaced by de novo synthesized D1). To allow for PSII repair, PSII is disassembled and the photodamaged D1 is removed by proteases (for review, see Nickelsen and Rengstl, 2013). Concomitantly, the Mn_4O_5Ca cluster is released into the thylakoid lumen. It is debated whether the de novo synthesized D1 can be inserted into PSII in thylakoid membranes or whether the repair takes place at the biogenesis centers with the participation of PratA (Nickelsen and Rengstl, 2013). It is also not clear whether the released Mn can be recycled or needs to be replaced by freshly imported Mn. Our observations that the Δ*mnx* mutant was highly susceptible to high light intensities (Fig. 4) and needed significantly longer to recover from a short-time high-light treatment (Fig. 4, D and E) are indications that, at least partly, the repair of PSII occurs on site and employs Mnx to import Mn into the thylakoid lumen for reincorporation into PSII. With regard to the slightly patchy distribution of Mnx::YFP in the thylakoid membrane (Fig. 7; Supplemental Fig. S3), it could be speculated that the transporter also might localize to the biogenesis centers. More detailed studies will be necessary to identify the specific site(s) of Mnx action. We suggest that Mnx functions in parallel with PratA to provide Mn to the OEC. While, under standard conditions, the contribution of Mnx seems to be marginal in comparison with PratA in contrast to Δ*mnx* (Fig. 4C), a mutant in *pratA* has reduced photosynthetic activity (Klinkert et al., 2004), and it becomes critical under high-light conditions with increased need for PSII repair. However, the expression of *mnx* is not changed during

Downloaded from www.plantphysiol.org on March 23, 2017 - Published by www.plantphysiol.org
Copyright © 2017 American Society of Plant Biologists. All rights reserved.

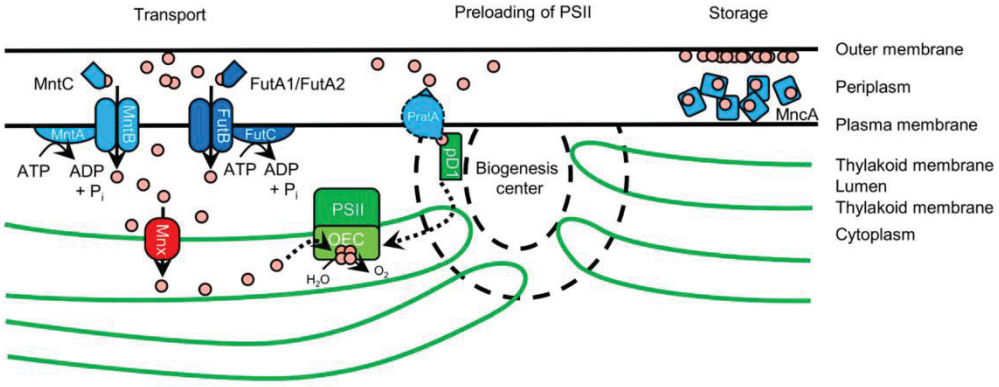

Figure 9. Hypothetical model for the function of Mnx in *Synechocystis*. Mn (Mn^{2+} ions represented as rose-colored circles; oxidation states Mn^{3+} and Mn^{4+} in the activated Mn_4O_5Ca cluster are not specifically accentuated) is stored mainly in the periplasm, with MncA as the most abundant Mn-containing protein. Mn also is suggested to bind to the outer membrane. To maintain cellular functionality, Mn is imported by the plasma membrane ABC transporter MntCAB under Mn-limiting conditions. The presence of a second, constitutively acting Mn importer has been hypothesized. Likely, the Fe ABC transporter FutABC fulfills this function. The pre-D1 (pD1) protein, which is the Mn_4O_5Ca cluster-binding core protein of PSII, is preloaded with Mn from the periplasm via PratA in biogenesis centers. The cytoplasmic surplus of Mn resulting from the turnover and degradation of Mn-containing proteins gets sequestered into the safekeeping environment thylakoid lumen via Mnx. Additionally, Mnx transports Mn from the cytoplasm into the thylakoid lumen to support Mn delivery to the OEC.

acclimation from low to high light intensities (Hihara et al., 2001). Another possible explanation for the high-light susceptibility and the retarded recovery in the Δ*mnx* mutant is that the Mn accumulation involves ROS production, as explained before, which inhibits the translation of D1 for the repair of PSII (Nishiyama et al., 2011). A more detailed analysis of PSII activity, as well as the photodamage and repair process in the mutant line, are necessary in future studies to clarify this question.

Our results indicate that both suggested biological functions of Mnx (i.e. Mn safekeeping in the thylakoid lumen and Mn provision to OEC) are critical for Mn homeostasis in *Synechocystis*. In Arabidopsis, the biological significance of the homologous thylakoid protein PAM71 is different. Since proteins homologous to PratA and biogenesis centers do not exist (Nickelsen and Rengstl, 2013), the incorporation of Mn into the OEC occurs on site in the thylakoid membrane. Mutants in *PAM71* are highly sensitive to low Mn concentrations and contain reduced amounts of Mn in isolated PSII complexes. Thus, it is suggested that PAM71 majorly serves the provision of Mn to the OEC (Schneider et al., 2016). The sequestration of surplus stromal Mn appears to be less important. This is expected because, in the highly compartmentalized plant cell, the vacuole, which is not present in cyanobacteria, serves as a reservoir for surplus metal ions, at least within physiological concentration ranges (Lanquar et al., 2010). Quite contrary to the situation in the cyanobacterial Δ*mnx* mutant, high-Mn treatment is beneficial for *pam71* mutants, since likely other, so far unknown, transporter(s) with lower affinity for Mn serve to import the Mn into the thylakoid lumen and, thereby, compensate the loss of PAM71 (Schneider et al., 2016).

Mnx Function as an Mn Transporter Is Conserved among Oxygenic Photosynthetic Organisms

The Mnx protein belongs to UPF0016, which contains only a few studied proteins. So far, only GDT1 from yeast and human TMEM165 have been investigated more closely. Both proteins are suggested to act as Ca^{2+}/H^+ antiporters in the Golgi apparatus membrane and, thus, to play important roles in Ca signaling and protein glycosylation (Demaegd et al., 2013; Colinet et al., 2016). When we treated the mutant Δ*mnx* with 12.5-fold higher concentrations of $CaCl_2$ than was used in standard BG11 medium, we did not detect any effect on the growth performance (Fig. 2B). Thus, in *Synechocystis*, Mnx is unlikely to play a major role as a Ca transporter. Interestingly, phylogenetically related proteins from green algae and land plants display similar specificity for Mn over Ca (Schneider et al., 2016). In the genome of the model plant Arabidopsis, five proteins orthologous to Mnx are encoded. Of these five proteins, PAM71 and PHOTOSYNTHESIS AFFECTED MUTANT71 HOMOLG (PAM71-HL) are targeted to the chloroplast. PAM71 resides in the thylakoid membrane and PAM71-HL in the chloroplast inner envelope (Schneider et al., 2016). The protein PAM71 was demonstrated recently to facilitate Mn uptake from the stroma into the thylakoid lumen, thus providing Mn for incorporation into the OEC of PSII (Schneider et al., 2016). Arabidopsis and

Downloaded from www.plantphysiol.org on March 23, 2017 - Published by www.plantphysiol.org
Copyright © 2017 American Society of Plant Biologists. All rights reserved.

C. reinhardtii knockout mutants in this protein both could be rescued by supplementation with Mn but not Ca, emphasizing the prominent role of Mnx homologs in Mn versus Ca transport (Schneider et al., 2016). The function of PAM71-HL remains to be studied. Importantly, the duplication of plastidial Mnx homologs is conserved throughout oxygenic photosynthetic eukaryotes (Schneider et al., 2016). This indicates the importance of the role of Mnx proteins as Mn transporters in chloroplasts, the cellular compartment where oxygenic photosynthesis takes place and, thus, makes Mn management a critical task. It remains to be clarified whether the other three Mnx homologs in Arabidopsis, which are predicted to reside in membranes of the secretory pathway (Schneider et al., 2016), function in Ca or Mn transport.

CONCLUSION

In this study, we identified and characterized the Mn transport protein Mnx in the cyanobacterium *Synechocystis*. Mnx resides in the thylakoid membrane and facilitates Mn export from the cytoplasm into the thylakoid lumen, first to avoid critical cytoplasmic accumulation of Mn by sequestration in the thylakoid lumen and second to back up Mn provision to the OEC. According to our results, in cyanobacteria, the cytoplasmic Mn pool must be maintained at a constant level within a narrow range. Therefore, the released Mn needs to be exported rapidly to prevent toxic accumulation. The export function of Mnx is important under standard growth conditions and becomes crucial under high-light conditions, since Mnx likely ensures Mn supply during the repair of PSII. Members of UPF0016 are widespread among all classes of organisms. However, while, in yeast and human cells, these proteins facilitate Ca transport in the membrane of the Golgi apparatus, cyanobacterial Mnx proteins and the plant and green algal orthologous proteins that are targeted to the plastid use preferentially Mn as a transport substrate. This altered substrate specificity might be a specialization of the proteins for oxygenic photosynthetic organisms, which strongly rely on Mn.

MATERIALS AND METHODS

Synechocystis Strains and Growth Conditions

A Glc-tolerant strain of *Synechocystis* sp. PCC 6803 served as the wild type. Axenic cultures were grown continuously at 30°C, 200 rpm, and 100 μmol photons m^{-2} s^{-1} constant light in BG11 medium buffered with 20 mM HEPES-KOH to pH 7.5 (Rippka et al., 1979). Growth medium for mutant lines was supplemented with appropriate antibiotics (50 μg mL^{-1} kanamycin [Km] and 20 μg mL^{-1} spectinomycin [Sp]). For experiments, precultures were generally Mn starved for 5 d to ensure the same preconditions for all lines. To this end, the cells were washed once with EDTA solution (HEPES-KOH, pH 7.5, and 5 mM EDTA; Keren et al., 2002) and two times with Mn-free BG11 medium to remove the periplasmic storage pool of Mn. Then, the cultures were grown for 5 d in Mn-free BG11 medium and subsequently used for experiments.

Generation of *mnx* Knockout and Overexpression Lines

The Δ*mnx* knockout mutant was generated by introduction of a Km resistance cassette obtained from the plasmid pUC4K (Pharmacia) into the unique *Sma*I site of the PCR-amplified (primers ME29 and ME30; Supplemental Table S2) open reading frame *sll0615*. After transformation and selection on Km-containing BG11 plates, full segregation of several independent clones was verified by PCR analysis as described (Eisenhut et al., 2006). To generate the overexpression line Δ*mnx/OEX*, full-length *mnx* was PCR amplified using primers ME57 and ME58 (Supplemental Table S2). After digestion with *Nde*I and *Hpa*I, the *mnx* fragment was introduced into the modified version of the overexpression vector pPSBAII (Lagarde et al., 2000), carrying an Sp resistance cassette for selection (Engel et al., 2008). The obtained plasmid was used for transformation of the Δ*mnx* mutant. The complementation/overexpression line Δ*mnx/OEX* was selected on BG11 plates containing both Km and Sp.

RNA Isolation and RT-qPCR Analysis

For RNA isolation, 10 mL of culture was harvested by centrifugation for 5 min at 4°C and 3,000*g*. Extraction was performed with the Universal RNA Purification Kit (Roboklon) using the bacterial cell protocol. DNase treatment was carried out using RQ1 RNA-Free DNase (Promega), and cDNA synthesis was performed using Moloney murine leukemia virus reverse transcriptase (Promega). For the RT-qPCR analysis, Mesa Blue MasterMix for SYBR Assay (Eurogentec) was used. The primers used for RT-qPCR were FB24 and FB25 (Supplemental Table S2; efficiency, 1.94) for the amplification of *mnx*. RNase P subunit B (*rnpB*) was used as a reference gene using the primers FB26 and FB27 (Supplemental Table S2; efficiency, 1.99). RT-qPCR was performed with the StepOne Plus Real-Time system (Applied Biosystems). Mean normalized expression was calculated from three biological replicates, each measured in three technical replicates, according to Simon (2003). Samples with a cycle threshold value higher than the water control were set as not detectable.

Drop Tests

The effect of metals was tested on solid medium. Two microliters of the cultures with an OD_{750} of 0.25 and 1:10, 1:100, and 1:1,000 dilutions were spotted onto agar plates (BG11; pH 7.5; solidified with 1.5% [w/v] bacto agar), which were supplemented with different concentrations of $MnCl_2$, $CaCl_2$, FeEDTA, $CuSO_4$, $NiSO_4$, $Co(NO_3)_2$, $CdCl_2$, or $ZnSO_4$. Plates were incubated under continuous illumination of 100 μmol photons m^{-2} s^{-1} at 30°C for 4 d.

Growth, Chlorophyll, and Oxygen Evolution Analysis

After 5 d of Mn limitation, the cultures were set to an OD_{750} of 0.3 and grown in Mn-free BG11 medium for another 5 d. Then, the cultures were diluted to an OD_{750} of 0.5 and kept under limitation (0 μM $MnCl_2$) or were treated with 9 and 150 μM $MnCl_2$. Growth and chlorophyll content were determined by monitoring the OD_{750} and OD_{680}, respectively. Before and after 4 h of Mn treatment, additional samples were taken to analyze oxygen evolution as a measure of photosynthesis with a Clark-type electrode.

Effects of High-Light Treatment on Photosynthetic Activity

Cultures were set to an OD_{750} of 0.5 in BG11 medium containing the standard concentration of 9 μM $MnCl_2$. At time point 0 min, the cultures were placed under a 50-W light-emitting diode lamp at 1,000 μmol photons m^{-2} s^{-1} for 45 min. Temperature (30°C) and continuous mixing were controlled by a magnetic stirrer with heating function. After 45 min, the cultures were returned to standard growth conditions (100 μmol photons m^2 s^{-1} and 30°C) for 75 min. During the experiment, oxygen evolution as a measure of photosynthesis was analyzed every 15 min with a Clark-type electrode. The experiment was repeated three times to get biological triplicates.

Subcellular Localization of Mnx

To determine the subcellular localization of Mnx, an eYFP from pUBC-YFP-Dest (Grefen et al., 2010) was C-terminally fused to Mnx. For selection, a KmR from the vector pUC4K (Pharmacia) was added downstream of the YFP open reading frame followed by 200 bp of the 3′ region of *mnx* for homologous recombination in the *Synechocystis* genome. All fragments were PCR amplified and assembled using the Gibson Assembly Master Mix (New England Biolabs). Primers FB16 and FB17 were used to amplify *mnx*, FB18 and FB19 to amplify *yfp*, FB20 and FB21 to amplify the *KmR*, and FB22 and FB23 to amplify the 3′ region of *mnx*. Genotypes of Km-resistant transformants were verified by PCR

Downloaded from www.plantphysiol.org on March 23, 2017 - Published by www.plantphysiol.org
Copyright © 2017 American Society of Plant Biologists. All rights reserved.

using primers ME57 and FB31 (Supplemental Fig. S2A), and the biological functionality of Mnx::YFP fusion proteins was tested by growth on BG11 medium supplemented with elevated $MnCl_2$ concentrations (Supplemental Fig. S2B). Before imaging, the cells were kept in darkness for 30 min to relax the proton gradient across the thylakoid membrane, because the low pH in the thylakoid lumen might affect the fluorescence of YFP. For imaging, transformed cells were mixed with wild-type cells to have a negative control in the same image. The cells were immobilized on microscopic glass slides by a thin layer of solid BG11 medium (1:1 mixture of 2-fold concentrated BG11 medium and 3% [w/v] bacto agar). A Leica TCS SP8 STED 3X microscope was used with a 100× oil objective (optical aperture 1.4) and Leica HyD hybrid detectors. YFP and chlorophyll were excited at 488 nm with a white-light laser at 70% output intensity.

ICP-MS Measurements

After precultivation under Mn limitation conditions, the cells were adjusted to an OD_{750} of 0.75 and treated with 200 μM $MnCl_2$. The higher $MnCl_2$ concentration compared with our other experiments was chosen to apply Mn stress proportional to the OD_{750} used in this experiment and thus make the effects comparable. Four-milliliter samples were pelleted via centrifugation (3,000*g* for 5 min at 4°C). The samples were washed two times with 4 mL of ice-cold EDTA solution (20 mM HEPES-KOH, pH 7.5, and 5 mM EDTA) to release the periplasmic Mn pool and measure the intracellular Mn pool only (Keren et al., 2002) and one time with 4 mL of ice-cold HEPES buffer (20 mM HEPES-KOH, pH 7.5). All steps were performed at 4°C or on ice. From here on, all steps were performed in a clean laboratory. For analysis, the samples were digested at 100°C with distilled HNO_3, evaporated to dryness, and reconstituted in double distilled water. Mn concentrations were determined using ICP-MS (PerkinElmer-Elan). For each time point, an additional sample was taken to determine the cell number per milliliter microscopically.

Radioactive Trace Experiments

After precultivation under Mn limitation conditions, the cells were adjusted to an OD_{750} of 0.3 and incubated for 3 d in BG11 medium supplemented with 0.18 μM ^{54}Mn and 0.82 μM cold ^{55}Mn. After incorporation of the radioactive Mn into the cells, the radioactive medium was washed off by one washing step with EDTA solution (20 mM HEPES-KOH, pH 7.5, and 5 mM EDTA) and two washing steps with Mn-free BG11 medium. The cultures were adjusted to an OD_{750} of 0.3 and treated with 9 μM $MnCl_2$. Samples of 500 μL were taken with a reusable syringe-type filter holder (Schleicher & Schuell) and nitrocellulose filters (Whatman). The filter residue was washed one time with EDTA solution (20 mM HEPES-KOH, pH 7.5, and 5 mM EDTA) and one time with pure water to remove the periplasmic pool of Mn. The radioactivity in the cells was monitored with a gamma counter (Kontron Analytical; GAMMAmatic I). The experiment was performed in biological triplicates, and every sample was measured in three technical replicates.

Expression of *mnx* in Yeast

The coding sequence of *mnx* was PCR amplified from *Synechocystis* genomic DNA using the primers SK102 and SK103 (Supplemental Table S2). The PCR product was subcloned into pJET1.2 (Thermo Fisher Scientific) and verified by sequencing. After restriction digestion with *Sal*I and *Spe*I, the fragment was cloned into the vector pDR196 (Rentsch et al., 1995; Loqué et al., 2007). All further experimental steps were performed as described (Schneider et al., 2016).

Supplemental Data

The following supplemental materials are available.

Supplemental Figure S1. Statistical analysis of growth rates and chlorophyll contents.

Supplemental Figure S2. Verification of the genotype and functionality of Mnx::YFP proteins.

Supplemental Figure S3. Overview of fluorescence microscopy images of wild-type and *mnx*::*yfp* cells.

Supplemental Table S1. GreenCut proteins strictly conserved in cyanobacterial genomes with predicted but so far unknown functions in chloroplast transport processes.

Supplemental Table S2. Oligonucleotides used in this study.

ACKNOWLEDGMENTS

We thank Petra Düchting (Ruhr University) and the Center of Advanced Imaging at Heinrich Heine University for excellent technical assistance.

Received December 16, 2016; accepted January 26, 2017; published January 30, 2017.

LITERATURE CITED

Anderson JM, Boardman NK, David DJ (1964) Trace metal composition of fractions obtained by digitonin fragmentation of spinach chloroplasts. Biochem Biophys Res Commun **17:** 685–689

Bartsevich VV, Pakrasi HB (1995) Molecular identification of an ABC transporter complex for manganese: analysis of a cyanobacterial mutant strain impaired in the photosynthetic oxygen evolution process. EMBO J **14:** 1845–1853

Bartsevich VV, Pakrasi HB (1996) Manganese transport in the cyanobacterium Synechocystis sp. PCC 6803. J Biol Chem **271:** 26057–26061

Clairmont KB, Hagar WG, Davis EA (1986) Manganese toxicity to chlorophyll synthesis in tobacco callus. Plant Physiol **80:** 291–293

Colinet AS, Sengottaiyan P, Deschamps A, Colsoul ML, Thines L, Demaegd D, Duchêne MC, Foulquier F, Hols P, Morsomme P (2016) Yeast Gdt1 is a Golgi-localized calcium transporter required for stress-induced calcium signaling and protein glycosylation. Sci Rep **6:** 24282

Csatorday K, Gombos Z, Szalontai B (1984) Mn and Co toxicity in chlorophyll biosynthesis. Proc Natl Acad Sci USA **81:** 476–478

Demaegd D, Foulquier F, Colinet AS, Gremillon L, Legrand D, Mariot P, Peiter E, Van Schaftingen E, Matthijs G, Morsomme P (2013) Newly characterized Golgi-localized family of proteins is involved in calcium and pH homeostasis in yeast and human cells. Proc Natl Acad Sci USA **110:** 6859–6864

Dürr G, Strayle J, Plemper R, Elbs S, Klee SK, Catty P, Wolf DH, Rudolph HK (1998) The medial-Golgi ion pump Pmr1 supplies the yeast secretory pathway with Ca^{2+} and Mn^{2+} required for glycosylation, sorting, and endoplasmic reticulum-associated protein degradation. Mol Biol Cell **9:** 1149–1162

Eisenhut M, Kahlon S, Hasse D, Ewald R, Lieman-Hurwitz J, Ogawa T, Ruth W, Bauwe H, Kaplan A, Hagemann M (2006) The plant-like C2 glycolate cycle and the bacterial-like glycerate pathway cooperate in phosphoglycolate metabolism in cyanobacteria. Plant Physiol **142:** 333–342

Engel N, Eisenhut M, Qu N, Bauwe H (2008) Arabidopsis mutants with strongly reduced levels of the T-protein subunit of glycine decarboxylase. *In* Photosynthesis: Energy from the Sun. Springer, The Netherlands. pp 819–822

Grefen C, Donald N, Hashimoto K, Kudla J, Schumacher K, Blatt MR (2010) A ubiquitin-10 promoter-based vector set for fluorescent protein tagging facilitates temporal stability and native protein distribution in transient and stable expression studies. Plant J **64:** 355–365

Hänsch R, Mendel RR (2009) Physiological functions of mineral micronutrients (Cu, Zn, Mn, Fe, Ni, Mo, B, Cl). Curr Opin Plant Biol **12:** 259–266

Hebbern CA, Laursen KH, Ladegaard AH, Schmidt SB, Pedas P, Bruhn D, Schjoerring JK, Wulfsohn D, Husted S (2009) Latent manganese deficiency increases transpiration in barley (*Hordeum vulgare*). Physiol Plant **135:** 307–316

Hihara Y, Kamei A, Kanehisa M, Kaplan A, Ikeuchi M (2001) DNA microarray analysis of cyanobacterial gene expression during acclimation to high light. Plant Cell **13:** 793–806

Houtz RL, Nable RO, Cheniae GM (1988) Evidence for effects on the in vivo activity of ribulose-bisphosphate carboxylase/oxygenase during development of Mn toxicity in tobacco. Plant Physiol **86:** 1143–1149

Karpowicz SJ, Prochnik SE, Grossman AR, Merchant SS (2011) The GreenCut2 resource, a phylogenomically derived inventory of proteins specific to the plant lineage. J Biol Chem **286:** 21427–21439

Kehres DG, Maguire ME (2003) Emerging themes in manganese transport, biochemistry and pathogenesis in bacteria. FEMS Microbiol Rev **27:** 263–290

Keren N, Kidd MJ, Penner-Hahn JE, Pakrasi HB (2002) A light-dependent mechanism for massive accumulation of manganese in the photosynthetic bacterium *Synechocystis* sp. PCC 6803. Biochemistry **41:** 15085–15092

Klinkert B, Ossenbühl F, Sikorski M, Berry S, Eichacker L, Nickelsen J (2004) PratA, a periplasmic tetratricopeptide repeat protein involved in biogenesis of photosystem II in Synechocystis sp. PCC 6803. J Biol Chem **279:** 44639–44644

Downloaded from www.plantphysiol.org on March 23, 2017 - Published by www.plantphysiol.org
Copyright © 2017 American Society of Plant Biologists. All rights reserved.

Lagarde D, Beuf L, Vermaas W (2000) Increased production of zeaxanthin and other pigments by application of genetic engineering techniques to *Synechocystis* sp. strain PCC 6803. Appl Environ Microbiol **66:** 64–72

Lanquar V, Lelièvre F, Bolte S, Hamès C, Alcon C, Neumann D, Vansuyt G, Curie C, Schröder A, Krämer U, et al (2005) Mobilization of vacuolar iron by AtNRAMP3 and AtNRAMP4 is essential for seed germination on low iron. EMBO J **24:** 4041–4051

Lanquar V, Ramos MS, Lelièvre F, Barbier-Brygoo H, Krieger-Liszkay A, Krämer U, Thomine S (2010) Export of vacuolar manganese by AtNRAMP3 and AtNRAMP4 is required for optimal photosynthesis and growth under manganese deficiency. Plant Physiol **152:** 1986–1999

Lapinskas PJ, Cunningham KW, Liu XF, Fink GR, Culotta VC (1995) Mutations in *PMR1* suppress oxidative damage in yeast cells lacking superoxide dismutase. Mol Cell Biol **15:** 1382–1388

Liberton M, Saha R, Jacobs JM, Nguyen AY, Gritsenko MA, Smith RD, Koppenaal DW, Pakrasi HB (2016) Global proteomic analysis reveals an exclusive role of thylakoid membranes in bioenergetics of a model cyanobacterium. Mol Cell Proteomics **15:** 2021–2032

Loqué D, Lalonde S, Looger LL, von Wirén N, Frommer WB (2007) A cytosolic trans-activation domain essential for ammonium uptake. Nature **446:** 195–198

Lynch JP, St. Clair SB (2004) Mineral stress: the missing link in understanding how global climate change will affect plants in real world soils. Crop Res **90:** 101–115

Maeda T, Sugiura R, Kita A, Saito M, Deng L, He Y, Yabin L, Fujita Y, Takegawa K, Shuntoh H, et al (2004) Pmr1, a P-type ATPase, and Pdt1, an Nramp homologue, cooperatively regulate cell morphogenesis in fission yeast: the importance of Mn^{2+} homeostasis. Genes Cells **9:** 71–82

Millaleo R, Reyes-Díaz M, Alberdi M, Ivanov AG, Krol M, Hüner NP (2013) Excess manganese differentially inhibits photosystem I versus II in *Arabidopsis thaliana*. J Exp Bot **64:** 343–354

Nable RO, Houtz RL, Cheniae GM (1988) Early inhibition of photosynthesis during development of Mn toxicity in tobacco. Plant Physiol **86:** 1136–1142

Nelson N, Junge W (2015) Structure and energy transfer in photosystems of oxygenic photosynthesis. Annu Rev Biochem **84:** 659–683

Nickelsen J, Rengstl B (2013) Photosystem II assembly: from cyanobacteria to plants. Annu Rev Plant Biol **64:** 609–635

Nishiyama Y, Allakhverdiev SI, Murata N (2011) Protein synthesis is the primary target of reactive oxygen species in the photoinhibition of photosystem II. Physiol Plant **142:** 35–46

Ogawa T, Bao DH, Katoh H, Shibata M, Pakrasi HB, Bhattacharyya-Pakrasi M (2002) A two-component signal transduction pathway regulates manganese homeostasis in *Synechocystis* 6803, a photosynthetic organism. J Biol Chem **277:** 28981–28986

Rentsch D, Laloi M, Rouhara I, Schmelzer E, Delrot S, Frommer WB (1995) NTR1 encodes a high affinity oligopeptide transporter in *Arabidopsis*. FEBS Lett **370:** 264–268

Rippka R, Deruelles J, Waterbury JB, Herdman M, Stanier RY (1979) Generic assignments, strain histories and properties of pure cultures of cyanobacteria. J Gen Microbiol **111:** 1–61

Rosch JW, Gao G, Ridout G, Wang YD, Tuomanen EI (2009) Role of the manganese efflux system *mntE* for signalling and pathogenesis in *Streptococcus pneumoniae*. Mol Microbiol **72:** 12–25

Salomon E, Keren N (2011) Manganese limitation induces changes in the activity and in the organization of photosynthetic complexes in the cyanobacterium *Synechocystis* sp. strain PCC 6803. Plant Physiol **155:** 571–579

Salomon E, Keren N (2015) Acclimation to environmentally relevant Mn concentrations rescues a cyanobacterium from the detrimental effects of iron limitation. Environ Microbiol **17:** 2090–2098

Schneider A, Steinberger I, Herdean A, Gandini C, Eisenhut M, Kurz S, Morper A, Hoecker N, Rühle T, Labs M, et al (2016) The evolutionarily conserved protein PHOTOSYNTHESIS AFFECTED MUTANT71 is required for efficient manganese uptake at the thylakoid membrane in *Arabidopsis*. Plant Cell **28:** 892–910

Sharon S, Salomon E, Kranzler C, Lis H, Lehmann R, Georg J, Zer H, Hess WR, Keren N (2014) The hierarchy of transition metal homeostasis: iron controls manganese accumulation in a unicellular cyanobacterium. Biochim Biophys Acta **1837:** 1990–1997

Simon P (2003) Q-Gene: processing quantitative real-time RT-PCR data. Bioinformatics **19:** 1439–1440

Socha AL, Guerinot ML (2014) Mn-euvering manganese: the role of transporter gene family members in manganese uptake and mobilization in plants. Front Plant Sci **5:** 106

Stengel A, Gügel IL, Hilger D, Rengstl B, Jung H, Nickelsen J (2012) Initial steps of photosystem II de novo assembly and preloading with manganese take place in biogenesis centers in *Synechocystis*. Plant Cell **24:** 660–675

Tobergte DR, Curtis S (2012) Marschner's Mineral Nutrition of Higher Plants. Academic Press, United Kingdom

Tottey S, Waldron KJ, Firbank SJ, Reale B, Bessant C, Sato K, Cheek TR, Gray J, Banfield MJ, Dennison C, et al (2008) Protein-folding location can regulate manganese-binding versus copper- or zinc-binding. Nature **455:** 1138–1142

Tsunekawa K, Shijuku T, Hayashimoto M, Kojima Y, Onai K, Morishita M, Ishiura M, Kuroda T, Nakamura T, Kobayashi H, et al (2009) Identification and characterization of the Na^+/H^+ antiporter Nhas3 from the thylakoid membrane of *Synechocystis* sp. PCC 6803. J Biol Chem **284:** 16513–16521

Yamaguchi K, Suzuki I, Yamamoto H, Lyukevich A, Bodrova I, Los DA, Piven I, Zinchenko V, Kanehisa M, Murata N (2002) A two-component Mn^{2+}-sensing system negatively regulates expression of the *mntCAB* operon in *Synechocystis*. Plant Cell **14:** 2901–2913

Zorina A, Sinetova MA, Kupriyanova EV, Mironov KS, Molkova I, Nazarenko LV, Zinchenko VV, Los DA (2016) *Synechocystis* mutants defective in manganese uptake regulatory system, ManSR, are hypersensitive to strong light. Photosynth Res **130:** 11–17

Downloaded from www.plantphysiol.org on March 23, 2017 - Published by www.plantphysiol.org
Copyright © 2017 American Society of Plant Biologists. All rights reserved.

SUPPLEMENTAL DATA

The *Synechocystis* MANGANESE EXPORTER Mnx is essential for manganese homeostasis in cyanobacteria

Fabian Brandenburg, Hanan Schoffman, Samantha Kurz, Ute Krämer, Nir Keren, Andreas P.M. Weber, Marion Eisenhut

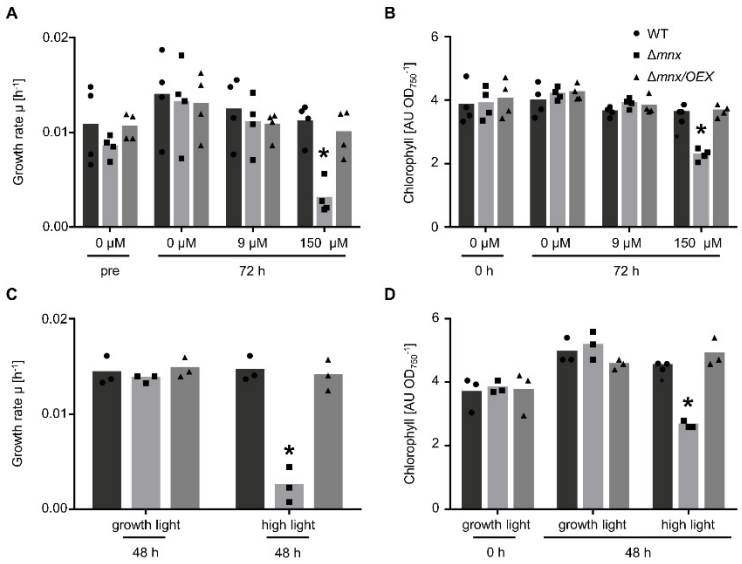

Fig. S1: Statistical analysis of growth rates and chlorophyll content. (A) Growth rates of WT, Δ*mnx*, and Δ*mnx/OEX* during 5 d of Mn limited pre-cultivation (pre) and during 72 h treatment with Mn concentrations as indicated. (B) Chlorophyll content after 5 d of Mn limited pre-cultivation (0 h) and after 72 h treatment with Mn concentrations as indicated. (C) Growth rates after 48 h cultivation under standard growth light (100 µmol photons m^{-2} s^{-1}) or high light (1,000 µmol photons m^{-2} s^{-1}) conditions. (D) Chlorophyll content at the beginning of the experiment (0 h) and after 48 h cultivation under standard growth light (100 µmol photons m^{-2} s^{-1}) or high light (1,000 µmol photons m^{-2} s^{-1}) conditions. Asterisks (*) indicate significant changes to the respective WT value according to a two-way ANOVA ($P \leq 0.05$).

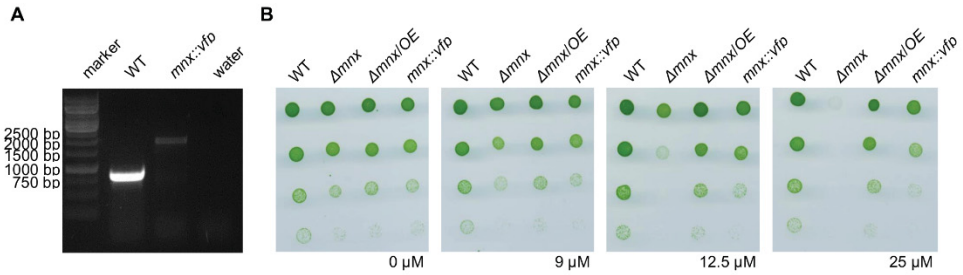

Fig. S2: Verification of genotype of *mnx::yfp* and functionality of Mnx::YFP proteins. (A) The genotype of the mutant *mnx::yfp* was verified by PCR using genomic DNA and primers binding to the *mnx* coding sequence and to the 3' region of *mnx*. The amplified fragment for *mnx::yfp* includes *mnx*, the inserted *yfp* and *KmR* genes, and 255 bp of the 3' region downstream of *mnx*. Water was used as a negative control. (B) The cells in mid log phase were diluted to an OD_{750} of 0.25. 2 µL of these cultures and subsequent 1:10, 1:100 and 1:1,000 dilutions were spotted onto BG11 plates with increasing concentrations of $MnCl_2$. Pictures were taken after incubation for 4 d. The concentration of $MnCl_2$ in standard BG11 medium is 9 µM.

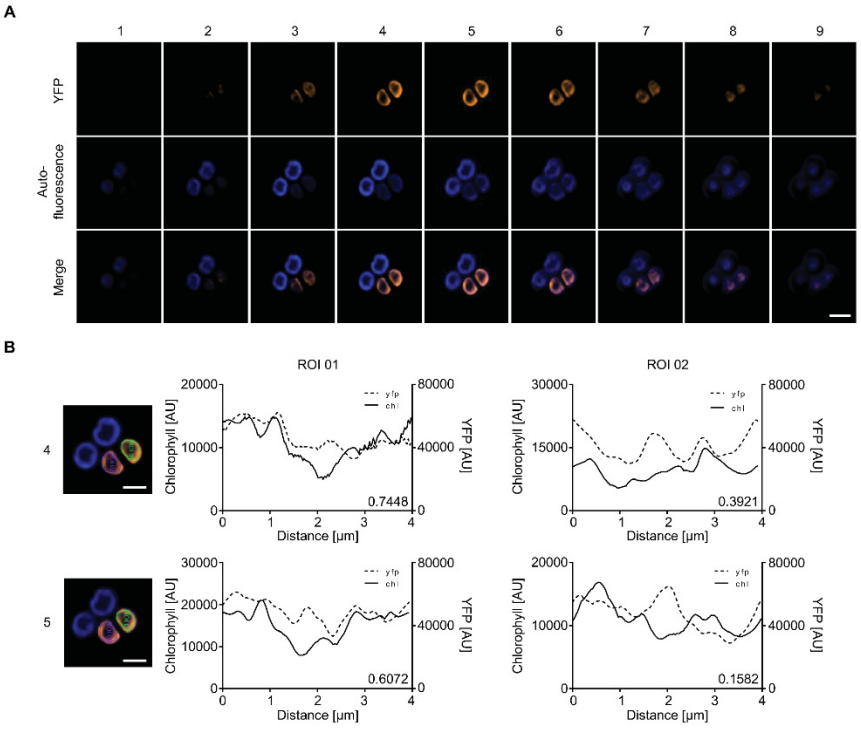

Fig. S3: Overview of fluorescence microscopy pictures of WT and *mnx::yfp* cells. (A) Full series of z-stacks used for localization of Mnx. Fig. 7 shows stack 5. The distance between two images is approximately 0.1 µm. (B) Quantification of YFP and chlorophyll fluorescence along the cellular circumference for images 4 and 5. Region of interest (ROI) 01 is indicated in green and ROI 02 in purple. Spearman's rank correlation coefficients are given for each graph. The length of the scale bars is 1 µm.

Table S1: List of GreenCut proteins strictly conserved in cyanobacterial genomes with predicted but so far unknown function in chloroplast transport processes. Proteins were extracted from the GreenCut2 inventory (Karpowicz et al., 2011). *Cre* protein ID according to JGI v3.0 of the Cre genome, *Syn* protein ID according to Cyanobase

C: Chloroplast; *Cre*: *Chlamydomonas reinhardtii;* iV: inner envelope; *Syn: Synechocystis* sp. PCC 6803;

Cre* protein name	***Cre* protein ID***	***Syn* protein ID**	**Proposed function***	**Domain***	**Predicted location***	**Encoded in cyanobacterial genomes (number)***
CGL98	114780	Sll0355		Integral membrane protein DUF6	C	37
PCD4	205606	Slr0941	possible lipid transport protein	Polyketide_cyc(1)	C	37
TIC21	183668	Sll1737	inner envelope membrane transporter protein, regulated by signaling pathway	Similar to AtTic20-like proteins	iV	37
CPLD63	105873	Sll0615	possible solute transporter	Uncharacterized protein family UPF0016	iV	36
SNR2	146768	Slr0305	SNARE associated Golgi protein, green tissues	SNARE associated Golgi protein	C	35

* according to Karpovicz et al., 2011

Table S2: Oligonucleotides used in this study. Restriction sites are underlined.

Name	**Sequence (5`-> 3`)**	**Experiment**
ME29	TTAACGGTCAGGCGATCA	Generation of knockout mutant in *mnx*
ME30	TAGATCTGATCGCCTTGC	Generation of knockout mutant in *mnx*
ME57	CATATGATGCTGACCGCTTTTACT	Generation of *mnx* overexpression line
ME58	GTTAACCTATGCAATCTTGGTCCA	Generation of *mnx* overexpression line
FB24	TCTTGGCCATACCATCTGTGC	RT-qPCR analysis, expression of *mnx*
FB25	CCACCAGGAAACCACAGCAA	RT-qPCR analysis, expression of *mnx*
FB26	AAGGTTGGTCTTTTTCCTGCC	RT-qPCR analysis, expression of *rnpB*
FB27	AGAGAGTTAGTCGTAAGCCGGG	RT-qPCR analysis, expression of *rnpB*
SK102	AGGAGTCGACATGCTGACCGCTTTTAC	Expression of *mnx* in yeast
SK103	AGGAACTAGTCTATGCAATCTTGGTCCACC	Expression of *mnx* in yeast
FB16	cgagtttttcagcaagatcaTTTGCCCTCACCTTTGTG	Generation of *mnx::yfp* line
FB17	tgctcactccTGCAATCTTGGTCCACCA	Generation of *mnx::yfp* line
FB18	caagattgcaGGAGTGAGCAAGGGCGAG	Generation of *mnx::yfp* line
FB19	gttgcaaaatTTATAACTTGTACAGCTCGTCCATG	Generation of *mnx::yfp* line
FB20	caagttataaATTTTGCAACAAATAACCAC	Generation of *mnx::yfp* line
FB21	aatccgagtcGAGAGTGAGGACCTGCAG	Generation of *mnx::yfp* line
FB22	cctcactctcGACTCGGATTTGCAGATC	Generation of *mnx::yfp* line
FB23	agaatattgtaggagatcttCACGTAGGGTTGAAACTTTTTC	Generation of *mnx::yfp* line
FB31	CACGTAGGGTTGAAACTTTTTCA	Together with ME57 verification of *mnx::yfp*

Authors' contribution to manuscript I

Fabian Brandenburg	Designed, performed and analyzed all experiments, wrote the manuscript, and designed the figures.
Hanan Schoffmann	Participated in design, execution, and analysis of the ICP-MS and radioactive trace experiments.
Samantha Kurz	Generated the yeast complementation lines and performed the assay.
Ute Krämer	Helped with a preliminary ICP-OES analysis of the lines and reviewed the manuscript.
Nir Keren	Supervised the ICP-MS and radioactive trace experiments, and reviewed the manuscript.
Andreas Weber	Helped with the experimental design and drafting the manuscript.
Marion Eisenhut	Generated the knockout and overexpression lines, supervised the experimental design, wrote the manuscript, and designed figure 8.

Manuscript II

Determination of Mn Concentrations in *Synechocystis sp*. PCC 6803 Using ICP-MS

bio-protocol www.bio-protocol.org/exxxx Vol x, Iss xx, xxx xx, 2017
DOI:10.21769/BioProtoc.xxxx

Determination of Mn Concentrations in *Synechocystis sp*. PCC6803 Using ICP-MS

Fabian Brandenburg[1, #], Hanan Schoffman[2, #], Nir Keren[2] and Marion Eisenhut[1, *]

[1]Institute of Plant Biochemistry, Heinrich Heine University, Duesseldorf, Germany; [2]Department of Plant and Environmental Sciences, Institute of Life Sciences, Hebrew University of Jerusalem, Jerusalem, Israel

*For correspondence: Marion Eisenhut (m.eisenhut@hhu.de)

[#]Contributed equally to this work

[Abstract] Manganese (Mn) is an essential micronutrient for all photoautotrophic organisms. Two distinct pools of Mn have been identified in the cyanobacterium *Synechocystis sp*. PCC 6803 (*Synechocystis*), with 80% of the Mn residing in the periplasm and 20% in cytoplasm and thylakoid lumen (Keren *et al.*, 2002). In this protocol, we describe a method to quantify the periplasmic and intracellular pools of Mn in *Synechocystis* accurately, using inductively coupled plasma mass spectrometry (ICP-MS).

Keywords: Cyanobacteria, *Synechocystis*, Manganese, Periplasm, ICP-MS

[Background] Mn plays a vital role in the active sites of several enzymes such as the oxygen-evolving complex in photosystem II. In contrast to its role as an important micronutrient, Mn can be toxic when present in excess. It is therefore of crucial importance for cyanobacteria to maintain the intracellular levels of Mn and in particular to avoid free Mn in the cytoplasm. The cyanobacterium *Synechocystis* addresses this challenge by storing about 80% of the Mn in the periplasm. Only 20% of the cellular content can be detected in the cytoplasm and thylakoid system (Keren *et al.*, 2002), with most of the Mn being incorporated into proteins, leaving virtually no free Mn in the cytoplasm. We recently identified the manganese transport protein Mnx, which resides in the thylakoid membrane and facilitates export of Mn from the cytoplasm into the thylakoid lumen in *Synechocystis*. According to our study, Mnx is a major player in maintaining the cellular Mn homeostasis (Brandenburg *et al.*, 2017). To analyze the biological significance of Mnx, we developed a protocol to measure the periplasmic and intracellular Mn pools separately. We chose ICP-MS for quantification, since it is a sensitive and reliable method to detect metals in biological samples. Detection limits can be in the range of [ng l^{-1}] and below. Prior to the analysis, all complex molecules of the sample are broken down to atomic compounds by digestion with nitric acid. Subsequently, the sample is ionized by an inductively coupled plasma and analyzed by mass spectrometry. In this protocol, we describe the detailed workflow for subcellular Mn quantification, from sampling to the calculation of Mn concentrations.

Materials and Reagents

1. 15 ml tubes (SARSTEDT, catalog number: 62.554.002)
2. Syringe filter filtropur S, 0.2 µm (SARSTEDT, catalog number: 83.1826.001)

bio-protocol www.bio-protocol.org/exxxx Vol x, Iss xx, xxx xx, 2017
DOI:10.21769/BioProtoc.xxxx

3. 10 ml Luer-Lok syringe without needle (BD, catalog number: 300912)
4. Milli-Q grade (or similar) water (Resistivity at 25 °C 18 MΩ cm)
5. Distilled AR grade nitric acid (Macron Fine Chemicals, VWR catalog number: MK140946)
6. ICP-MS multi element standard solution VI (Merck, catalog number 1105800100)
7. Na_2-Ethylenediaminetetraacetic acid (EDTA) (Carl Roth, catalog number: 8043.2)
8. 4-(2-hydroxyethyl)-1-piperazineethanesulfonic acid (HEPES) (Carl Roth, catalog number: 6763.3)
9. EDTA wash buffer (see Recipes)

Equipment

1. Cooling centrifuge for 15 ml tubes (Beckman Coulter, model: GS6)
2. Teflon cups (Savillex, custom made)
3. Analytical balance (Kern, model: ALJ220 4M)
4. Vortex Mixer (Eppendorf, model: MixMate)
5. Clean lab (Class 5000)
6. Chemical hood (Wesemann GmbH)
7. Hot plate (IKA 3581001 Ceramic Stirring Hot Plate)
8. ICP-MS 7500cx (Agilent Technologies, model: ICP-MS 7500cx)
9. Neubauer-improved hemocytometer (Marienfeld, Art. No. 0650030)

Procedure

1. Sampling and washing (Figure 1)

   Notes:

   i. Keep samples on ice to slow down the metabolic activity.

   ii. The washing steps are time sensitive, since they stop the experiment by removing all external Mn. Removing all external Mn conserves the sample in the state of the timepoint it was taken and the elemental composition of the sample cannot change anymore.

   iii. Sample volumes and final elution volumes are accounted for in the calculation under data analysis. All volumes in this protocol are therefore approximate volumes, as long as they are weighted accurately. All transfers can be done by pouring. Pipetting is not necessary and may even add contaminants.

bio-protocol www.bio-protocol.org/exxxx Vol x, Iss xx, xxx xx, 2017
DOI:10.21769/BioProtoc.xxxx

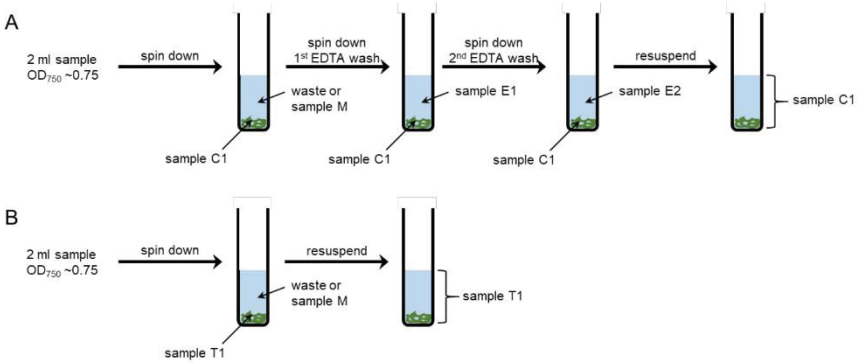

Figure 1. Workflow for sampling and washing. A. Intracellular (sample C) and periplasmic (samples E1 and E2) Mn pools are separated by EDTA washing steps. B. To measure the total cellular Mn content (sample T), cells are separated from the medium and resuspended in Milli-Q water.

a. For each sample, prepare four 15 ml test tubes, labeled with sample number and T1 (total cell), E1 (first EDTA wash), E2 (second EDTA wash) and C1 (intracellular Mn content).
b. Weigh and note weight of all test tubes, including cap.
c. Take 2 ml samples (OD_{750} ~0.75, Note 3) and transfer them into tubes T1 and C1 (Note 4).
d. Remove 30 µl from tube T1 for cell counting.
e. Weigh and note weight for both tubes T1 and C1.
   Note: Subtracting the weight of the tube only from the tube with sample gives you the weight of the sample.
f. Centrifuge tubes T1 and C1 at 3,000 *x g* and 4 °C for 5 min.
g. Discard the supernatant.
   Note: The supernatant can be analyzed as sample M (medium) if wanted. If so, weigh the sample before filtering them through a 0.2 µm syringe filter to get rid of remaining cells. Growth of remaining cells would change the Mn composition of the medium and require sample digestion. After filtering, the sample does not need further processing.
h. Resuspend samples T1 by vortexing in approximately 4 ml of Milli-Q water. Store the samples at room temperature until sample digestion.
i. Add 4 ml EDTA wash buffer to samples C and resuspend by vortexing. Repeat step 1f.
j. Transfer the EDTA supernatant to the test tube labeled E1. Weigh and note weight. Store tube E1 at room temperature. The sample does not need further processing (Note 5).
   Note: Most ICP-MS facilities do not accept undigested or unfiltered samples. Therefore, it may be necessary to filter the EDTA washes as described above. However, potentially remaining cells cannot grow, since they are in EDTA wash buffer and not medium.
k. Add 4 ml EDTA wash buffer to samples C and resuspend by vortexing. Repeat step 1f.

bio-protocol www.bio-protocol.org/exxxx Vol x, Iss xx, xxx xx, 2017
DOI:10.21769/BioProtoc.xxxx

l. Transfer the EDTA supernatant to the test tube labeled E2. Weigh and note weight. Store tube E2 at room temperature. The sample does not need further processing.
m. Add 4 ml Milli-Q water and resuspend by vortexing.
n. Remove 30 µl from the tube for cell counting.

2. Sample digestion

Note: From here on, it is essential to carry out all steps in clean room conditions.

a. For each sample, prepare another set of two 15 ml test tubes (label with sample number and C2 or T2).
b. Weigh out 4 ml of Milli-Q water to the test tubes C2 and T2
c. Add 2 ml of nitric acid to each of samples T1 and C1.
d. Gently shake or turn for 5 min.
e. Preheat hot plate in chemical hood to 200 °C (Note 6).
f. Place each sample (T1 and C1 only) into Teflon cups suitable for hot plate and place the samples on hot plate.
g. Let the samples evaporate until minimal droplet remains; remove from hot plate before sample evaporates completely (Note 7).
h. Add all water from corresponding test tube to the Teflon cup, re-suspend the sample carefully and return the sample to the same test tube (eg. water from tube T2 to the evaporated sample T and back to tube T2).

3. Sample measurement (clean room not required)

a. Transfer 2 ml from each sample (T2, C2, E1, and E2) to appropriate sample tubes for the ICP-MS sample handler.
b. Store the remaining 2 ml of each sample for potential extra measurements.
c. Analyze the samples according to the instructions of your ICP-MS facility.

4. Cell counting

a. Perform cell counting on the samples from sampling and washing (steps 1d and 1n) according to the instructions manual of your hemocytometer.

Data analysis

The periplasmic Mn concentration is the sum of the Mn in samples E1 and E2. Sample C2 is the intracellular concentration of Mn, namely cytosol and thylakoid system. Apply equation 1 to calculate the periplasmic Mn concentration using samples E1, E2 as well as volume and cell count from C1. Similarly, use equation 2 to calculate the intracellular Mn concentration in [atoms cell^{-1}] using samples C1 and C2.

$$\frac{atoms}{cell} = \frac{\text{Result E1}\left[\frac{\mu g}{mL}\right] * \frac{Volume\ E1\,[g]}{Volume\ C1[g]} + Result\ E2\left[\frac{\mu g}{mL}\right] * \frac{Volume\ E2\,[g]}{Volume\ C1[g]}}{MW\left[\frac{\mu g}{mol}\right] * cell\ count\left[\frac{cells}{mL}\right]} * Avogadro\ constant\left[\frac{atoms}{mol}\right] \quad \text{(Eq. 1)}$$

bio-protocol www.bio-protocol.org/exxxx Vol x, Iss xx, xxx xx, 2017
DOI:10.21769/BioProtoc.xxxx

$$\frac{atoms}{cell} = \frac{\text{Result C}\left[\frac{\mu g}{mL}\right] * \frac{Volume\ C2\ [g]}{Volume\ C1\ [g]}}{MW\left[\frac{\mu g}{mol}\right] * cell\ count\left[\frac{cells}{mL}\right]} * Avogadro\ constant\ [\frac{atoms}{mol}] \quad \text{(Eq. 2)}$$

ICP-MS results usually come in parts per million (ppm), which is equivalent to [µg ml^{-1}] or parts per billion (ppb), which is equivalent to [µg l^{-1}]. Make sure to convert the input data into the correct units. Please note that the molecular weight (MW) in equations 1 and 2 is in [µg mol^{-1}]

Instead of cell counting, you can use OD_{750} or chlorophyll content for normalization as well. However, we recommend cell counting. As a control, the sum of the Mn in samples C2, E1 and E2 should equal the Mn concentration in sample T2. You can calculate sample T2 in the same way as sample C2.

Figure 2 shows an example for the calculations. The numbers used for this calculation were obtained from a WT sample grown at our standard conditions (Note 1).

Periplasm: $$\frac{0.0183\left[\frac{\mu g}{mL}\right] * \frac{4.2406\,[g]}{0.8905[g]} + 0.00119\left[\frac{\mu g}{mL}\right] * \frac{4.0783\,[g]}{0.8905[g]}}{54.938\text{x}10^{3}\left[\frac{\mu g}{mol}\right] * 51\text{x}10^{6}\left[\frac{cells}{mL}\right]} * 6.0221\text{x}10^{23}\,[\frac{atoms}{mol}] = 8.82\text{x}10^{6}\,\frac{atoms}{cell}$$

Intracellular: $$\frac{0.00381\left[\frac{\mu g}{mL}\right] * \frac{4.1766\,[g]}{0.8905\,[g]}}{54.938\text{x}10^{3}\left[\frac{\mu g}{mol}\right] * 51\text{x}10^{6}\left[\frac{cells}{mL}\right]} * 6.0221\text{x}10^{23}\,[\frac{atoms}{mol}] = 1.75\text{x}10^{6}\,\frac{atoms}{cell}$$

Total: $$\frac{0.01495\left[\frac{\mu g}{mL}\right] * \frac{4.089\,[g]}{1.3049\,[g]}}{54.938\text{x}10^{3}\left[\frac{\mu g}{mol}\right] * 49.5\text{x}10^{6}\left[\frac{cells}{mL}\right]} * 6.0221\text{x}10^{23}\,[\frac{atoms}{mol}] = 1.06\text{x}10^{7}\,\frac{atoms}{cell}$$

Control: $$(8.82\text{x}10^{6} + 1.75\text{x}10^{6}) - 1.06\text{x}10^{7} = -9.08\text{x}10^{2}$$

Figure 2. Example calculation of Mn concentration. Make sure the input data is in the correct units. In our case for example, the ICP-MS results were in [µg l^{-1}]. Please note that the molecular weight (MW) of Mn is in [µg mol^{-1}]. In our experiments, the difference between E1+E2+C2 and T2 was in the range of 0.1 - 10x10^{3} [atoms cell^{-1}].

Notes

1. Mutant lines are based on and compared to a Japanese WT of *Synechocystis* sp. PCC 6803 obtained from Martin Hagemann (University of Rostock, Germany). Our standard growth conditions are 30 °C, 100 rpm shaking, and 100 µmol photons m^{-2} s^{-1}.
2. This is an elemental analysis that does not differentiate between Mn incorporated into proteins, complexed Mn and free Mn.

bio-protocol www.bio-protocol.org/exxxx Vol x, Iss xx, xxx xx, 2017
DOI:10.21769/BioProtoc.xxxx

3. The amount of original sample to be analyzed depends on the cell density of the sample. Dense samples require less volume and dilute samples require more. There is no need to adjust the other volumes. In our experiments, we took 2 ml samples with an OD_{750} ~0.75.
4. There is no need to use a pipette following this protocol. This minimizes the contamination of the sample. All transfers from one tube to another should be done by pouring.
5. In principal, it is possible to combine samples E1 and E2 and measure them together. If doing so, the sample volume in the calculation needs then to be changed accordingly. However, depending on the physiological conditions of the experiment, the amount of Mn found in these samples can be close to the detection limit already in Sample E1. Therefore, we prefer to not further dilute sample E1 with sample E2.
6. The temperature of the hot plate can be set as low as 180 °C if handling a large number of samples. Doing this will slow down the process allowing for better tracking of all samples on the hot plate to avoid burning.
7. The minimal possible droplet size mostly depends on the experience of the person conducting the experiment. Importantly, the droplet size gets included in the sample weight before the measurements meaning larger droplets do not affect the measurements. This step is solely to protect the ICP-MS pump by reducing the amount of nitric acid in the sample. If samples do evaporate completely, add 1 ml of nitric acid and mix well. Continue evaporation carefully.
8. All samples can be stored at room temperature until digestion, as soon as the experiment has stopped by the washing steppes. All possible contaminations will be eliminated in the digestion process but cannot change the elemental composition of the sample. We are not aware of any specific shelf life of the samples before digestion, however, the longest time we stored samples before digestion was three weeks. After digestion, we recommend to freeze the samples to prevent microbial growth, which may affect the ICP-MS machine rather than the sample composition.

Recipes

1. EDTA wash buffer
   20 mM HEPES-KOH, pH 7.5
   5 mM EDTA
   Note: EDTA wash buffer can be stored at room temperature for several months.

Acknowledgments

This research was supported by the German Science Foundation (EI 945/3-1 to M.E.) and the Israeli Science Foundation (2733/16 to N.K.).

bio-protocol www.bio-protocol.org/exxxx Vol x, Iss xx, xxx xx, 2017
DOI:10.21769/BioProtoc.xxxx

References

1. Brandenburg, F., Schoffman, H., Kurz, S., Kramer, U., Keren, N., Weber, A. P. and Eisenhut, M. (2017). The *Synechocystis* manganese exporter Mnx is essential for manganese homeostasis in cyanobacteria. *Plant Physiol* 173(3): 1798-1810.
2. Keren, N., Kidd, M. J., Penner-Hahn, J. E. and Pakrasi, H. B. (2002). A light-dependent mechanism for massive accumulation of manganese in the photosynthetic bacterium *Synechocystis* sp. PCC 6803. *Biochemistry* 41(50): 15085-15092.

Authors' contribution to manuscript II

Fabian Brandenburg	Wrote the manuscript and designed the figures.
Hanan Schoffmann	Wrote the manuscript.
Nir Keren	Supervised the project and reviewed the manuscript.
Marion Eisenhut	Supervised the project and reviewed the manuscript.

Manuscript III

The *Synechocystis* Hemi Manganese Exchanger Hmx1 and Hmx2 Elucidate the Importance of Manganese Export in Manganese Homeostasis in Cyanobacteria

Short title: Manganese transport in cyanobacteria

The *Synechocystis* Hemi Manganese Exchangers Hmx1 and Hmx2 Elucidate the Importance of Manganese Export in Manganese Homeostasis in Cyanobacteria [1]

Fabian Brandenburg, Anastasija Plett, Andreas P.M. Weber, Marion Eisenhut*

Author affiliations:

Institute of Plant Biochemistry, Cluster of Excellence on Plant Science (CEPLAS), Heinrich Heine University, Düsseldorf, Germany (F.B., A.P, A.P.M.W., M.E.)

One sentence summary:

The hemi manganese exchangers Hmx1 and Hmx2 function as heteromers in export of manganese from the cytoplasm into the periplasm to prevent toxic accumulation of the metal inside the cell and represent a second export system besides the manganese exporter Mnx.

[1] This research was supported by the German Science Foundation (EI 945/3-1 to M.E., EXC 1028 to A.P.M.W).
* Address correspondence to m.eisenhut@uni-duesseldorf.de.
F.B., M.E., and A.P.M.W. designed the study. F.B., M.E, A.P., and S.M. carried out laboratory experiments. F.B., M.E., A.P., and A.P.M.W. interpreted the data. F.B. and M.E. wrote the manuscript. A.P.M.W. edited and approved the manuscript.

ABSTRACT

Although the micronutrient manganese (Mn) is essential for photosynthetic organisms, elevated intracellular concentrations are detrimental to the organism and accumulation needs to be avoided. We identified two proteins with so far unknown function and characterized their role as a heterodimeric Mn transporter in the cyanobacterium *Synechocystis* sp. PCC 6803 (*Synechocystis*). According to their proposed function and size, we named the proteins Hemi Mn Exchanger (Hmx) 1 and 2. The knockout mutant Δ*hmx1* showed sensitivity towards externally applied Mn and a double-knockout with the Mn exporter Mnx – which belongs to the same protein family – resulted in increased Mn accumulation inside the cell as compared to a single-knockout of Mnx. We found Hmx1 and Hmx2 to interact via the C-terminus in a yeast two-hybrid assay. Furthermore, heterologous expression of both proteins had a stronger positive effect on growth of *Escherichia coli* at increased concentrations of Mn than either Hmx1 or Hmx2 alone. In *Synechocystis*, we localized CFP-tagged Hmx1 and Hmx2 proteins to the plasma membrane. Based on our results we propose that Hmx1 and Hmx2 form a heterodimer and facilitate the export of Mn from the cytoplasm into the periplasm. We discuss the biological function of Hmx1 and Hmx2 in the interplay with Mnx and the importance of Mn export in the network of Mn homeostasis of *Synechocystis*.

INTRODUCTION

The transition metal Mn is of crucial importance for all organisms performing oxygenic photosynthesis (Hänsch and Mendel, 2009). Mn serves as catalytically active metal, fulfills an activating role for several proteins, and acts as direct cofactor of a variety of enzymes (Burnell, 1988; Hänsch and Mendel, 2009). It is involved in ATP synthesis, the reactions of ribulose-1,5-bisphosphate carboxylase/oxygenase (RuBisCO), and the biosynthesis of fatty acids and proteins (Ness and Woolhouse, 1980; Pfeffer et al., 1986; Houtz et al., 1988). However, the most prominent role of Mn is in the oxygen-evolving complex (OEC) of photosystem II (PSII) where a Mn_4O_5Ca cluster (Mn-cluster) mediates the water-splitting reaction (Nelson and Junge, 2015).

In the cyanobacterium *Synechocystis* sp. PCC 6803 (*Synechocystis*), the network of Mn homeostasis were investigated over the past decades. Two distinct Mn pools have been identified and up to 80% of the cellular content was found to accumulate in the periplasm, while only 20% reside inside the cytoplasmic membrane (Keren et al., 2002). In the periplasmic space, Mn is most likely loosely bound to the outer membrane by the negative membrane potential or bound to soluble Mn-binding proteins such as MncA (Keren et al., 2002; Tottey et al., 2008).

Inside the cell, roughly 80% of the Mn is associated with the Mn-cluster of the OEC (Anderson et al., 1964). This major sink of Mn is assumed to being supplied from the periplasmic storage and with the tetratricopeptide repeat protein PratA delivering Mn from the periplasm directly to the precursor of the D1 reaction center protein in the biogenesis centers of the cell (Stengel et al., 2012).

Mn demands other than PSII are supplied by active transport of Mn across the plasma membrane via the high-affinity ATP-binding cassette (ABC)- type transporter MntCAB (Bartsevich and Pakrasi, 1995; Bartsevich and Pakrasi, 1996). However, *mntCAB* knockout lines show Mn uptake when supplemented with micromolar amounts of Mn, indicating the

presence of a second, yet unidentified Mn uptake system (Bartsevich and Pakrasi, 1996). In contrast to MntCAB, which is competitively inhibited by cadmium (Cd), cobalt (Co), and zinc (Zn), this second system is hypothesized to be highly specific (Bartsevich and Pakrasi, 1996). Sharon and coworkers suggest that iron (Fe) transporters like FutABC transport Mn as co-substrate by a piggybacking mechanism (Sharon et al., 2014).

Recently, we identified the Mn export protein Mnx as a Mn export protein in *Synechocystis* (Brandenburg et al., 2017b). The thylakoid membrane protein Mnx exports Mn from the cytoplasm to the thylakoid lumen to prevent toxic concentrations in the cytoplasm.

Mnx belongs to the unknown protein family (UPF) 0016 that contains integral membrane proteins mostly of unknown function. Most members of the family consist of two copies of a domain that contains a conserved ExGD motif in the first of three predicted transmembrane helices (Demaegd et al., 2014). In *Arabidopsis thaliana* (*Arabidopsis*) the Mnx orthologue PAM71 is mediating the uptake of manganese (Mn) from the chloroplast stroma to the thylakoid lumen in order to provide Mn for in cooperation in the OEC of PSII (Schneider et al., 2016). Interestingly, two members of this highly conserved protein family, TMEM165 and Gdt1, have been described as calcium/proton (Ca^{2+}/H^{+}) exchangers in the Golgi apparatus of yeast and human, respectively, and play important roles in Ca^{2+}-signaling (Demaegd et al., 2013; Colinet et al., 2016). Together, these results suggest different conserved functions of UPF0016 in Mn- and Ca-transport between species performing oxygenic photosynthesis compared to non-photosynthetic species, respectively.

In this study, we provide further evidence for the hypothesis that the role of UPF0016 members in photosynthetic organisms is Mn- rather than Ca-transport. We identified two homologues of Mnx as Mn export proteins and named the proteins Hmx1 and Hmx2. Based on our results we present an updated model of the intricate model of Mn homeostasis in *Synechocystis*.

RESULTS

Identification of Proteins Homologous to Mnx

The UPF0016 seems to have different functions in photosynthetic organisms in comparison to non-photosynthetic organisms. While the proteins TMEM165 and Gdt1 have been described as Ca^{2+}-exchangers in human and yeast, respectively (Demaegd et al., 2013; Colinet et al., 2016), PAM71 and Mnx function as Mn transporter in *Arabidopsis* and *Synechocystis*, respectively (Schneider et al., 2016; Brandenburg et al., 2017b).

To investigate the function of UPF0016 in cyanobacteria further, we searched for additional members of UPF0016 in the Pfam database (Finn et al., 2016) and found two additional proteins of UPF0016, Slr1170 and Ssr1558, encoded in the genome of *Synechocystis*. BlastP analysis revealed that Slr1170 and Ssr1558 have a 35% and 31% sequence identity to Mnx, respectively.

Importantly, both proteins share the for UPF0016 typical ExGD motif in the first of three predicted transmembrane spans with Mnx (Figure 1A). However, Slr1170 and Ssr1558 are approximately half the size of Mnx, and thus lack the internal repeat of the conserved domain (Figure 1A). Among the prokaryotes, proteins of UPF0016 have been found encoded by one gene that has undergone an internal duplication resulting in a two-domain protein, or by one or two smaller genes encoding for a homodimer or heterodimer, respectively (Demaegd et al., 2014). Furthermore, we found orthologues of *slr*1170 and *ssr*1558 to be neighboring genes in 72% of the cyanobacterial species we looked at, while in only 16% of the species they were dispersed in the genome like in *Synechocystis*. Interestingly, we found a third gene in close proximity upstream in most of the species (Figure 2B). The upstream genes were either completely uncharacterized, belonged to UPF0153, or were predicted as iron-sulfur oxdireductases. In *Cyanothece* sp. ATCC 51142 we found *psb28-2* upstream of the *slr*1170 orthologue, which is involved in PSII biogenesis and chlorophyll biosynthesis (Dobakova et al., 2008; Nowaczyk et al., 2012).

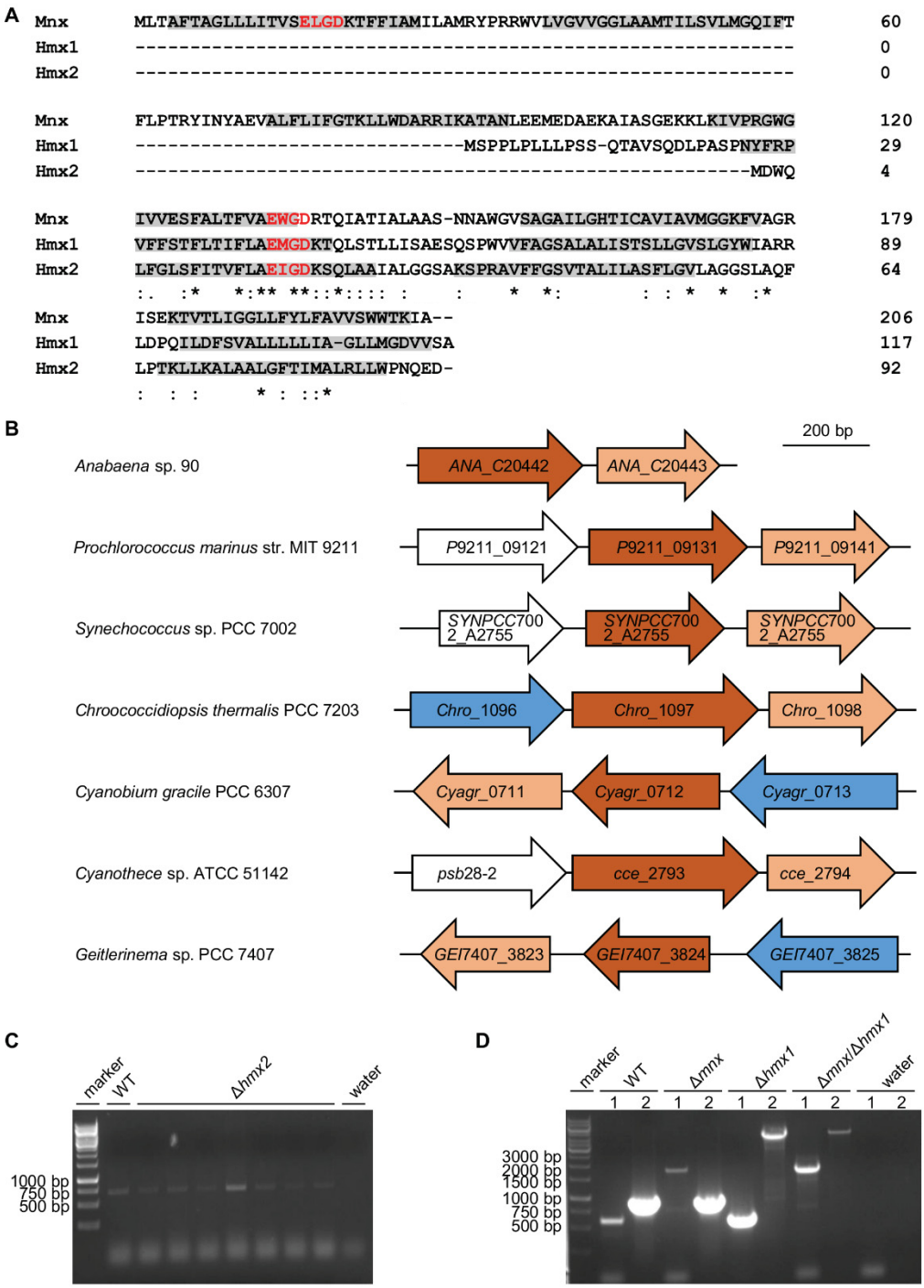

Figure 1: Sequence analysis and generation of mutant lines. (A) Alignment of the protein sequences of Mnx, Hmx1, and Hmx2. Grey boxes indicate predicted transmembrane spans. The conserved ExGD motiv is highlighted in red. Asteriks (*) indicated fully conserved residues and a colon (:) residues with similar properties. (B) Genomic organization of Hmx1 (dark orange) and Hmx2 (light orange) in selected cyanobacterial species. The direction of arrows indicates the orientation in the genome. Genes encoding for UPF0153 members are highlighted in blue. (C) PCR analysis of not segregated Δ*hmx2* mutants. (D) The genotypes of the mutants used in this study were verified by PCR using gene specific primers for amplification of *mnx* (lanes 1) and *hmx1* (lanes 2). Water was used as a negative control.

The close proximity in the genome of most cyanobacteria is an indicator for an operon structure. Therefore, we hypothesized *slr*1170 and *ssr*1558 to form a heterodimer. Interestingly, for 12% of the analyzed species, we found the same orthologues gene for both *slr*1170 and *ssr*1558, indicating that the organization as a homodimer is also possible.

In all species with two orthologous, the orthologue for *slr*1170 was located upstream of the orthologue for *ssr*1558 (Figure 1B). Due to their similarity to Mnx, we choose Slr1170 and Ssr1558 as candidate genes and hypothesize they form a heterodimer and function as Mn transporter in *Synechocystis*. Based on the hypothesized function, their size and their relative position to each other in the genome of most cyanobacterial species we named Slr1170 and Ssr1558 hemi Mn exchanger (Hmx) 1 and 2, respectively.

Loss of Hmx1-function causes sensitivity towards high concentration of externally supplied Mn

To investigate the function of Hmx1 and Hmx2 we aimed to generate the *Synechocystis* knockout line Δ*hmx1* and Δ*hmx2* by insertional inactivation. Although WT cells transformed with the knockout construct for *hmx2* formed colonies on selective plates, we could not verify the knockout of *hmx2* by PCR analysis (Figure 1C). In contrast, the generation of Δ*hmx1* and the *mnx*/*hmx1* double-knockout line Δ*mnx*/Δ*hmx1* by inactivation of *hmx1* in the Δ*mnx* mutant background yielded fully segregated mutants (Figure 1D).

To investigate the biological function of Hmx1 we exposed the different lines to increased amounts of Mn as compared to the 9 µM commonly used in BG11 medium (Herdman et al., 1979) and Mn limiting conditions (Figure 2A). All lines grew comparably well at 0 and 9 µM of $MnCl_2$. Growth of Δ*hmx1* was not affected by $MnCl_2$ concentrations up to 200 µM (22-fold increase). At 400 µM $MnCl_2$ (44-fold increase), *Δhmx1* was unable to grow, while the WT cells were only partially impaired in growth.

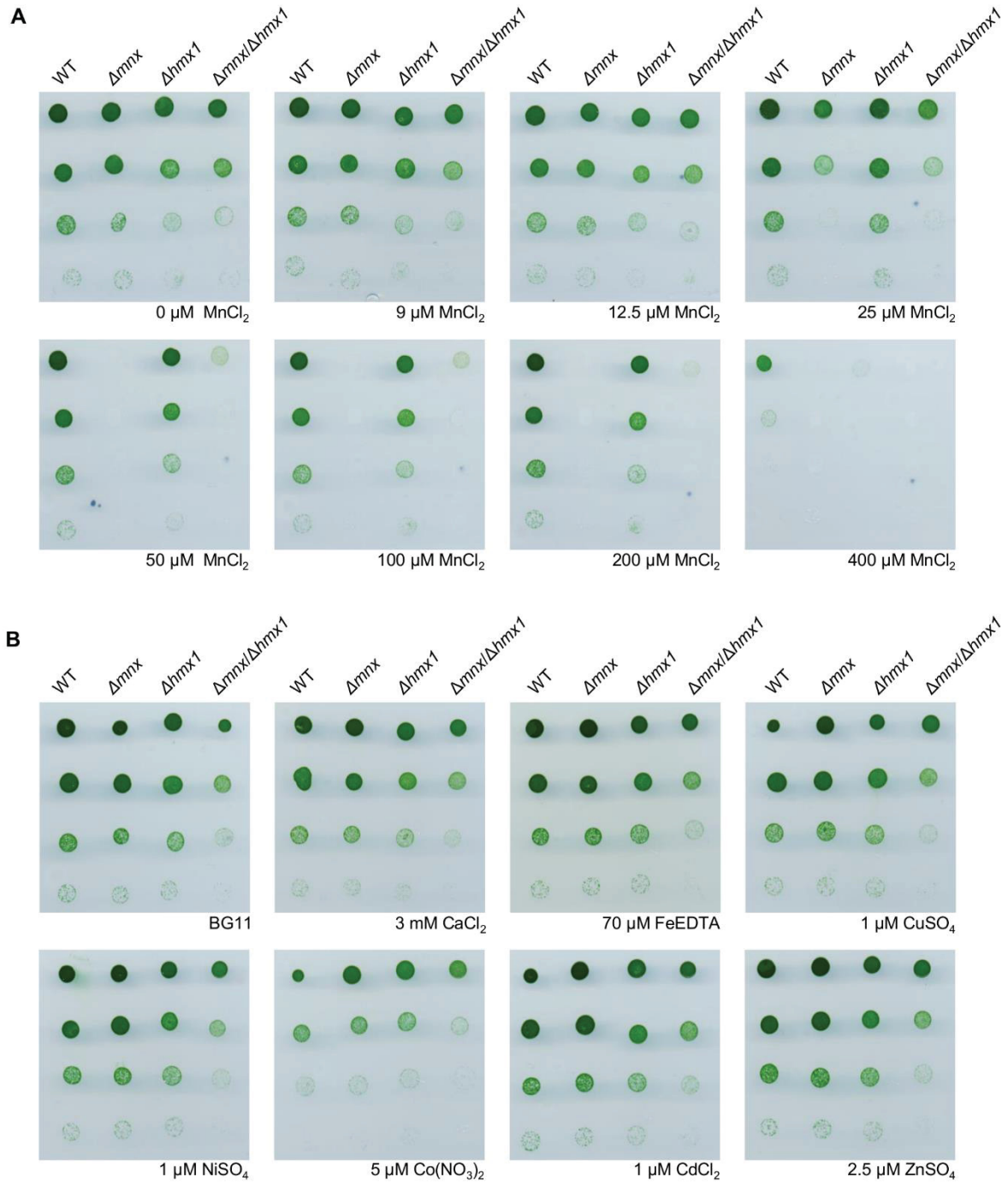

Figure. 2: Sensitivity of *Synechocystis* WT, Δ*mnx*, Δ*hmx1*, and Δ*mnx*/Δ*hmx1* lines toward divalent transition metals. Cells in mid log phase were diluted to an OD_{750} of 0.25. 2 µL of these cultures and subsequent 1:10, 1:100 and 1:1,000 dilutions were spotted onto BG11 plates supplemented with different transition metals as indicated. Pictures were taken after incubation for 5 d. (A) Growth of cells on BG11 medium containing 0, 9, 12.5, 25, 50, 100, 200, or 400 µM $MnCl_2$. 9 µM is the standard concentration of $MnCl_2$ in BG11 medium. (B) Growth of cells on BG11 medium containing elevated levels of divalent transition metals. The concentrations were 12-fold elevated for Ca^{2+} and 3-fold elevated for Fe^{2+}, Cu^{2+}, Zn^{2+}, and Co^{2+}-ions compared to standard BG11 medium. Additionally, 1 µM Cd^{2+} and Ni^{2+}-ions were added, which are not contained in standard BG11 medium.

As described previously, Δ*mnx* is impaired in growth when exposed to only slightly increased concentrations of Mn (Brandenburg et al., 2017b). In our experiments, Δ*mnx* was impaired in growth starting at 25 µM (2.5-fold increase) and Δ*mnx*/Δ*hmx1* neither showed an increased nor repressed phenotype as compared to Δ*mnx* at any of the tested conditions (Figure 2A).

Moreover, we tested the sensitivity towards other divalent transition metals, because it has been shown that Mn transporters in plants frequently accept multiple transport substrates (Socha and Guerinot, 2014). None of the mutant lines showed distinguishable growth to the WT when exposed to 12-fold elevated concentrations of Ca^{2+} ions or 3-fold elevated Fe^{2+}, Cu^{2+}, Zn^{2+}, and Co^{2+} as compared to standard BG11 (Figure 2B). In addition, 1 µM Cd^{2+} and Ni^{2+} ions, which are not contained in standard BG11, did not affect the mutant lines.

Based on the dose-dependent and Mn-specific phenotype towards elevated concentrations of Mnx, we specified our hypothesis for Hmx1 to a function in Mn export.

Double-knockout of hmx1 *and* mnx *leads to hyper-accumulation of Mn inside the cell*

Previously, we reported that the knockout of the Mn exporter Mnx causes significant over-accumulation of the intracellular pool of Mn within 4 h after treatment with Mn (Brandenburg et al., 2017b). To test the hypothesis Hmx1 functions in Mn export, we quantified the cellular amounts of Mn for Δ*hmx1* and Δ*mnx*/Δ*hmx1*. To ensure equal cellular concentration of Mn before the experiment for all cultures, we removed the periplasmic Mn storage with an EDTA-washing step and incubated the cells for 5 d at Mn-limiting conditions (Keren et al., 2002; Brandenburg et al., 2017b). After this precultivation, we found the intracellular Mn pools strongly reduced and significantly increased in Δ*mnx* to the WT (Figure 3). Within 4 h after addition of 300 µM $MnCl_2$, the intracellular Mn concentrations strongly increased in all lines. As expected, Δ*mnx* accumulated significantly more (1.5-fold) Mn inside the cell than the WT, while Δ*hmx1* showed no

difference. Remarkably, Δ*mnx*/Δ*hmx1* significantly over-accumulated (6-fold) Mn inside the cell.

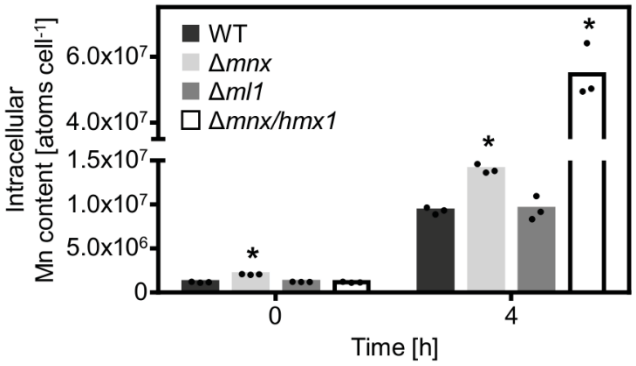

Figure 3: Cellular Mn accumulation in WT, WT, Δ*mnx*, Δ*hmx1*, and Δ*mnx*/Δ*hmx1* lines. Cells were grown under Mn-limiting conditions for 5 d and then treated with 300 µM $MnCl_2$. ICP-MS analysis was performed after limitation (0 h) and 4 h after treatment with $MnCl_2$. Each bar represents three biological replicates. The periplasmic and total Mn content is shown in Supplemental Figure S1. Asterisks (*) indicate significant changes to the respective WT value according to an unpaired t-test ($P \leq 0.05$).

Expression of Hmx1 *and* Hmx2 *supports growth of* E. coli *at high concentrations of Mn*

With Mnx, *Synechocystis* has at least one backup system to compensate for a loss of the hypothesized Mn export function of Hmx1. To investigate the function of Hmx1 independent from potential compensating mechanisms in the native organism, we expressed Hmx1 and Hmx2 heterologously in *Escherichia coli* (*E. coli*) under control of an isopropyl-β-D-thiogalactopyranosid (IPTG) inducible T7-promotor. The expression strains were challenged with high Mn concentrations to test for their resistance towards this metal. Cells expressing either Hmx1, Hmx2 or both proteins had slower but insignificantly changed growth rates compared to cells carrying only the empty expression vector in the control medium without extra supplemented Mn (Figure S2). For this reason, we analyzed the changes in growth rates upon Mn treatment of each strain relative to the same strain

without additional Mn added to the medium. Cells expressing either Hmx1 or Hmx2 grew significantly better than cells not expressing the proteins with 5 mM $MnCl_2$ added to standard LB-medium, while both proteins also grew better with 10 mM $Mncl_2$ added (Figure 4). With 20 mM $Mncl_2$ supplemented to the medium, none of the lines showed significant growth differences to the WT (Figure 4).

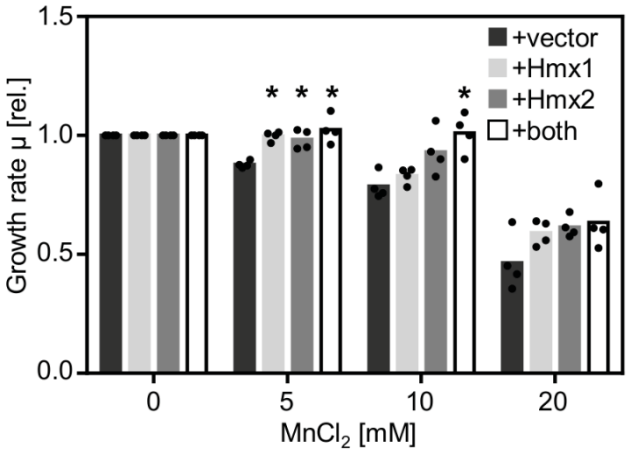

Figure 4: Mn dependent growth phenotype of *E. coli* expressing Hmx1 and/or Hmx2 heterelogously. Dilute cultures (OD_{600} 0.2) of *E. coli* cells expressing either Hmx1, Hmx2, or both proteins have been exposed to increasing concentrations of $MnCl_2$ while being incubated aerobically shaking at 37°C in LB medium plus ampicillin. Cell density was measured before and after 4 h of incubation. Shown are the growth rates μ [h^{-1}] relative to the respective untreated culture. Each bar represents four individual colonies of the same transformation. Asterisks (*) indicate significant changes to the respective WT value according to an unpaired t-test ($P \leq 0.05$).

Hmx1 and Hmx2 reside in the plasma membrane

To assign a biological meaning to the hypothesized export function, we investigated the subcellular localization of Hmx1 and Hmx2. We generated mutant lines expressing either Hmx1 (*hmx1::cfp*) or Hmx2 (*hmx2::cfp*) with a C-terminal cyan fluorescent protein (CFP) in their native genomic context under control of the respective native promotor and replacing the untagged protein. Confocal fluorescent microscopy revealed that the CFP

signals of both Hmx1 and Hmx2 do not overlap completely with the signal of the chlorophyll autofluorescence but are oriented towards the outside of the cell, indicating a localization in the plasma membrane (Figure 5A+B and 5D+E). Furthermore, in some cases the signals show local maxima at regions of low chlorophyll fluorescence (Figure 5 C+F),which are typical for biogenesis centers (Heinz et al., 2016).

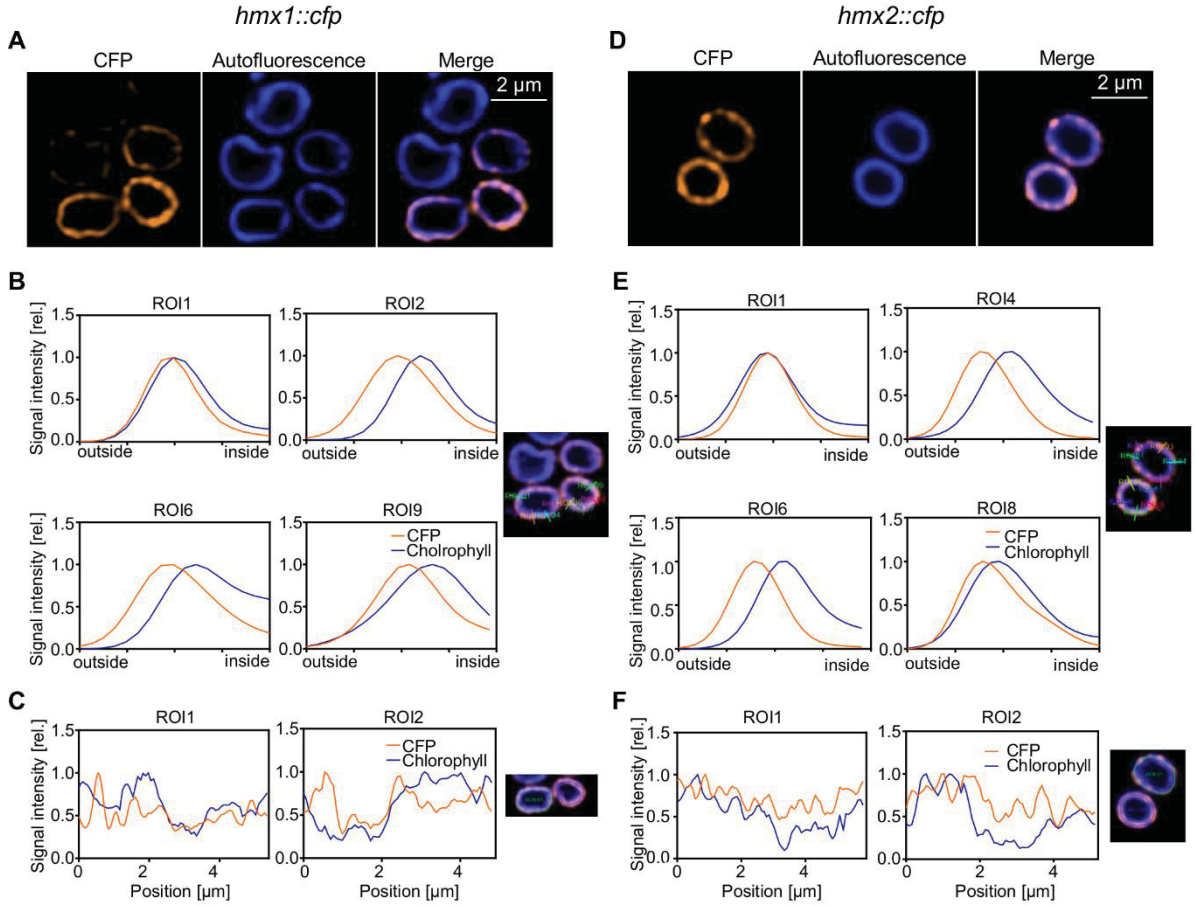

Figure 5: Subcellular localization of Hmx1 and Hmx2. Hmx1 and Hmx2 were C-terminally fused to a CFP. All results are shown for Hmx1::CFP (A, B, and C) and Hmx2::CFP (D, E, and F). CFP fluorescence is shown in orange, chlorophyll autofluorescence in blue, and a merged image shows both signals at the same time (A and D). Intensities of the signals from the outside to the inside of the cell at various positions of the cell circumference were analyzed as indicated by the regions of interest (ROIs) (B and E). Additional positions analyzed are shown in Supplemental Figure S3. Intensities of the signals along the cell circumference were analyzed as indicated by the ROIs (C and F).

Hmx1 and Hmx2 interact via the C-terminus

To investigate an interaction between Hmx1 and Hmx2, we established a yeast two-hybrid membrane system with a split ubiquitin mechanism (Stagljar et al., 1998). Yeast cells were transformed with either Hmx1 or Hmx2 fused to the N-terminal half (Nub) or the C-terminal half (Cub) of the yeast protein ubiquitin. Interaction of the tagged proteins Nub and Cub re-assemble into the so-called 'split-ubiquitin', which resembles the native fold of ubiquitin and is immediately recognized and cleaved by ubiquitin specific proteases (Johnsson and Varshavsky, 1994). Upon cleavage, release of reporter genes allows autotrophic growth on selective plates lacking the respective amino acids.

Growth on selective plates lacking the amino acids leucine and tryptophan (-Leu, -Trp) of all lines verified the successful transformation of all tested lines and controls. Growth on medium additionally lacking histidine and adenine (-His, -Ade) indicates an interaction of the tagged proteins. According to our results, Hmx1 and Hmx2 interact via the C-terminus, but not the C- and N-terminus (Figure 6A). The interaction was verified by a β-galactosidase assay, where the interaction of the tagged proteins is indicated by the blue color of the cells (Figure 6B).

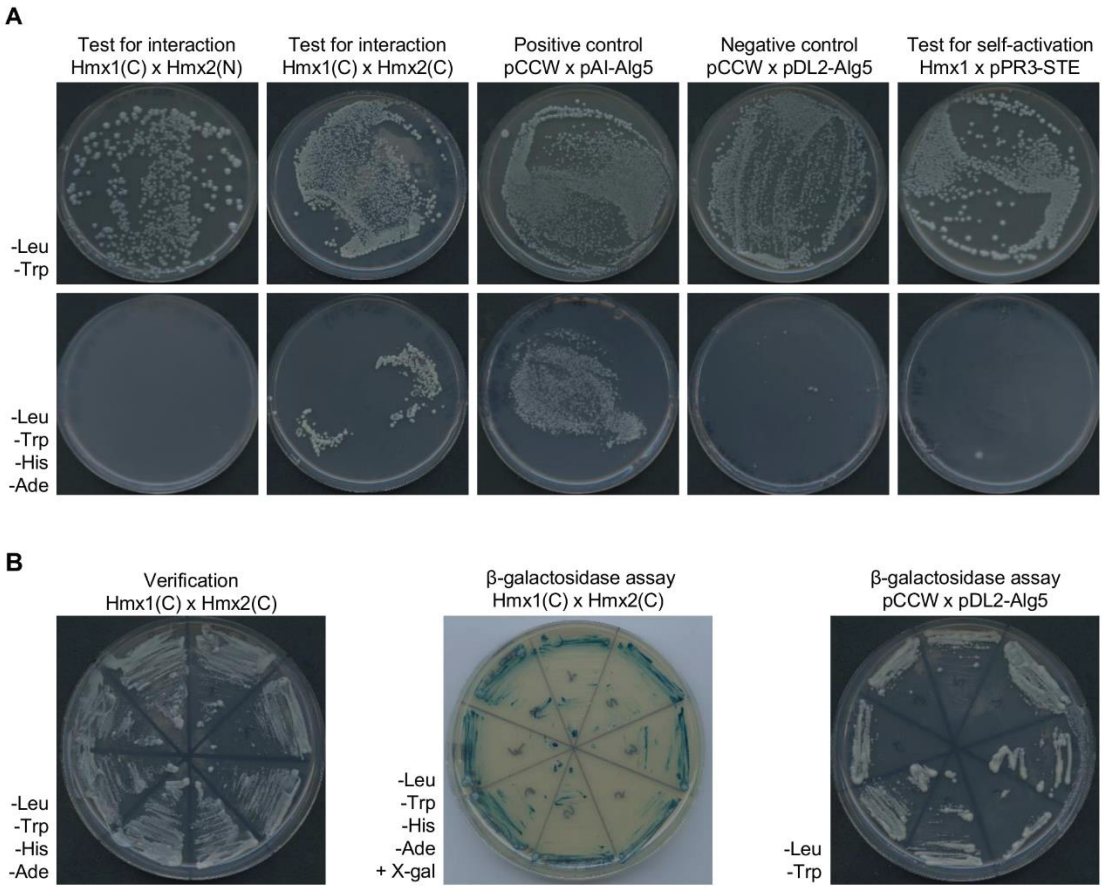

Figure 6: Interaction studies in *Saccharomyces cerevisiae*. NMY51 yeast cells were transformed with 'bait' and 'prey' constructs as indicated ('bait' x 'prey') and grown on selective plates. (A) The double dropout (-Leucin, -Tryptophan) selects for cells carrying both plasmids. Growth on quadruple dropout plates (-Leucin, -Tryptophan, -Histedin, -Adenin) selects for cells carrying both plasmids and interacting 'bait' and 'prey' proteins. A C-terminal Hmx1 fusion [Hmx1(C)] was tested as 'bait' for interaction with a N- and C-terminal Hmx2 fusion as 'prey' [Hmx2(N) and Hmx2(C), respectively]. The WT split ubiquitin proteins from the 'bait' control-vector pCCW and the 'prey' control-vector pAI-Alg5 will strongly interact regardless if they are fused to interacting proteins and thus serve as positive control. In contrast to this, the mutated N-terminal ubiquitin in pDL2-Alg5 will only interact in close proximity to the C-terminal half from pCCW and thus serves as negative control. Co-transformation of the Hmx1 'bait' vector with the empty library vector pPR3-STE was carried out to test for self-activation of the 'bait' construct. (B) The growth of the line Hmx1(C) x Hmx2(C) was verified by re-streaking eight colonies on quadruple dropout plates (left) and a β-galactosidase assay (middle). The β-galactosidase was also performed for the negative control (pCCW x pDL2-Alg5).

DISCUSSION

Hmx1 and Hmx2 form a heterodimer and facilitate Mn export from the cytoplasm into the periplasm in Synechocystis

The UPF0016 contains integral membrane proteins of unknown function. Most members of the family are composed of a duplicated domain, each containing a conserved ExGD motif in the first of three predicted transmembrane helices (Demaegd et al., 2014). Based on studies in human and yeast members of UPF0016 are Ca/H^+ exchangers and have important functions in Ca signaling (Demaegd et al., 2013; Colinet et al., 2016). However, studies in *Arabidopsis* and *Synechocystis* revealed a different function in Mn- rather than Ca-transport. This Mn specialization might have evolved in photosynthetic organisms (Schneider et al., 2016; Brandenburg et al., 2017b). To gain further insight in the function of UPF0016 members in photosynthetic organisms, we chose the *Synechocystis* Mnx-homologues Hmx1 and Hmx2 encoded by the open reading frames *slr*1170 and *ssr*1558, respectively, as candidats to analyze for their transport characteristics. In this study, we provide evidence that Hmx1 and Hmx2 form a heterodimer and represent, besides Mnx, a second cytoplasmic Mn export system.

The knockout mutant Δ*hmx1* showed sensitivity towards 44-fold (400 µM) increased concentrations of $MnCl_2$ in the medium (Figure 2A). This phenotype is typical for a mutant defective in Mn export capacity and different physiological mechanisms for Mn toxicity have been suggested (Brandenburg et al., 2017b). However, the sensitivity of Δ*hmx1* was lower than for Δ*mnx*, as previously (Brandenburg et al., 2017b) and in this study (Figure 2A) reported. Thus, the export capacity of Mnx is higher than that of Hmx1 and compensates the loss of Hmx1 function up to a concentration of 200 µM $MnCl_2$. The phenotype of Δ*mnx*/Δ*hmx1* corresponded to the phenotype of Δ*mnx* (Figure 2A) and supported this hypothesis. The hypothesis was supported further by ICP-MS analysis before and after treatment with 300 µM $MnCl_2$ (Figure 3). Δ*mnx* accumulated 1.5-fold more Mn in the cell than the WT. This increase was lower than reported previously (Brandenburg et al., 2017b),

but still significant. Interestingly, Δ*hmx1* showed internal Mn concentrations comparable to the WT, indicating that the function of Mnx was sufficient to maintain Mn homeostasis at 300 µM external $MnCl_2$, at least for the analyzed 4 h time course. Importantly, the loss of both export systems in Δ*mnx*/Δ*hmx1* caused a stronger increase of the intracellular Mn content as compared to Δ*mnx* (6-fold vs. 1.5-fold, Figure 3). In summary, we postulate two Mn export systems operating in *Synechocystis*, (i) a high-capacity system via Mnx and (ii) a low-capacity system via Hmx1.

We did not observe any phenotype upon the addition of Ca, Fe, Cu, Ni, Co, Cd, and Zn indicating the transport activity of Hmx1 is rather specific for Mn (Figure 2B). However, our results also show that Mnx is able to compensate for the phenotype of a loss of Hmx1 to a certain extent, which is why we cannot rule out that Hmx1 is accepting other metals as transport substrates.

To test if Hmx1 and Hmx2 indeed mediate Mn transport or have a regulatory function, we expressed the proteins heterologously in *E. coli*. Cells expressing either Hmx1, Hmx2 or both proteins grew significantly better after the addition of 5 mM $MnCl_2$ and only cells expressing both proteins grew significantly better after the additions of 10 mM $MnCl_2$ (Figure 4). The results show that Hmx1 and Hmx2 have indeed a transport function, and indicates that both proteins are needed for a fully functional protein. If the hypothesis, Mnx has a higher transport capacity than Hmx1 and Hmx2, was true, the expression of Mnx in E. coli should have a stronger effect on growth than Hmx1 and/or Hmx2.

Based on these results and because we found orthologues of Hmx1 and Hmx2 to be neighboring genes in most cyanobacterial species (Figure 1B), we hypothesized them to form a heterodimer. In a yeast two-hybrid assay we found the C-terminus of Hmx1 to interact with the C-terminus of Hmx2, while an interaction via the C-terminus of Hmx1 and the N-terminus of Hmx2 could not be shown (Figure 6). In bacteria, the cytosolic side of a membrane protein is determined by the higher number of positively charged amino acid residues (Arginin, R and Lysin, K) in cytosolic loops in comparison to non-cytosolic loops

(R+K rule) (von Heijne, 1986). For members of UPF0016 consisting of two proteins, one protein has more positive residues in even loops, while the other has more positive residues in odd loops, which suggests an interaction via the C- and N-terminus and results in an antiparallel organization of the subunits (Demaegd et al., 2014). However, Hmx1 shows only a weak R+K bias and Hmx2 does not follow the R+K rule at all (Supplemental Figure S4). Based on our results indicating a C-terminal interaction of Hmx1 and Hmx2 we hypothesize the proteins to insert into the plasma membrane in a parallel manner. If the orientation in the membrane is affecting the transport mechanism has not been investigated so far and cannot be concluded from our results.

To gain more insight into the biological function of a second Mn export system besides Mnx, we investigated the subcellular localization of Hmx1 and Hmx2. Mnx was shown to reside in the thylakoid membrane and to facilitate the export of Mn from the cytoplasm into the thylakoid lumen (Brandenburg et al., 2017b). In our microscopic analysis, the signals of CFP-tagged Hmx1 and Hmx2 do not overlap completely with the signal of the chlorophyll fluorescence (Figure 5A+D), but are oriented towards the periphery of the cell (Figure 5 B+E). Furthermore, the signals indicate a local accumulation of Hmx1 and Hmx2 in the biogenesis centers of the cell in some cases (Figure 5 C+F). The results indicate Hmx1 and Hmx2 have a function in the plasma membrane of *Synechocystis* and might be involved in the functions of the biogenesis centers. Demaegd and colleagues suggested antiport with H^+ as transport mechanism for all members of UPF0016 (Demaegd et al., 2014). Across the thylakoid membrane, a ΔpH of about 2.5 units has been reported for several species and is also hypothesized for *Synechocystis* (Teuber et al., 2001). Hence, Mnx and its *Arabidopsis* homologue PAM71 have been proposed to function as Mn transporter into the thylakoid lumen, using the H^+ gradient across the thylakoid membrane (Schneider et al., 2016; Brandenburg et al., 2017b). In the biogenesis centers, Hmx1 and Hmx2 might transport Mn provided by PratA to the thylakoid lumen, using the proton gradient across the thylakoid membrane, and thus provide Mn for the incorporation in D1 (Figure 7).

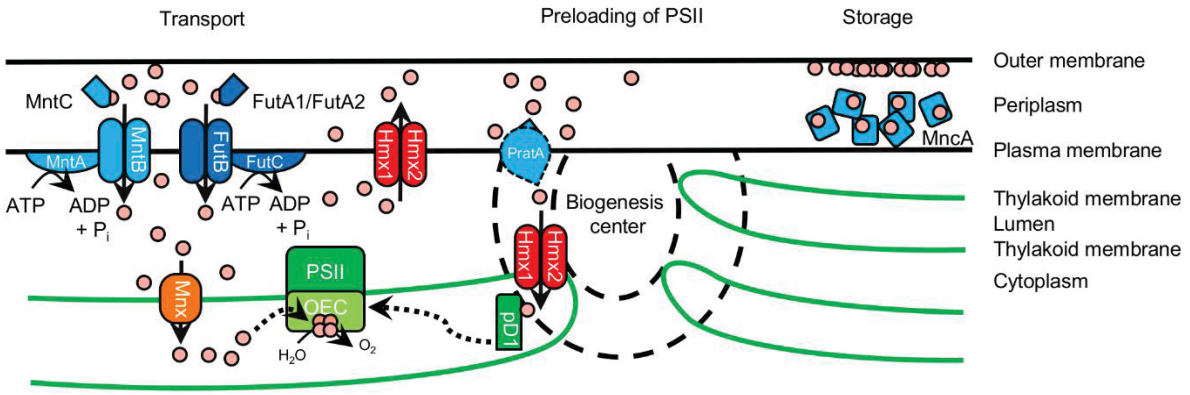

Figure 7: Hypothetical model for the function of Hmx1 and Hmx2 in *Synechocystis*. Mn (Mn^{2+} ions represented as rose-colored circles; oxidation states Mn^{3+} and Mn^{4+} in the activated Mn_4O_5Ca cluster are not specifically accentuated) is stored mainly in the periplasm, bound to the outer membrane or proteins with MncA being the most abundant Mn containing protein in the periplasm. To maintain cellular functionality, the plasma membrane ABC transporter MntCAB imports Mn under Mn-limiting conditions. Fe transporters like FutABC are hypothesized to accept Mn as transport substrate as well. The cytoplasmic surplus of Mn resulting from the turnover and degradation of Mn- containing proteins is sequestered into the safekeeping environment thylakoid lumen via Mnx. Additionally, Mnx transports Mn from the cytoplasm into the thylakoid lumen to support Mn delivery to the OEC. In the plasma membrane, Hmx1 and Hmx2 export Mn from the cytoplasm directly into the periplasm, using the inwards H^+ gradient generated upon illumination. In the biogenesis centers, Hmx1 and Hmx2 provide Mn for the pre-D1 (pD1) protein, which is the Mn_4O_5Ca cluster-binding core protein of PSII in corporation with PratA.

This hypothesis is supported further by the organization of *psb*28-2, which is involved in the biogenesis of PSII (Dobakova et al., 2008; Nowaczyk et al., 2012), in an operon with the homologues of Hmx1 and Hmx2 in *Cyanothece* sp. ATCC 5142.

The localization in the plasma membrane requires a more sophisticated discussion of the direction of Mn transport of Hmx1 and Hmx2 and the implemented biological function. Across the plasma membrane, extrusion of protons by both respiration and ATP hydrolysis have been shown to result in a proton gradient from the periplasm to the cytoplasm (Teuber et al., 2001). This process is thought to be important for energy dissipation during periods of high light (Schultze et al., 2009). Interestingly, the work with Mnx indicates an increased need for Mn export of *Synechocystis* during periods of high light (Brandenburg et al., 2017b). Similarly, we postulate that Hmx1 and Hmx2 use the H^+ gradient across the

plasma membrane formed during periods of high light to facilitate Mn extrusion from the cell (Figure 7).

However, the H^+ gradient across the plasma membrane is likely smaller than across the thylakoid membrane. This might explain the lower transport capacity of Hmx1 and Hmx2 compared to Mnx, which was hypothesized earlier. If this hypothesis was true, a lower pH might suppress the Mn sensitivity of Δ*mnx* due to a higher transport activity of Hmx1 and Hmx2. Furthermore, the effect of high light on mutants lacking Hmx1 and Hmx2 needs to be investigated.

In summary, we propose different directions of Mn transport for Hmx1 and Hmx2 based on their location (Figure 7). While Hmx1 and Hmx2 provide Mn for PSII biogenesis in cooperation with PratA in the biogenesis centers, they function as Mn exporter from the cytoplasm to the periplasm across the plasma membrane to maintain intracellular Mn homeostasis. We hypothesize that the latter is especially important under high light conditions.

Toward the importance of Mn export proteins in Mn homeostasis

The importance of Mn for the function of a photosynthetic cell has been described in the introduction and is reviewed widely in the literature (Shcolnick and Keren, 2006; Millaleo et al., 2010; Socha and Guerinot, 2014). However, most research focusses on Mn limitation and Mn import, even though it is known that for example for *Synechocystis* Mn concentrations of 100 nM are sufficient for growth without any physiological effects (Salomon and Keren, 2011). Even in the complete absence of Mn and with their periplasmic storage pool removed, cyanobacteria grow for several weeks before they show symptoms of Mn starvation (Salomon and Keren, 2015). The typical symptoms like reduced growth, reduced PSII activity and an increased phycocyanin to chlorophyll ratio can be reverted

within hours by the addition of sufficient concentrations of Mn to the medium (Salomon and Keren, 2015).

In contrast to the effect of Mn limitation, the effects of excess Mn are devastating and not revertible. Several mechanisms are discussed including the inhibition of chlorophyll biosynthesis (Csatorday et al., 1984), impaired abundance of the photosystem I (PSI) reaction center proteins PsaA and PsaB (Millaleo et al., 2013), and the generation of reactive oxygen species (ROS) in a Fenton reaction (Lynch and St.Clair, 2004). Therefore, free Mn in the cytoplasm resulting from turnover of Mn-containing proteins needs to be avoided. The PSII reaction center protein D1 contains about 80% of the intracellular Mn and is the largest cellular sinks for Mn (Anderson et al., 1964). With a half-life of 19 minutes (Tyystjärvi et al., 1994), turnover of D1 is likely the largest source for free Mn inside the cell. In our previous work, we identified the first cyanobacterial Mn exporter Mnx and investigated its role in Mn homeostasis (Brandenburg et al., 2017b). We demonstrated that increased cellular concentration of Mn have a massive impact on photosynthesis and eventually cause cell death (Brandenburg et al., 2017b). Plants have evolved multiple tolerance mechanisms to address this issue. Here, Mn gets sequestered in the Golgi apparatus and secreted via the secretory pathway (Ducic and Polle, 2005), or exported to the vacuole and inactivated by the formation of insoluble phosphate-Mn- (Dučić and Polle, 2007) or malate-Mn-complexes (Chen et al., 2015). The gram-negative bacterium *E. coli* uses the Mn exporter MntP to compensate for over activity of the Mn importer MntH during transitions from low- to high-Mn environments (Martin et al., 2015). Similarly, *Synechocystis* has evolved two parallel export systems for Mn, which are both important under high light, when increased D1 turnover causes a transition from low to high intracellular concentrations of Mn. The presence of two parallel export systems, underlines the crucial importance of maintaining Mn homeostasis within a narrow range and strictly avoiding the accumulation of free Mn inside the cell.

In most species containing orthologous of Hmx1 and Hmx2 in an operon, we found proteins of UPF0153 upstream of the orthologue to Hmx1. The function of the cysteine rich UPF0153 is unknown. However, cysteine rich proteins are often metallothioneins (de Miranda et al., 1990). Methallotioneins function as chaperon for various heavy metals and are one cellular mechanism in plants for heavy metal safe-keeping (Hall, 2002; Guo et al., 2003). In human the metal-responsive transcription factor 1 (MTF1) contains a cysteine cluster and specifically activates genes important during heavy metal stress (Chen et al., 2004). Future work with UPF0153 might also contribute to a better understanding of the function of Hmx1 and Hmx2 and the integral understanding of *Synechocystis*' strategy to face heavy metal stress in its natural environment.

CONCLUSION

In this study, we identified and characterized the Mn transport proteins Hmx1 and Hmx2 in the cyanobacterium *Synechocystis*. The two proteins form a heterodimer via their C-termini and reside in the plasma membrane with local accumulations in the biogenesis centers. In the plasma membrane, Hmx1 and Hmx2 facilitate the export of Mn from the cytoplasm into the periplasm and form a second Mn export system besides the recently published Mn transport protein Mnx. The presence of a second Mn export system elucidates the toxic nature of elevated intracellular levels of Mn and the importance of strictly regulated Mn homeostasis for *Synechocystis*. While the cyanobacterium needs only trace amounts of Mn for sufficient cell growth, the effects of increased cellular concentration of Mn are devastating and therefore surplus of Mn needs to be exported immediately. In the biogenesis centers, Hmx1 and Hmx2 might provide Mn for PSII biogenesis in cooperation with PratA. The toxic nature of Mn together with the increased demand for Mn of a photosynthetic cell in comparison with a non-photosynthetic cell might be the reason for the changed substrate specificity of UPF0016 from Ca in human and yeast to Mn in photosynthetic organisms.

MATERIAL and METHODS

Sequence Analysis and Identification of Candidate Genes

Proteins of interest were identified using Pfam (http://pfam.xfam.org) (Finn et al., 2016) and BlastP (https://blast.ncbi.nlm.nih.gov/Blast.cgi) analysis (Altschul et al., 1990). DNA and protein sequences and the predicted trans-membrane spans were obtained from the genome database CyanoBase (http://genome.microbedb.jp/cyanobase). Clustal Omega (https://www.ebi.ac.uk/Tools/msa/clustalo) was used for sequence alignment (Sievers et al., 2014). The protein models were designed with the online tool Protter (http://wlab.ethz.ch/protter/start) (Omasits et al., 2014).

Synechocystis Strains and Growth Conditions

A Glc-tolerant Japanese strain of *Synechocystis* sp. PCC 6803 obtained from Martin Hagemann (University of Rostock, Germany) severed as wild type. Axenic cultures were grown at 30°C and 200 rpm, illuminated with 100 µmol photons m^{-2} s^{-1} constant white light, in the defined medium BG11 (Rippka et al., 1979). Growth medium of the mutant lines was supplemented with appropriate antibiotics (50 µg mL^{-1} kanamycin [Km], 20 µg mL^{-1} spectinomycin [Sp], or 2 µg mL^{-1} gentamycine [Gm]).

Generation of Knockout and Double-Knockout Lines

The Δ*hmx1* knockout mutant was generated by introduction of the Sm resistance cassette from the plasmid pUC4S (Vinnemeyer, University Rostock, Germany) into the *NaeI* restriction site of the PCR amplified open reading frame of the PCR-amplified (primers FB69 and FB70; Supplemental Table 1) open reading frame of *slr*1170. The cloning vector pJET1.2 (ThermoFisher) served as vector backbone. In the same way the construct to knockout *hmx2* was generated using primers FB71 and FB72 (Supplemental Table 1) and

by adding a Gm resistance cassette derived from the plasmid used for CFP localization (provided by the group of Jörg Nickelsen, LMU Munich) to the *SmaI* restriction site of *hmx2*.

Transformation, selection on Sm- or Gm-containing BG11 plates and segregation of independent clones was verified by PCR analysis as described in (Eisenhut et al., 2006). The Δ*mnx*/*hmx1* double knockout mutant was generated by transformation of the Δ*mnx* mutant with the *hmx1*-knockout-construct, following the same protocol.

Drop Tests

The effect of varying amounts of $MnCl_2$ on the different lines was tested on solid BG11 medium. Cultures were grown until mid-log phase, before 2 µL of culture with an OD_{750} of 0.25 and subsequent 1:10, 1:100, and 1:1000 dilutions were spotted onto agar plates (BG11, pH 7.5 with 24 mM sodium thiosulfate added; solidified with 1.5% [w/v] bacto agar). The plates were supplemented with $MnCl_2$ or other divalent transition metals as indicated and did not contain antibiotics. Plates were incubated under continuous white-light illumination of 100 µmol photons m^{-2} s^{-1} at 30°C for 5 d.

ICP-MS Measurements

Cells were washed with EDTA (HEPES-KOH, pH7.5, and 5mM EDTA; Kerenet al., 2002) before and after pre-cultivation under Mn-limiting conditions for 5 days, to ensure similar intracellular Mn concentrations in all lines. Before the experiment, cells were adjusted to an OD_{750} of 1.0 and treated with 300 µM $MnCl_2$. Before the experiment and after 4 h of treatment, samples were taken and washed as described in Brandenburg et al. (2017a).The washed samples were re-suspended 0.5 mL 67% nitric acid and digested for 2 h at 70°C. The digested samples were diluted to ~6,7% nitric acid with 4.5 mL Mili-Q grade water (18

MΩ cm). The elemental composition of the samples was determined by ICP-MS (Agilent 7700). The cell numbers of the samples were estimated using a Neubauer-improved hemocytometer (Marienfeld).

E. coli Expression and Growth Curves

NcoI and *AflII* restriction sites were added to the *hmx1* coding sequence (incl. STOP codon) via PCR amplification (primers FB123 and FB124; Supplemental Table 1). In the same way, *NdeI* and *PacI* restriction sites were added to the *hmx2* coding sequence (incl. STOP codon) (primers FB125 and FB126; Supplemental Table 1). The PCR products were sub-cloned in the cloning vector pJET1.2 (ThermoFisher), and subsequently cloned into the expression vector pETDuet-1 (Novagen), using restriction digest (NEB enzymes) and T4 DNA Ligase (NEB). To express both proteins in the same cell, both genes were cloned into pETDuet-1. In pETDuet-1 the genes are under the control of an IPTG inducible T7-promotor. The *E. coli* expression strain Rosetta 2(DE3)pLysS Singles (Novagen) was transformed with the constructs. The successful transformation of four individual colonies per transformation was verified by PCR before the colonies were inoculated overnight and diluted to 20 mL culture with an OD_{600} of 0.2. All cultures were grown in standard LB-medium supplemented with 200 µg mL^{-1} Ampicillin. Each pre-culture was split in 4x5 mL cultures and supplemented with a final concentration of 0, 5, 10, or 20 mM $MnCl_2$. Protein expression was induced by addition of 1 mM IPTG. The cells were incubated at 37°C and 140 rpm for 4 h. The OD_{600} was determined using a microplate reader (BioTek Synergy HT).

Subcellular localization of Hmx1

XhoI and *NheI* restriction sites were added to a PCR amplified *hmx1* (primers FB105 and FB106; Supplemental Table 1) open reading frame including its 800 bp upstream region.

Similarly, the 800 bp downstream region of *hmx1* was PCR amplified with *EcoRI* restriction sites added to both ends (primers FB107 and FB108; Supplemental Table 1). Restriction digest and T4 DNA Ligase (all NEB enzymes) were used to first clone the 3'region of hmx1 downstream of a CFP and Gm resistance cassette, before hmx1 including the 5'region of hmx1 was cloned upstream of the CFP. A GSGSG peptide linker separates the gene of interest and *hmx1* to allow proper folding of both proteins. A *hmx2::cfp* fusion was generated in the same way using primers FB109, FB110 and FB111, FB112 (Supplemental Table 1). WT *Synechocystis* cells were transformed as described above using Gm for selection. Successful transformation was verified by PCR using primers FB104 (*hmx1::cfp*) or (*hmx2::cfp*) together with a Gm reverse primer (FB114; Supplemental Table 1).

For imaging, the cells were immobilized on microscopic glass slides by a thin layer of solid BG11 medium (1:1 mixture of 2-fold concentrated BG11medium, with 24 mM sodium thiosulfate added and 3% [w/v] bacto agar). A Leica TCS SP8 STED 3X microscope with a HC PL APO CS2 100x/1.40 OIL objective was used. An argon laser at 488 nm and 70 W output intensity was used for excitation. Emission was detected using Leica HyD hybrid detectors from 470-530 nm (CFP) and 660-700 nm (chlorophyll).

Interaction studies

A split ubiquitin yeast two-hybrid assay was used to investigate a potential interaction of Hmx1 and Hmx2. The vector pBT3-STE (Dualsystems Biotech, Switzerland) was used to generate the Hmx1 'bait' construct (primers ME318 and ME319; Supplemental Table 1) and the vectors pPR3-N and pPR3-STE (Dualsystems Biotech, Switzerland) to generate the respective Hmx2 N-and C-terminal 'prey' constructs (primers ME321, ME323 and ME330 and ME331, respectively; Supplemental Table 1). The vectors pCCW-Alg5, pAl-Alg5, pDL2-Alg5, and an empty pPR3-STE were used as control vectors (all MoBiTec GmbH, Germany). The constructs were transformed in *Saccharomyces cerevisiae* strain NMY51 (MoBiTec

GmbH, Germany) using the lithium acetate method (Gietz and Shiestl, 2007). Transformed cells were grown on selective plates with the appropriate 'drop outs' according to the auxotrophies conferred by the respective vectors as stated by the manufacturers manual. Eight colonies from transformed cells showing interaction were re-streaked on selective plates with 0.1 mg/mL 5-bromo-4-chloro-3-indolyl-β-D-galactopyranoside (X-gal) added for blue white screening.

ACKNOWLEDGMENTS

We thank Tabea Mettler-Altmann and Sabine Metzger from the Plant Metabolism and Metabolomics Facility and the Center of Advanced Imaging, in particular Stefanie Weidtkamp-Peters and Thomas Zobel, at the Heinrich Heine University for excellent technical assistance. We thank the group of Jörg Nickelsen for providing us with the codon optimized CFP.

LITERATURE CITED

Altschul SF, Gish W, Miller W, Myers EW, Lipman DJ (1990) Basic local alignment search tool. J Mol Biol **215**: 403–10

Anderson JM, Boardman NK, David DJ (1964) Trace metal composition of fractions obtained by digitonin fragmentation of spinach chloroplasts. Biochem Biophys Res Commun **17**: 685–689

Bartsevich V V, Pakrasi HB (1995) Molecular identification of an ABC transporter complex for manganese : analysis of a cyanobacterial mutant strain impaired in the photosynthetic oxygen evolution process. EMBO J **14**: 1845–1853

Bartsevich V V, Pakrasi HB (1996) Manganese Transport in the Cyanobacterium *Synechocystis* sp . PCC 6803. J Biol Chem **271**: 26057–26061

Brandenburg F, Schoffman H, Keren N, Eisenhut M (2017a) Determination of Mn Concentrations in *Synechocystis* sp. PCC 6803 Using ICP-MS. Bio-protocol **x**: 1–7

Brandenburg F, Schoffman H, Kurz S, Krämer U, Keren N, Weber APM, Eisenhut M (2017b) The *Synechocystis* Manganese Exporter Mnx Is Essential for Manganese Homeostasis in Cyanobacteria. Plant Physiol **173**: 1798–1810

Burnell J (1988) The Biochemistry of Manganese in Plants. Manganese in Soils and Plants. pp 125–137

Chen X, Zhang B, Harmon PM, Schaffner W, Peterson DO, Giedroc DP (2004) A Novel Cysteine Cluster in Human Metal-responsive Transcription Factor 1 Is Required for Heavy Metal-induced Transcriptional Activation in Vivo. J Biol Chem **279**: 4515–4522

Chen Z, Sun L, Liu P, Liu G, Tian J, Liao H (2015) Malate Synthesis and Secretion Mediated by a Manganese-Enhanced Malate Dehydrogenase Confers Superior Manganese Tolerance in *Stylosanthes guianensis*. Plant Physiol **167**: 176–88

Colinet A-S, Sengottaiyan P, Deschamps A, Colsoul M-L, Thines L, Demaegd D, Duchêne M-C, Foulquier F, Hols P, Morsomme P (2016) Yeast Gdt1 is a Golgi-localized calcium transporter required for stress-induced calcium signaling and protein glycosylation. Sci Rep **6**: 1–11

Csatorday K, Gombos Z, Szalontai B (1984) Mn^{2+} and Co^{2+} toxicity in chlorophyll biosynthesis. Proc Natl Acad Sci **81**: 476–478

Demaegd D, Colinet A-S, Deschamps A, Morsomme P (2014) Molecular Evolution of a Novel Family of Putative Calcium Transporters. PLoS One **9**: e100851

Demaegd D, Foulquier F, Colinet A-S, Gremillon L, Legrand D, Mariot P, Peiter E, Van Schaftingen E, Matthijs G, Morsomme P (2013) Newly characterized Golgi-localized family of proteins is involved in calcium and pH homeostasis in yeast and human cells. Proc Natl Acad Sci U S A **110**: 6859–64

Dobakova M, Sobotka R, Tichy M, Komenda J (2008) Psb28 Protein Is Involved in the Biogenesis of the Photosystem II Inner Antenna CP47 (PsbB) in the Cyanobacterium *Synechocystis* sp. PCC 6803. Plant Physiol **149**: 1076–1086

Ducic T, Polle A (2005) Transport and detoxiification of manganese and copper in plants. Brazilian J Plant Physiol **17**: 103–112

Dučić T, Polle A (2007) Manganese toxicity in two varieties of Douglas fir (*Pseudotsuga menziesii var. viridis* and *glauca*) seedlings as affected by phosphorus supply. Funct Plant Biol **34**: 31–40

Eisenhut M, Kahlon S, Hasse D, Ewald R, Lieman-Hurwitz J, Ogawa T, Ruth W, Bauwe H, Kaplan A, Hagemann M (2006) The Plant-Like C2 Glycolate Cycle and the Bacterial-Like Glycerate Pathway Cooperate in Phosphoglycolate Metabolism in Cyanobacteria. Plant Physiol **142**: 333–342

Finn RD, Coggill P, Eberhardt RY, Eddy SR, Mistry J, Mitchell AL, Potter SC, Punta M, Qureshi M, Sangrador-Vegas A, et al (2016) The Pfam protein families database: Towards a more sustainable future. Nucleic Acids Res **44**: D279–D285

Gietz RD, Shiestl HR (2007) Yeast transformation by the LiAc/SS carrier DNA/PEG method. Nat Protoc **2**: 31–35

Guo WJ, Bundithya W, Goldsbrough PB (2003) Characterization of the *Arabidopsis* metallothionein gene family: Tissue-specific expression and induction during senescence and in response to copper. New Phytol **159**: 369–381

Hall JL (2002) Cellular mechanisms for heavy metal detoxification and tolerance. J Exp Bot **53**: 1–11

Hänsch R, Mendel RR (2009) Physiological functions of mineral micronutrients (Cu, Zn, Mn, Fe, Ni, Mo, B, Cl). Curr Opin Plant Biol **12**: 259–66

von Heijne G (1986) The distribution of positively charged residues in bacterial inner membrane

proteins correlates with the trans-membrane topology. EMBO J **5**: 3021–3027

Heinz S, Rast A, Shao L, Gutu A, Gügel IL, Heyno E, Labs M, Rengstl B, Viola S, Nowaczyk MM, et al (2016) Thylakoid Membrane Architecture in *Synechocystis* Depends on CurT, a Homolog of the Granal CURVATURE THYLAKOID1 Proteins. Plant Cell. doi: 10.1105/tpc.16.00491

Herdman M, Janvier M, Waterbury JB, RIPPKA R, STANIER RY, Mandel M (1979) Deoxyribonucleic Acid Base Composition of Cyanobacteria. J Gen Microbiol **111**: 63–71

Houtz RL, Nable RO, Cheniae GM (1988) Evidence for Effects on the in Vivo Activity of Ribulose-Bisphosphate Carboxylase/Oxygenase during Development of Mn Toxicity in Tobacco. Plant Physiol **86**: 1143–1149

Johnsson N, Varshavsky A (1994) Split ubiquitin as a sensor of protein interactions in vivo. Proc Natl Acad Sci U S A **91**: 10340–4

Keren N, Kidd MJ, Penner-hahn JE, Pakrasi HB (2002) A Light-Dependent Mechanism for Massive Accumulation of Manganese in the Photosynthetic Bacterium *Synechocystis* sp. PCC 6803. Biochemistry **41**: 15085–15092

Lynch JP, St.Clair SB (2004) Mineral stress: the missing link in understanding how global climate change will affect plants in real world soils. F Crop Res **90**: 101–115

Martin JE, Waters LS, Storz G, Imlay JA (2015) The *Escherichia coli* Small Protein MntS and Exporter MntP Optimize the Intracellular Concentration of Manganese. PLoS Genet **11**: 1–32

Millaleo R, Ivanov AG, Mora ML, Alberdi M (2010) Manganese as Essentail and Toxic Element for Plant: Transport, Accumulation and Resistance Mechanisms. Journale Soil Sci Plant Nutr.ition **10**: 476–494

Millaleo R, Reyes-Díaz M, Alberdi M, Ivanov AG, Krol M, A HNP (2013) Excess manganese differentially inhibits photosystem I versus II in Arabidopsis thaliana. J Exp Bot **64**: 343–354

de Miranda JR, Thomas MA, Thurman DA, Tomsett AB (1990) Metallothionein genes from the flowering plant Mimulus guttatus. FEBS Lett **260**: 281–284

Nelson N, Junge W (2015) Structure and Energy Transfer in Photosystems of Oxygenic Photosynthesis. Annu Rev Biochem **84**: 659–683

Ness PJ, Woolhouse HW (1980) RNA Synthesis in Phaseolus Chloroplasts. **31**: 235–245

Nowaczyk MM, Krause K, Mieseler M, Sczibilanski A, Ikeuchi M, Rögner M (2012) Deletion of

psbJ leads to accumulation of Psb27-Psb28 photosystem II complexes in *Thermosynechococcus elongatus*. Biochim Biophys Acta - Bioenerg **1817**: 1339–1345

Omasits U, Ahrens CH, M??ller S, Wollscheid B (2014) Protter: Interactive protein feature visualization and integration with experimental proteomic data. Bioinformatics **30**: 884–886

Pfeffer PE, Tu SI, Gerasimowicz W V, Cavanaugh JR (1986) In vivo 31P NMR studies of corn root tissue and its uptake of toxic metals. Plant Physiol **80**: 77–84

Rippka R, Deruelles J, Waterbury JB, Herdman M, Stanier RY (1979) Generic Assignments, Strain Histories and Properties of Pure Cultures of Cyanobacteria. J Gen Microbiol **111**: 1–61

Salomon E, Keren N (2011) Manganese limitation induces changes in the activity and in the organization of photosynthetic complexes in the cyanobacterium *Synechocystis* sp. strain PCC 6803. Plant Physiol **155**: 571–9

Salomon E, Keren N (2015) Acclimation to environmentally relevant Mn concentrations rescues a cyanobacterium from the detrimental effects of iron limitation. Environ Microbiol **17**: 2090–2098

Schneider A, Steinberger I, Herdean A, Morper A, Rühle T, Labs M, Gandini C, Flugge UI, Geimer S, Spetea Wiklund C, et al (2016) The Evolutionarily Conserved Protein PHOTOSYNTHESIS AFFECTED MUTANT71 is Required for Efficient Manganese Uptake at the Thylakoid Membrane in *Arabidopsis*. Plant Cell. doi: 10.1105/tpc.15.00812

Schultze M, Forberich B, Rexroth S, Dyczmons NG, Roegner M, Appel J (2009) Localization of cytochrome b6f complexes implies an incomplete respiratory chain in cytoplasmic membranes of the cyanobacterium *Synechocystis* sp. PCC 6803. Biochim Biophys Acta - Bioenerg **1787**: 1479–1485

Sharon S, Salomon E, Kranzler C, Lis H, Lehmann R, Georg J, Zer H, Hess WR, Keren N (2014) The hierarchy of transition metal homeostasis: Iron controls manganese accumulation in a unicellular cyanobacterium. Biochim Biophys Acta **1837**: 1990–1997

Shcolnick S, Keren N (2006) Metal Homeostasis in Cyanobacteria and Chloroplasts . Balancing Benefits and Risks to the Photosynthetic Apparatus. Plant Physiol **141**: 805–810

Sievers F, Wilm A, Dineen D, Gibson TJ, Karplus K, Li W, Lopez R, McWilliam H, Remmert M, Soding J, et al (2014) Fast, scalable generation of high-quality protein multiple sequence alignments using Clustal Omega. Mol Syst Biol **7**: 539–539

Socha AL, Guerinot M Lou (2014) Mn-euvering manganese: the role of transporter gene family members in manganese uptake and mobilization in plants. Front Plant Sci **5**: 106

Stagljar I, Korostensky C, Johnsson N, te Heesen S (1998) A genetic system based on split-ubiquitin for the analysis of interactions between membrane proteins *in vivo*. Proc Natl Acad Sci U S A **95**: 5187–92

Stengel A, Gügel IL, Hilger D, Rengstl B, Jung H, Nickelsen J (2012) Initial steps of photosystem II de novo assembly and preloading with manganese take place in biogenesis centers in *Synechocystis*. Plant Cell **24**: 660–675

Teuber M, Rögner M, Berry S (2001) Fluorescent probes for non-invasive bioenergetic studies of whole cyanobacterial cells. Biochim Biophys Acta - Bioenerg **1506**: 31–46

Tottey S, Waldron KJ, Firbank SJ, Reale B, Bessant C, Sato K, Cheek TR, Gray J, Banfield MJ, Dennison C, et al (2008) Protein-folding location can regulate manganese-binding versus copper- or zinc-binding. Nature **455**: 1138–42

Tyystjärvi T, Aro EM, Jansson C, Mäenpää P (1994) Changes of amino acid sequence in PEST-like area and QEEET motif affect degradation rate of D1 polypeptide in photosystem II. Plant Mol Biol **25**: 517–526

SUPPLEMENTAL DATA

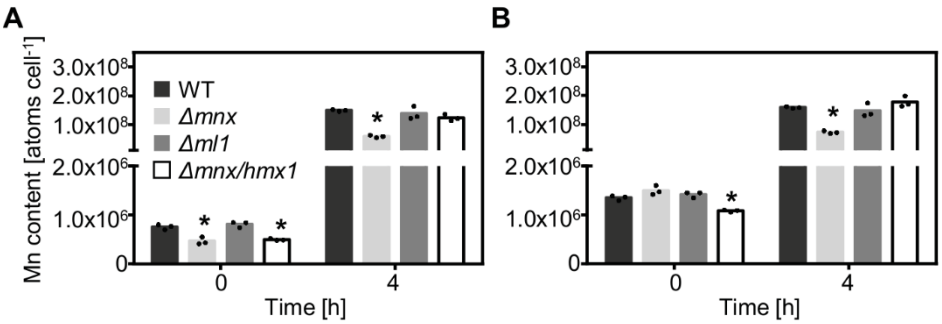

Figure S1: (A) Periplasmic and total (B) Mn accumulation in WT, WT, Δ*mnx*, Δ*hmx1*, and Δ*mnx*/Δ*hmx1* lines. Cells were grown under Mn-limiting conditions for 5 d and then treated with 300 µM $MnCl_2$. ICP-MS analysis was performed after limitation (0 h) and 4 h after treatment with $MnCl_2$. Each bar represents three biological replicates. The intracellular Mn content is shown in Figure 3. Asterisks (*) indicate significant changes to the respective WT value according to an unpaired t-test ($P \leq 0.05$).

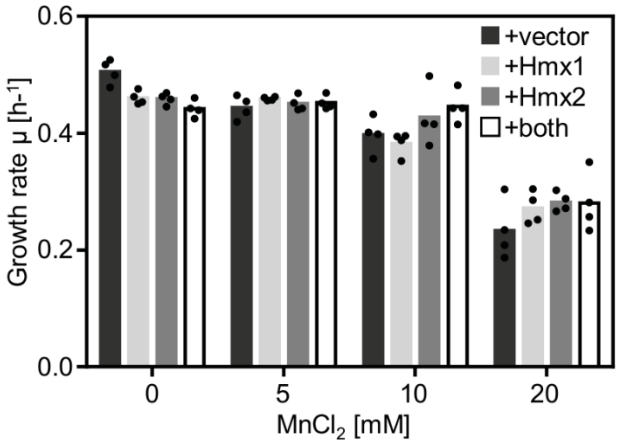

Figure S2: Mn dependent growth phenotype of *E. coli* expressing Hmx1 and/or Hmx2 heterelogously. Dilute cultures (OD_{600} 0.2) of *E. coli* cells expressing either Hmx1, Hmx2, or both proteins have been exposed to increasing concentrations of $MnCl_2$ while being incubated aerobically shaking at 37°C in LB medium plus ampicillin. Cell density was measured before and after 4 h of incubation. Shown are the growth rates µ [h^{-1}]. Each bar represents four individual colonies of the same transformation. Asterisks (*) indicate significant changes to the respective WT value according to an unpaired t-test ($P \leq 0.05$).

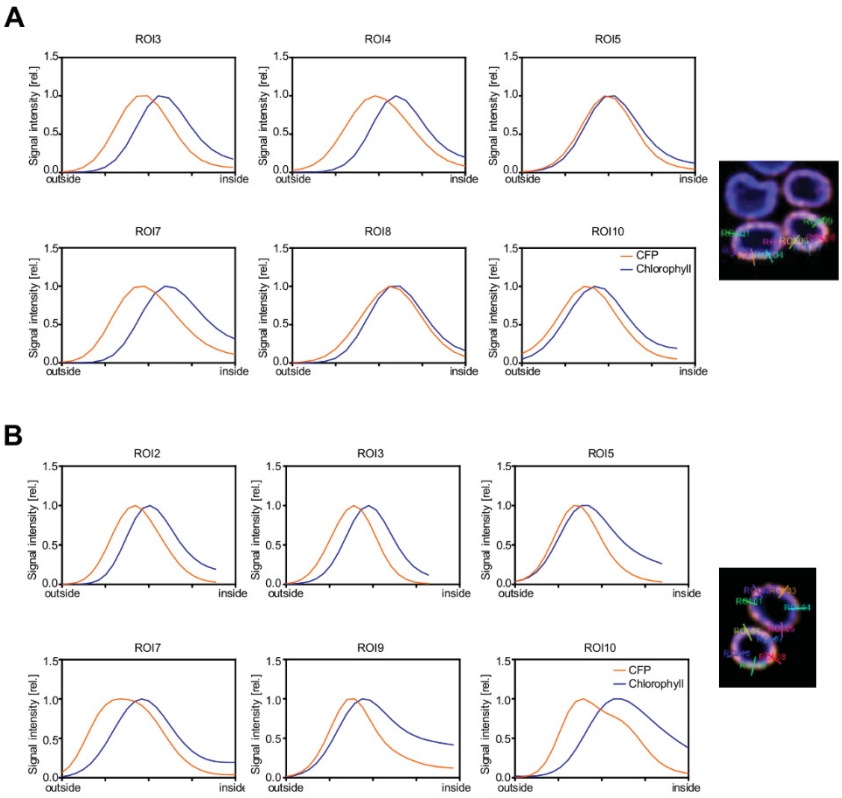

Figure S3: Signal intensities across the cell circumference. Hmx1 and Hmx2 were C-terminally fused to a CFP. CFP fluorescence is shown in orange, chlorophyll autofluorescence in blue. Intensities of the signals from the outside to the inside of the cell at various positions of the cell circumference were analyzed as indicated by the regions of interest (ROIs) for Hmx1::CFP (A) and Hmx2::CFP (B).

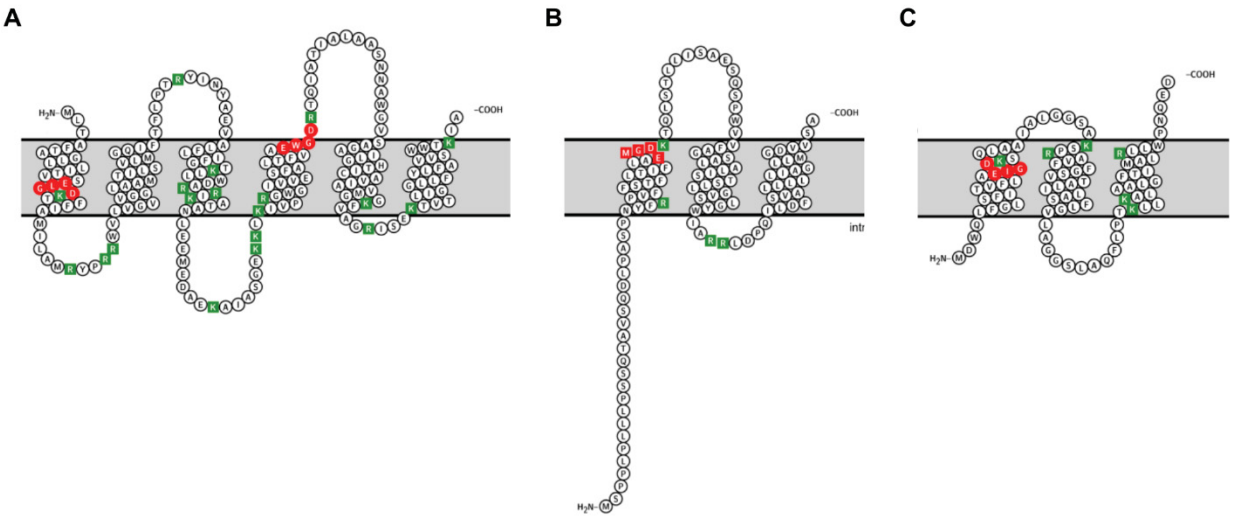

Figure S4: Organization of Mnx (A), Hmx1 (B), and Hmx2 (C) in the membrane. Red circles highlight the conserved ExGD motif. Green boxes mark positive arginine (R) and lysine (K) residues, which define the orientation of the protein towards the cytosol.

Table S1: Oligonucleotides used in this study. Restriction sites are in small letters.

Name	Sequence (5′ ➔ 3′)	Experiment
FB69	CTATTTATTCTCAGCAATATCGCCC	Generation of knockout mutant in *hmx1*
FB70	AACAGCACTTTACCTTCAAAGTCC	Generation of knockout mutant in *hmx1*
FB71	CCAGGATGCTGACGAAGTACAG	Generation of knockout mutant in *hmx2*
FB72	ATTTTACCGCCCCATGGTC	Generation of knockout mutant in *hmx2*
FB105	ctcgagCACCCTGGGAGTTTTCACCA	Generation of *hmx1::cfp*
FB106	gctagcGGCGCTGACCACGTCCC	Generation of *hmx1::cfp*
FB107	gaattcGCTCAGCACCACAAACATTCC	Generation of *hmx1::cfp*
FB108	gaattcTGCGGTTAAAAACTTAAATAGGGG	Generation of *hmx1::cfp*
FB109	ctcgagATTTGATTACCCTGCCTTTATTGG	Generation of *hmx2::cfp*
FB110	gctagcATCTTCTTGGTTAGGCCAAAGTAA	Generation of *hmx2::cfp*
FB111	gaattcATCACCGATCGCAATTTTTCC	Generation of *hmx2::cfp*
FB112	gaattcAGTGTGTTTGTGGCCCCAGT	Generation of *hmx2::cfp*
FB114	CGCTCCTGAAAAAAGGGGA	Verification of CFP-mutants
FB123	ccatgGTGTCCCCACCATTGCCG	Expression of Hmx1 in *E. coli*
FB124	cttaagCTAGGCGCTGACCACGTCC	Expression of Hmx1 in *E. coli*
FB125	catatgATGGATTGGCAACTGTTTGGTC	Expression of Hmx2 in *E. coli*
FB126	taataaCTAATCTTCTTGGTTAGGCCAAAGTA	Expression of Hmx2 in *E. coli*
ME318	ggccattacggccGTGTCCCCACCATTGCC	Generation of Hmx1 bait
ME319	ggccgaggcggccCCGGCGCTGACCACGTCC	Generation of Hmx1 bait
ME321	ggccattacggccATGGATTGGCAACTGTTTGGT	Generation of Hmx2 N-terminal prey
ME323	ggccgaggcggccCTAATCTTCTTGGTTAGGCCAAAGTA	Generation of Hmx2 N-terminal prey
ME330	ggccattacggccGGATGGATTGGCAACTGTTTGGT	Generation of Hmx2 C-terminal prey
ME331	ggccgaggcggccGAATCTTCTTGGTTAGGCCAAAGTAAAC	Generation of Hmx2 C-terminal prey

Authors' contribution to manuscript III

Fabian Brandenburg	Designed, performed and analyzed all experiments except the interaction studies, wrote the manuscript, and designed the figures.
Anastasija Plett	Planned and performed the interaction studies.
Andreas Weber	Helped with the experimental design
Marion Eisenhut	Generated the *ml1* knockout line, supervised the experimental design, and reviewed the manuscript.

Concluding Remark

In the beginning of this PhD thesis, the knowledge on Mn homeostasis in *Synechocystis* was limited to import mechanisms. The first Mn importer MntCAB was identified in 1995 and the presence of a second, still unidentified, Mn import system was hypothesized at the same time (Bartsevich and Pakrasi, 1995; Bartsevich and Pakrasi, 1996). A third route for Mn inside the cell, independent from transport proteins, was identified in 2004 with the description of the Mn binding protein PratA (Klinkert et al., 2004) and further characterization of its role in PSII biogenesis (Stengel et al., 2012).

The initial goal of this thesis was the characterization of the UPF0016 protein Sll0615. Up to this point, UPF0016 was characterized as a family of Ca^{2+}/H^{+} exchangers based on work with yeast protein Gdt1 and its human orthologue TMEM165 (Demaegd et al., 2013; Demaegd et al., 2014). Interestingly, the first results obtained in this thesis did not only indicate that Sll0615 functions in Mn and not Ca transport, but also that the protein is involved in export of Mn. Thus, Sll0615 was named Mnx, for manganese exporter. Work with the plant orthologue PAM71, done in parallel to the work with Mnx of this thesis, supported the hypothesis of an evolutionary conserved altered substrate specificity of UPF0016 towards Mn among photosynthetic organisms (Schneider et al., 2016). In the beginning of 2017, the results of the work with Mnx, included in this thesis as Manuscript I, were published in Plant Physiology (Brandenburg et al., 2017b). In the process of the characterization of Mnx, a novel protocol for the differential determination of periplasmic and intracellular Mn concentrations via ICP-MS in *Synechocystis* was established. The protocol is part of this thesis as Manucript II and was published in Bio-protocol (Brandenburg et al., 2017a). Based on the results of Manuscript I, Mnx resides in the thylakoid membrane and exports Mn from the cytoplasm into the thylakoid lumen. Although Mnx does not transport Mn through the plasma membrane out of the cell, several independent lines of evidence demonstrate that Mnx is involved in Mn export and serves important roles in the prevention of critical cytosolic Mn accumulation and the supply of PSII with Mn. However, it remains unclear how Mn sequestered in the thylakoid lumen is extruded from the cell eventually. Even though,

PAM71 facilitates transport of Mn across the thylakoid membrane into the thylakoid lumen, similar to Mnx, PAM71 is not involved in Mn export but the supply of PSII with Mn and replaces the function of PratA, which has no homologues in plants.

Shortly after the publication of the results obtained for Mnx in this thesis, Gandini and colleagues published their characterization of Sll0615 and named the protein SynPAM71 for *Synechocystis* PAM71, in conformity to the plant orthologue PAM71 (Gandini et al., 2017). The results of this publication mostly coincide with the model developed in this thesis. Interestingly, based on their results Mnx might also reside in the plasma membrane, an instance that cannot be excluded based on our results.

In the progress of the work with Mnx, the two paralogues Slr1170 and Ssr1558 identified as candidates for an additional Mn transport system in *Synechocystis*. Based on the results summarized in Manuscript III, Slr1170 and Ssr1558 form a heterodimer and export Mn across the plasma membrane from the cytoplasm to the periplasm using the inwards H^+ gradient, which is generated upon illumination by the extrusion of H^+ (Teuber et al., 2001). Local accumulation in the biogenesis centers of *Synechocystis* also indicate a function in the biogenesis of PSII. Here, a H^+ gradient from the thylakoid lumen to the periplasm indicates a function in Mn preloading of D1 in coordination with PratA. Due to their size and function, Slr1170 and Ssr1558 were named Hmx1 and Hmx2 for hemi Mn exchanger 1 and 2, respectively. If the UPF0153, located upstream of *hmx1* in most cyanobacterial species contributes to the tolerance of Mn or other heavy metals remains unknown.

In summary, the results of this thesis contributed significantly to the understanding of Mn homeostasis in *Synechocystis*. They demonstrate the importance of strictly regulated intracellular levels of Mn to avoid detrimental effects. The large Mn demands of PSII together with the short half-life of the D1 subunit result in a high turnover of Mn in photosynthetic cells and require immediate and rapid export to prevent accumulation of free Mn inside the cell. The presence of two different Mn export systems in *Synechocystis* elucidates the importance of Mn export over other tolerance mechanisms like a reduced import or the formation of insoluble complexes.

REFERENCES

Bartsevich V V, Pakrasi HB (1995) Molecular identification of an ABC transporter complex for manganese : analysis of a cyanobacterial mutant strain impaired in the photosynthetic oxygen evolution process. EMBO J **14**: 1845–1853

Bartsevich V V, Pakrasi HB (1996) Manganese Transport in the Cyanobacterium *Synechocystis* sp . PCC 6803. J Biol Chem **271**: 26057–26061

Brandenburg F, Schoffman H, Keren N, Eisenhut M (2017a) Determination of Mn Concentrations in *Synechocystis* sp. PCC6803 Using ICP-MS. Bio-protocol, accepted

Brandenburg F, Schoffman H, Kurz S, Krämer U, Keren N, Weber APM, Eisenhut M (2017b) The *Synechocystis* Manganese Exporter Mnx Is Essential for Manganese Homeostasis in Cyanobacteria. Plant Physiol **173**: 1798–1810

Demaegd D, Colinet A-S, Deschamps A, Morsomme P (2014) Molecular Evolution of a Novel Family of Putative Calcium Transporters. PLoS One **9**: e100851

Demaegd D, Foulquier F, Colinet A-S, Gremillon L, Legrand D, Mariot P, Peiter E, Van Schaftingen E, Matthijs G, Morsomme P (2013) Newly characterized Golgi-localized family of proteins is involved in calcium and pH homeostasis in yeast and human cells. Proc Natl Acad Sci U S A **110**: 6859–64

Gandini C, Schmidt SB, Husted S, Schneider A, Leister D (2017) The transporter SynPAM71 is located in the plasma membrane and thylakoids, and mediates manganese tolerance in *Synechocystis* PCC6803. New Phytol. doi: 10.1111/nph.14526

Klinkert B, Ossenbühl F, Sikorski M, Berry S, Eichacker L, Nickelsen J (2004) PratA, a periplasmic tetratricopeptide repeat protein involved in biogenesis of photosystem II in *Synechocystis* sp. PCC 6803. J Biol Chem **279**: 44639–44644

Schneider A, Steinberger I, Herdean A, Morper A, Rühle T, Labs M, Gandini C, Flugge UI, Geimer S, Spetea Wiklund C, et al (2016) The Evolutionarily Conserved Protein PHOTOSYNTHESIS AFFECTED MUTANT71 is Required for Efficient Manganese Uptake at the Thylakoid Membrane in *Arabidopsis*. Plant Cell. doi: 10.1105/tpc.15.00812

Stengel A, Gügel IL, Hilger D, Rengstl B, Jung H, Nickelsen J (2012) Initial steps of photosystem II de novo assembly and preloading with manganese take place in biogenesis centers in Synechocystis. Plant Cell **24**: 660–675

Teuber M, Rögner M, Berry S (2001) Fluorescent probes for non-invasive bioenergetic studies of whole cyanobacterial cells. Biochim Biophys Acta - Bioenerg **1506**: 31–46

Acknowledgment

In the following, I want to acknowledge some people who supported me either scientifically or mentally throughout my time as a PhD student. As every acknowledgment ever written, this list limited by space and therefore highly incomplete.

First and foremost, my supervisor, main discussion partner, and motivator since my Master's thesis Marion Eisenhut, who initiated this PhD project in the first place, and introduced me to the fascinating world of cyanobacteria with their amazing scientific community.

My doctoral advisor Prof. Andreas Weber who hosted me in his lab throughout my Bachelor's thesis, Master's thesis and PhD thesis and provided valuable feedback to all of my projects.

My committee members Prof. Peter Westhoff and Prof. Peter Jahns as well as my auditors Prof. Ilka Axmann and Prof. Michael Feldbrügge for their time and feedback.

Our collaborators Nir Keren and Hanan Schoffman from the Hebrew University in Jerusalem, without whom the Mnx-story would have probably never been finished, for a irradiant scientific and cultural exchange.

All the former and present scallywags of the 'Schlauch', the 'Metal Lab' and the 'Räuberhöhle', of whom many have become good friends, some even better than it would have been beneficial for both parties. I am thinking in particular about Thomas Wrobel, Nils Koppers, Marc-Sven Röll, Lennart Charton and Dominik 'Ipanak' Brilhaus. So long, and thanks for all the fish!

Nadine Hocken (for the occasional 'Ahuhu' in the morning and lots of discussions), Olena Tetyuk (for clarifying the difference between the prepositions 'in', 'on', and 'at'), and Kristian Kaiser (embarrassingly, for helping me to translate some expressions in to proper German).